Superconducting RF I
- Basics for SRF Cavity -

K.Saito KEK

1. Superconductivity
2. Niobium Material
3. Cavity Design
4. HOM Issue
5. Lorentz Detuning
6. RF input coupler
7. Cavity Fabrication

1. Superconductivity

1.1 Superconductivity

1.2 Surface Resistance of SRF Cavity

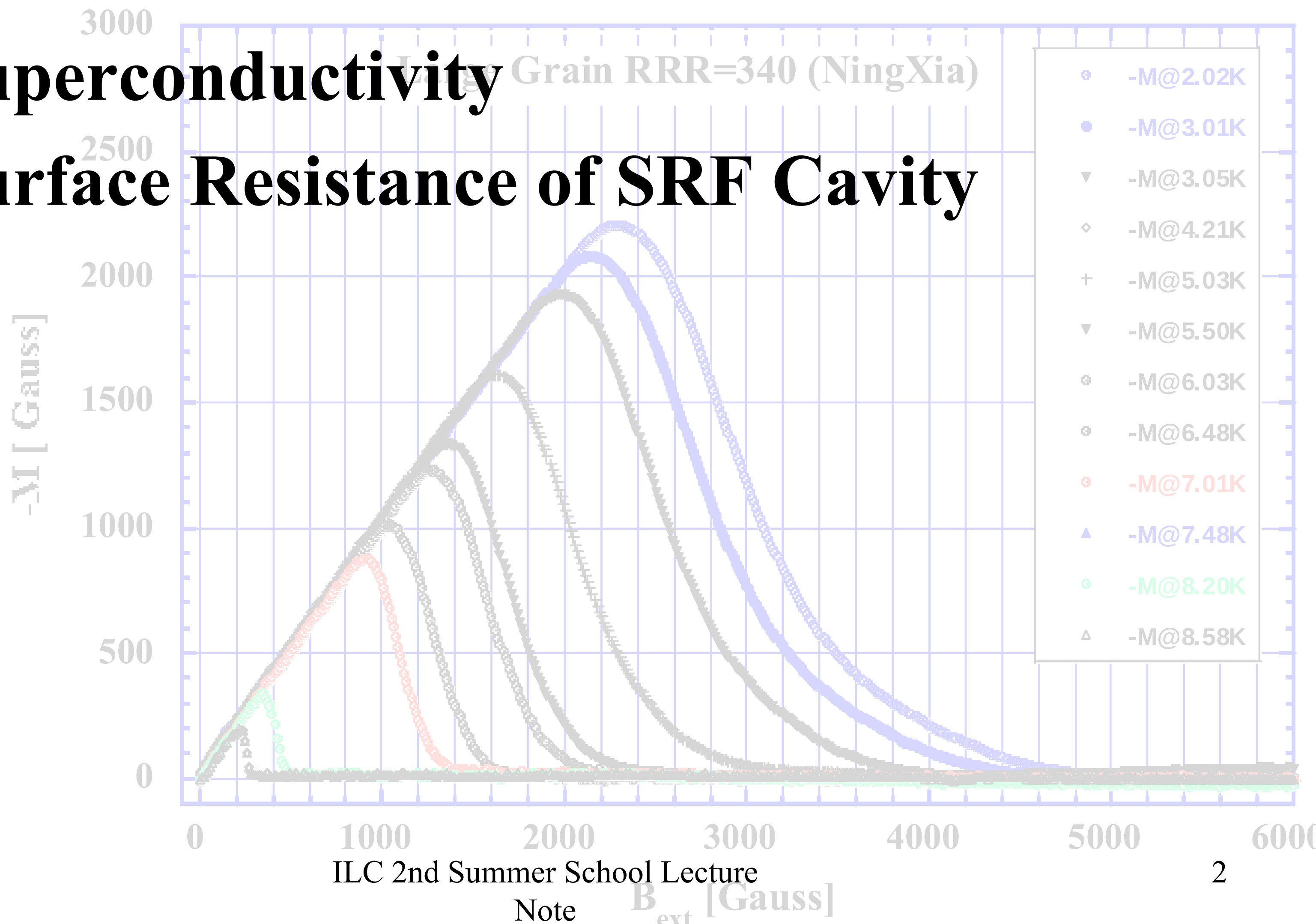

1.1 Superconductivity

1911 by K.Onnes

19933 by Meissner and Ochsenfeld (experiment)
1935 Phenomenological theory by F.and H.London

Zero resistance @ Tc

Perfect diamagnetism < Hc

Miessner effect

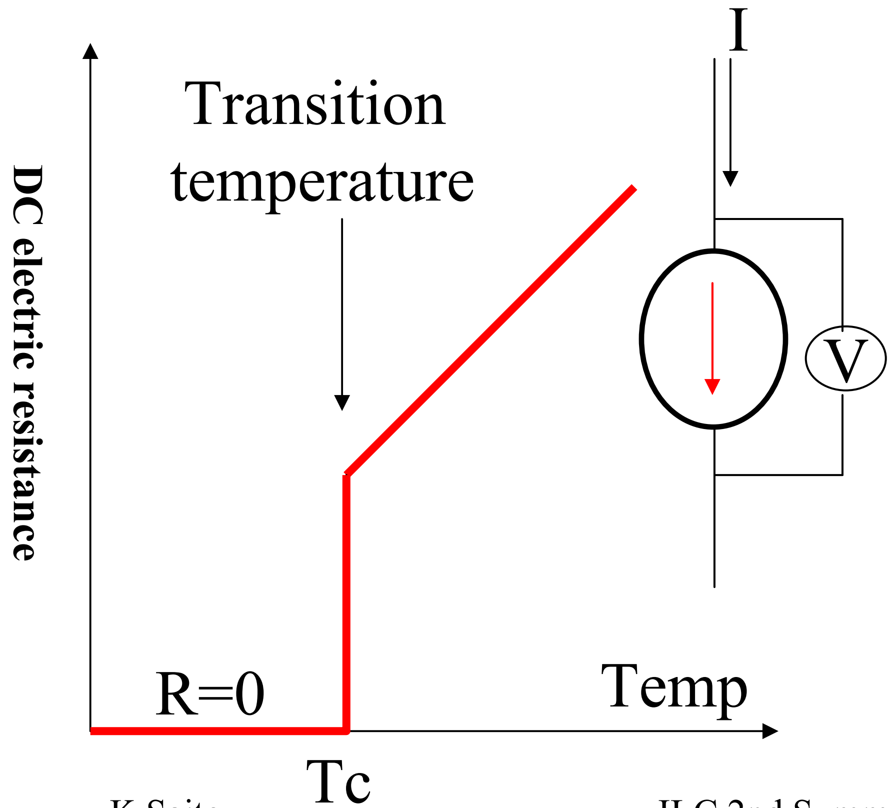

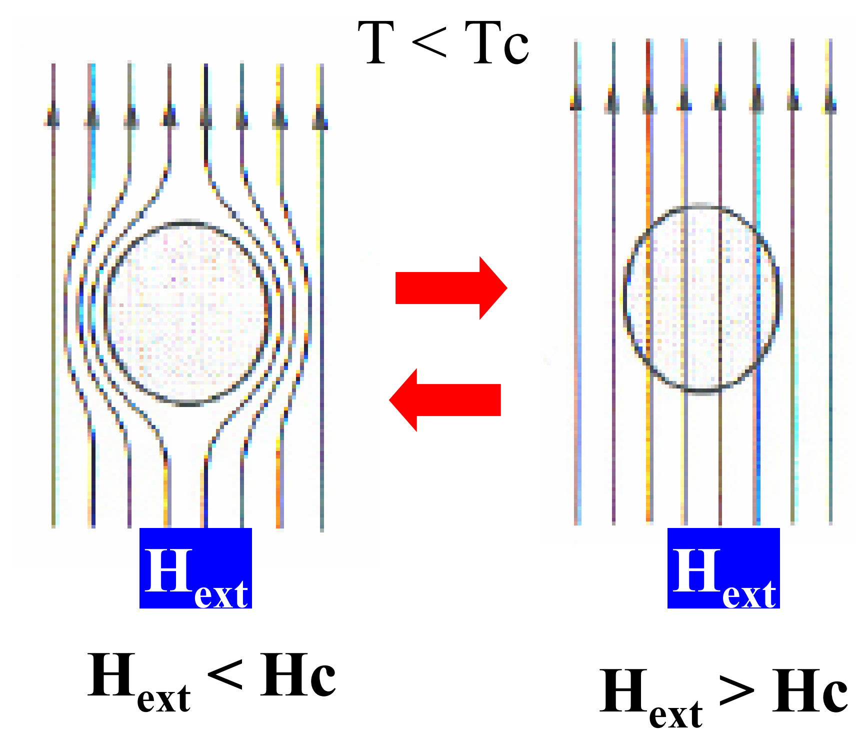

Microscopic Theory

Two electrons having opposite spin and momentum get an attractive interaction through lattice/electron interaction.

Attractive interaction through lattice

$$V = \frac{\left|V_{\mathbf{p}-\hbar\mathbf{k},\mathbf{p}}\right|^2}{\varepsilon(\mathbf{p}) - \varepsilon(\mathbf{p}-\hbar\mathbf{k}) - \hbar\omega(\mathbf{k})}$$

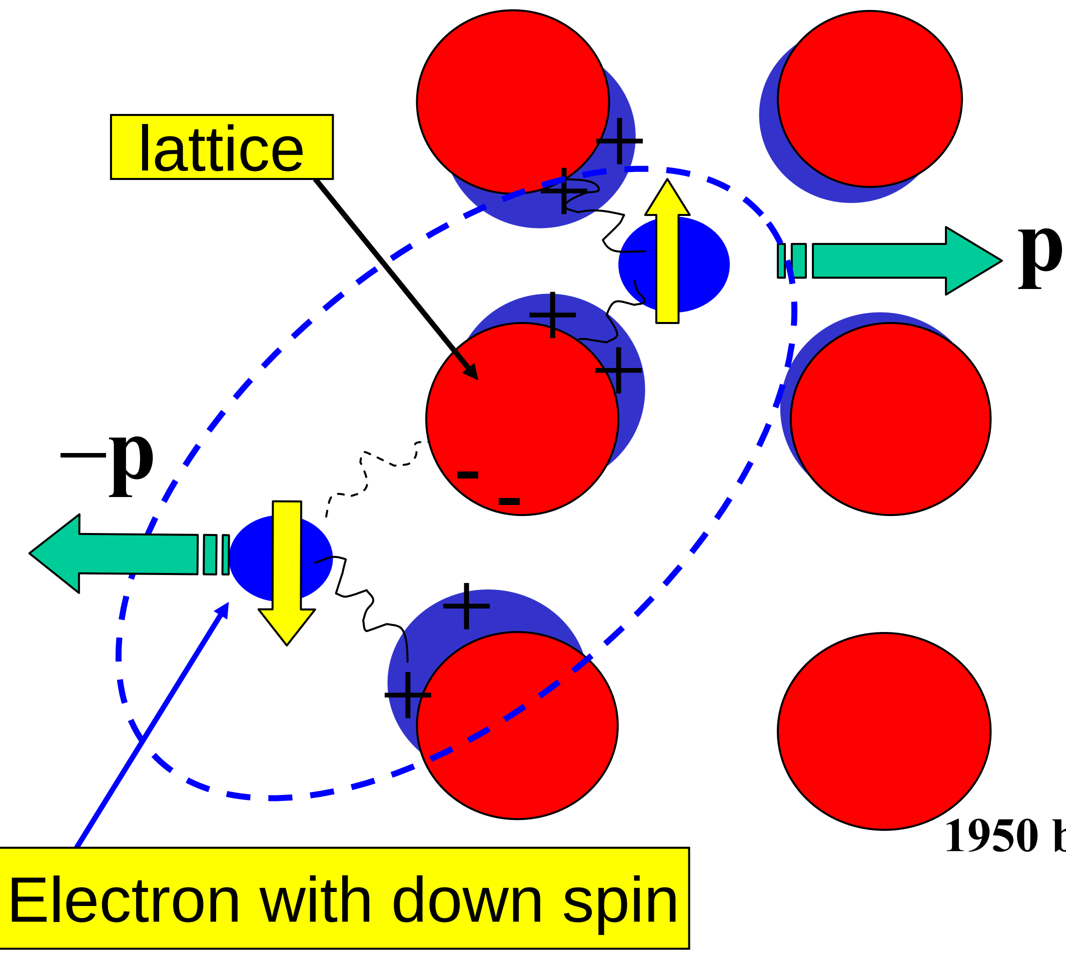

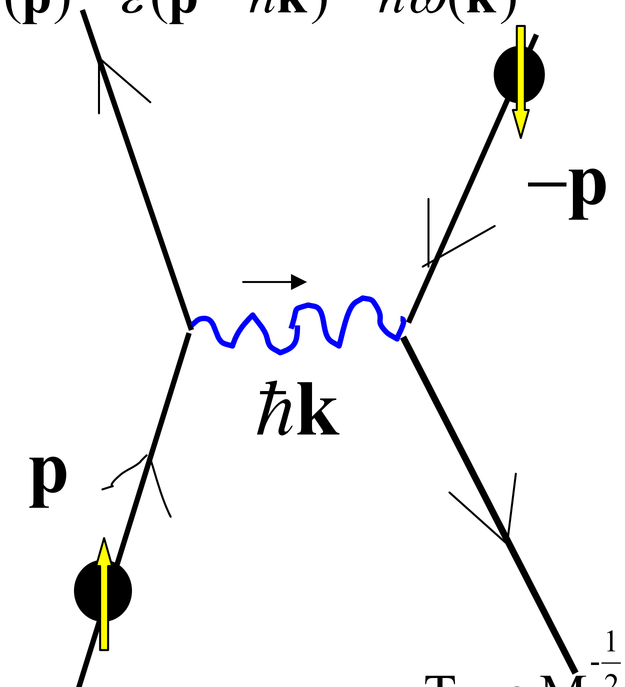

Isotope effect of Tc
1950 by Reynolds and Maxwell

$$T_C \propto M^{-\frac{1}{2}},$$

$$H_C \propto M^{-\frac{1}{2}}$$

BCS theory
1957 by Bardeen, Cooper, and Schrieffer

Two Types of superconductor

1937 by Schubnikov (experiment), 1957 Abrikosov (theory)

Type-I

$$\frac{\lambda}{\xi} \le \frac{1}{\sqrt{2}}$$

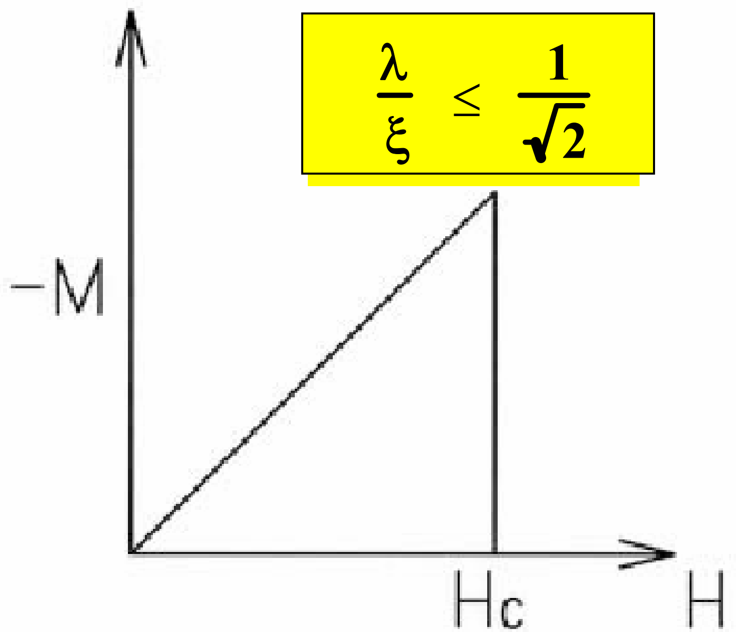

Type-II

$$\frac{\lambda}{\xi} > \frac{1}{\sqrt{2}}$$

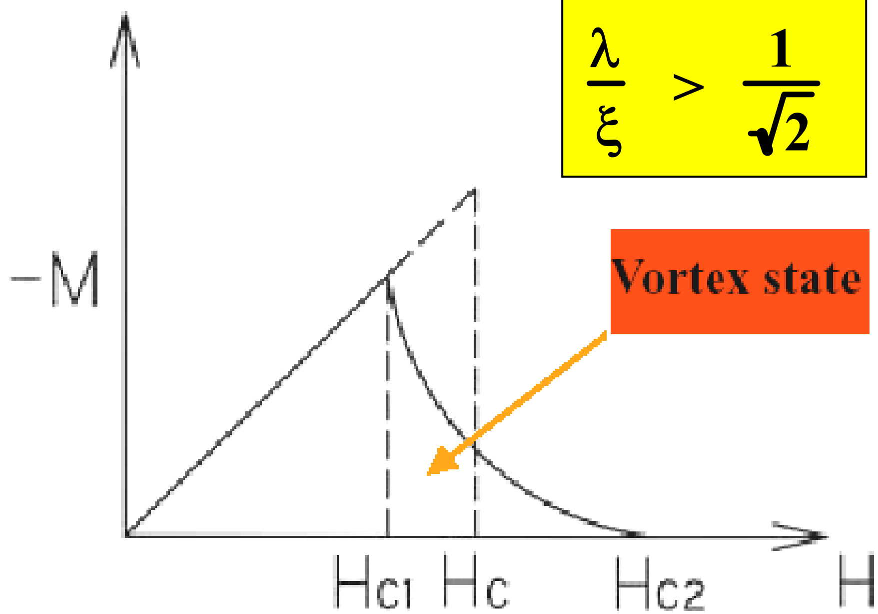

$$G_n - G_s = \frac{1}{2}\mu H_C^2 \equiv \int_0^{H_{c2}} M dH$$

Vortex state

Flux quantization, 1961 by Deaver and Fairbank

Observed by iron powder

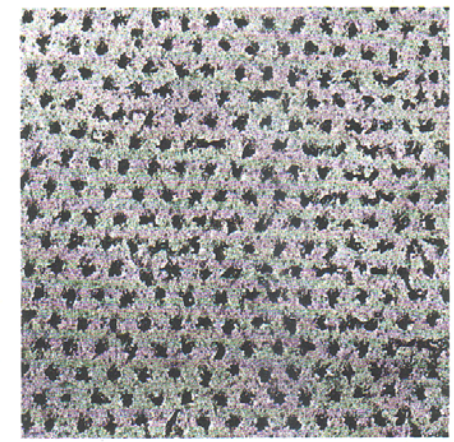

Figure 19 Triangular lattice of fluxoids through top surface of a superconducting cylinder. The points of exit of the flux lines are decorated with fine ferromagnetic particles. The electron microscope image is at a magnification of 8300, by U. Essmann and H. Träuble.

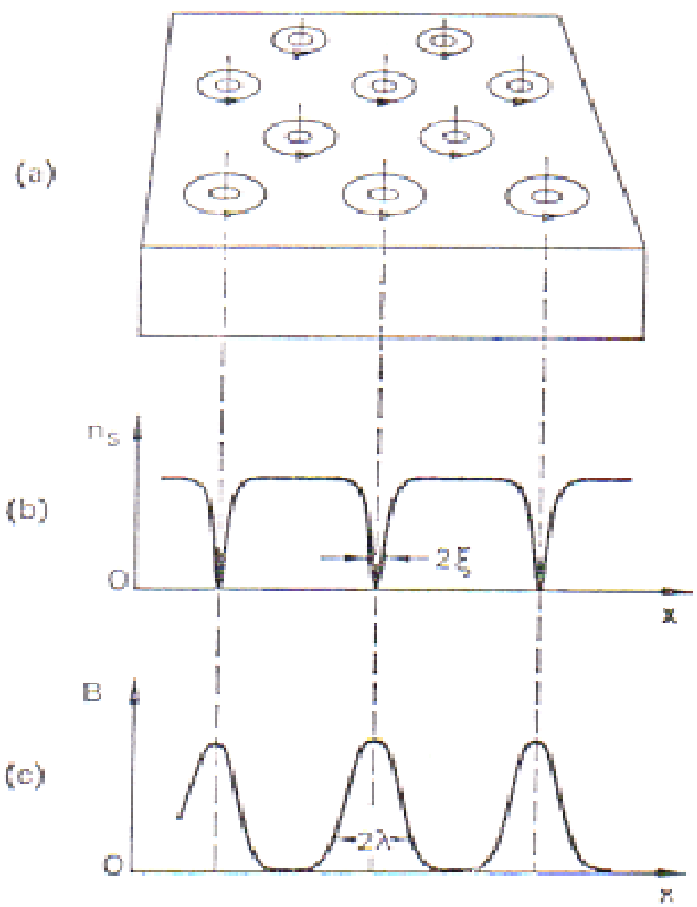

Vortex state

ξ : Coherence length
size of Cooper pair

λ_L : London penetration depth

Depth of penetration of the magnetic field

Note

Critical magnetic field measurement

$$V = V_A + V_B = -\frac{d}{dt}\Phi_A + \frac{d}{dt}\Phi_B$$

$$(\ -nS_0\mu\frac{d}{dt}B_{ext} + \frac{d}{dt}M\ ) + nS_0\mu\frac{d}{dt}B_{ext}$$

$$= \frac{d}{dt}M$$

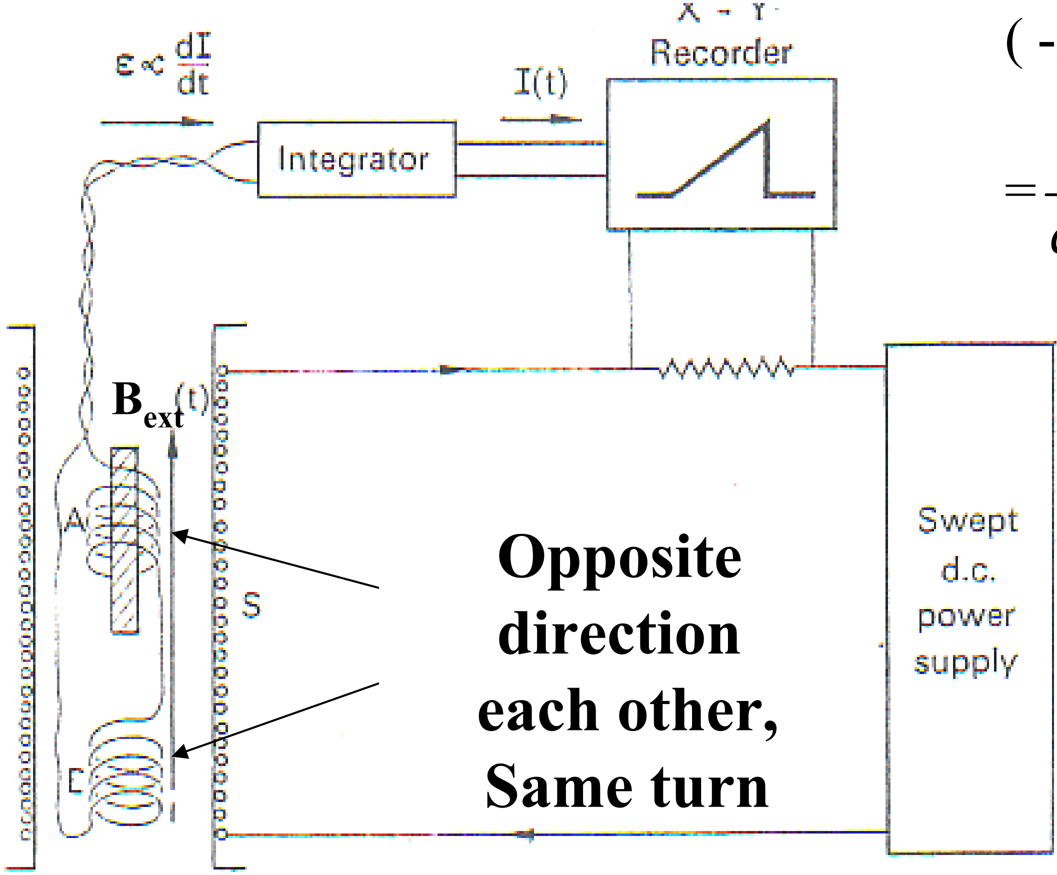

$$M = \int_0^t V dt$$

Example of demagnetization curve on Niobium
(NingXia, Large Grain RRR=340)

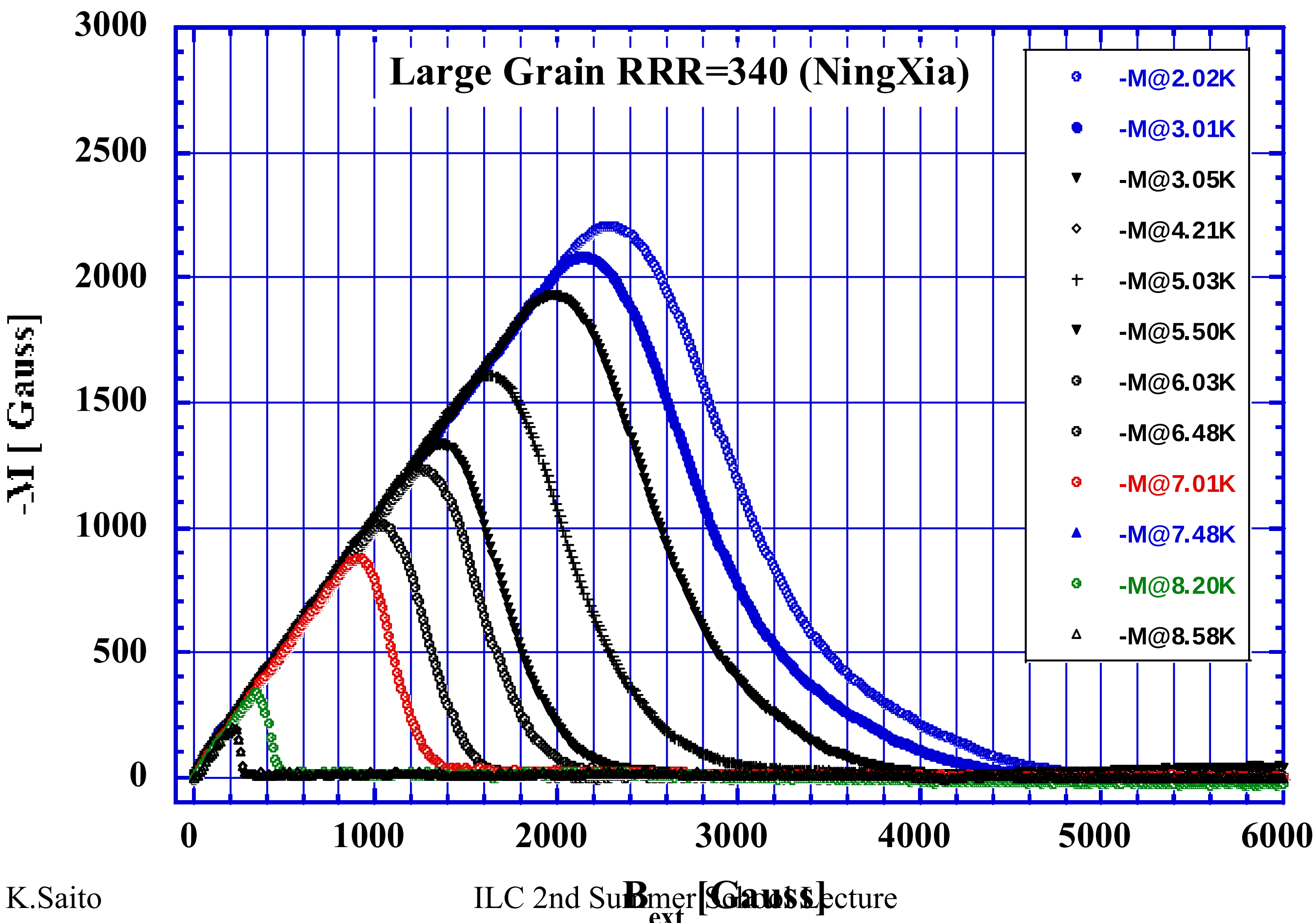

Abrikosov's Theory for Type-II

$$H_c = \frac{\kappa}{\lambda^2}\frac{\hbar c}{\sqrt{2}e^*} = \frac{\kappa}{\lambda^2}\frac{(hc/2e)}{2\pi\sqrt{2}} = \frac{\phi_0}{2\pi\sqrt{2}\lambda\xi}$$

$$H_{c2} = \sqrt{2}\frac{\lambda}{\xi}\frac{\phi_0}{2\pi\sqrt{2}\lambda\xi} = \frac{\phi_0}{2\pi\xi^2}$$

$$H_{c1} = \frac{\phi_o}{4\pi\lambda^2}\ln(\frac{\lambda}{\xi} + 0.08)$$

$$\phi_0 = hc/2e = 2.0678 \times 10^{-7} Gauss \cdot cm^2$$

$$= 2.0678 \times 10^{-15}\ T \cdot m^2$$

Perturbation theory T ~Tc

$$H_C(T) = H_C(0)\left[1-(T/T_C)^2\right]$$

$$\lambda(T) = \frac{\lambda(0)}{\sqrt{1-(T/T_C)^4}}$$

Expand for all T range (assumption)

$$\xi(T) = \xi(0)\cdot\sqrt{\frac{1+(T/T_C)^2}{1-(T/T_C)^2}} \qquad \kappa(T) = \frac{\kappa(0)}{1+(T/T_C)^2}$$

T-dependence of H_{C1}, H_C, H_{C2}

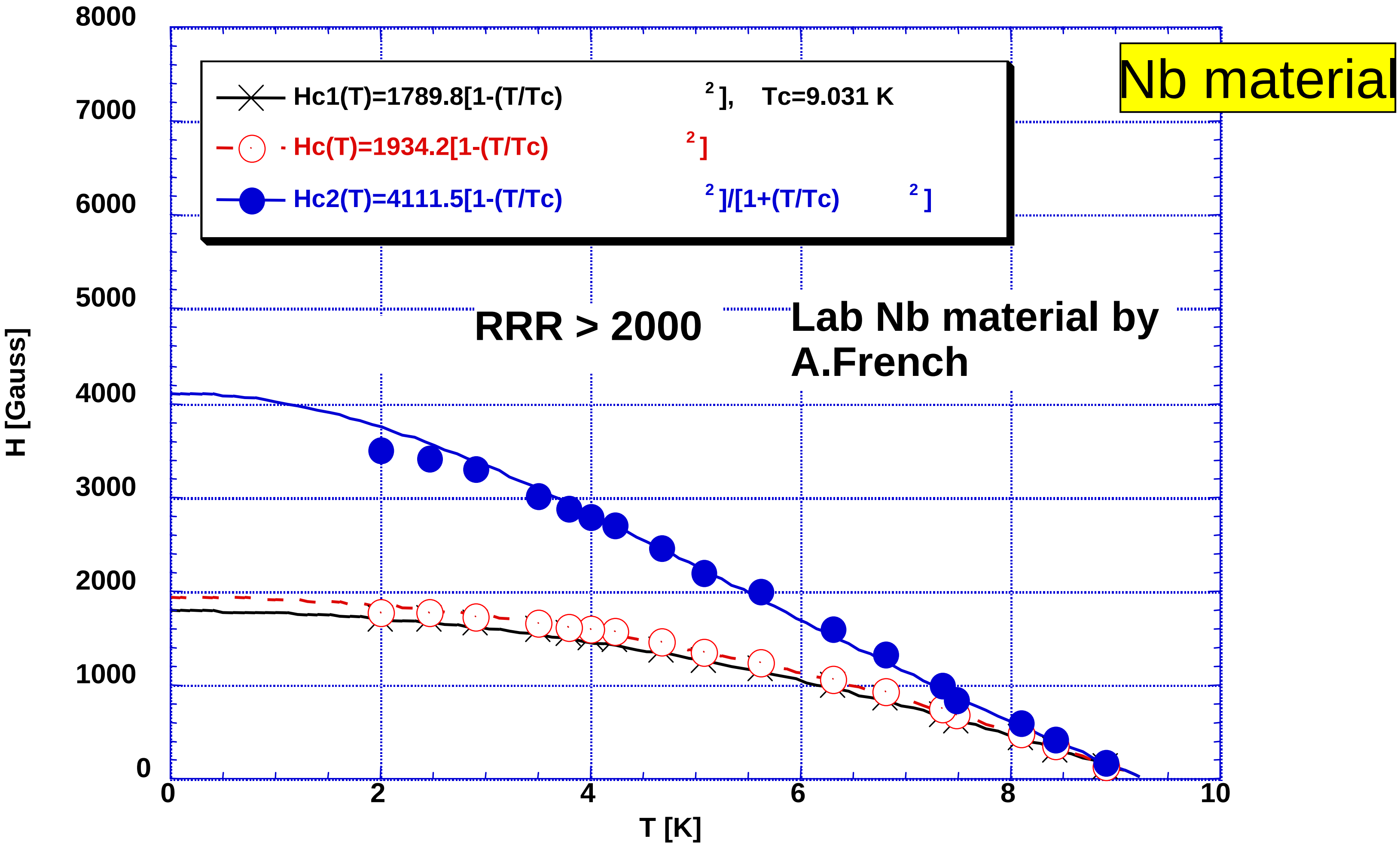

$$H_c(T) = H_c(0)\cdot\left[\,1-\left(\frac{T}{T_c}\right)^2\right]$$

T–dependence of λ and ξ

Lab material, RRR>2000

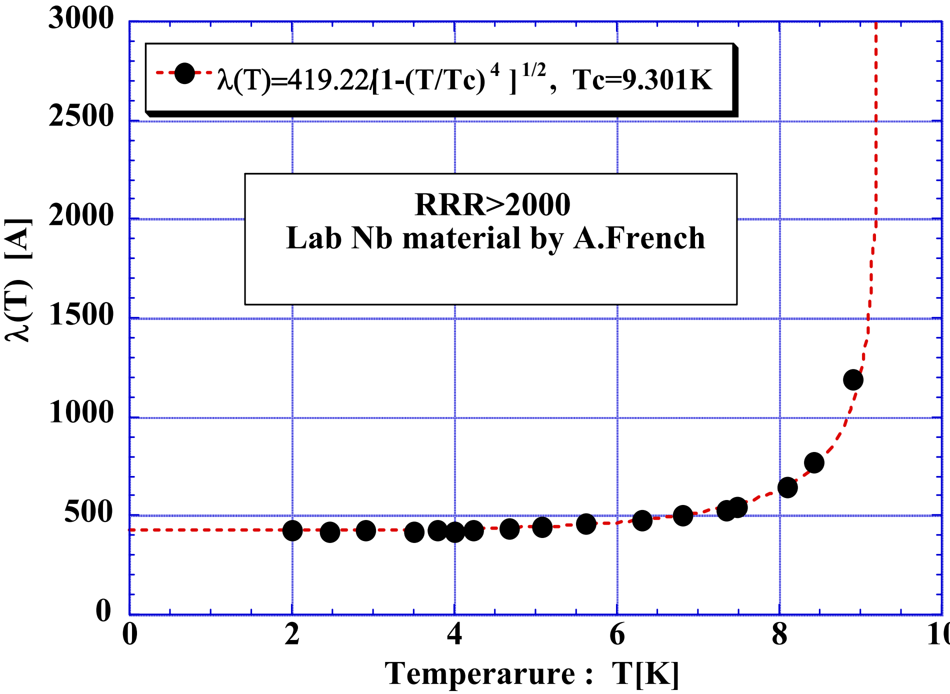

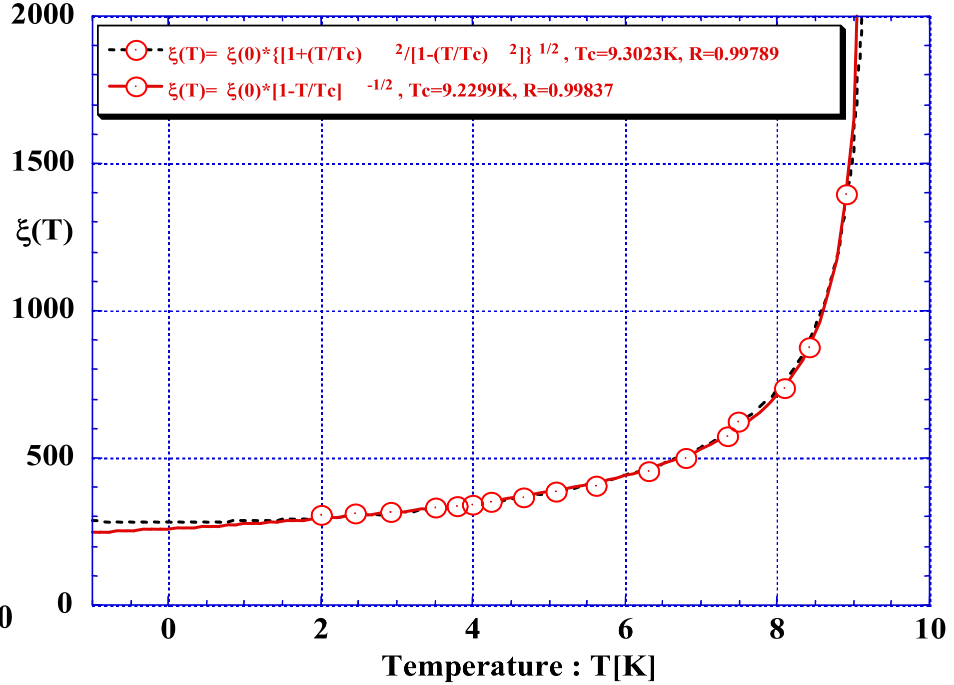

$$\lambda(T)=\frac{\lambda(0)}{\sqrt{1-(T/T_C)^4}},\qquad \xi(T)=\xi(0)\cdot\sqrt{\frac{1+(T/T_C)^2}{1-(T/T_C)^2}}$$

T-dependence of κ with Lab material

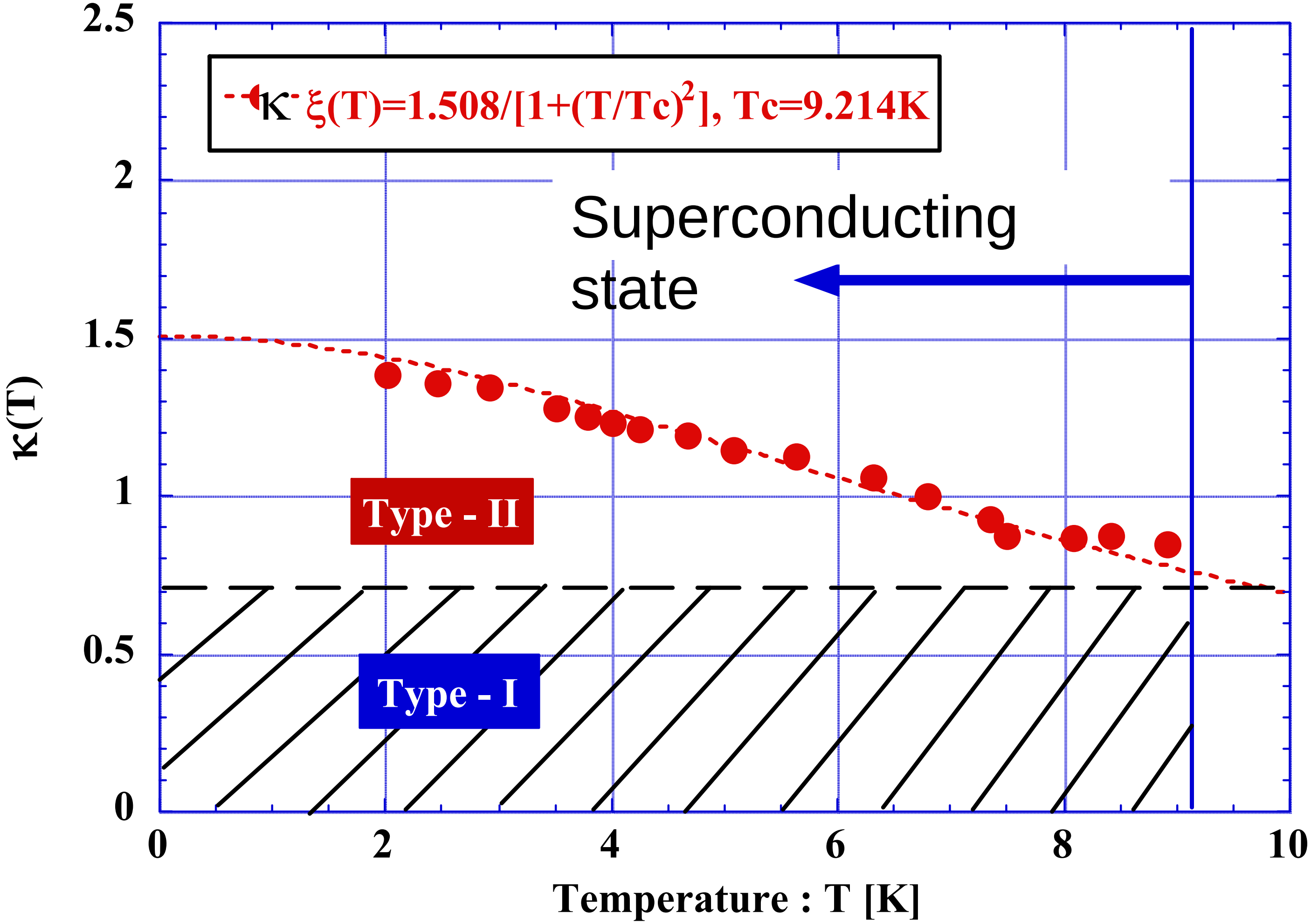

$$\kappa(T) = \frac{\kappa(0)}{1+(T/T_C)^2}$$

Attempt for RF Field limitation model

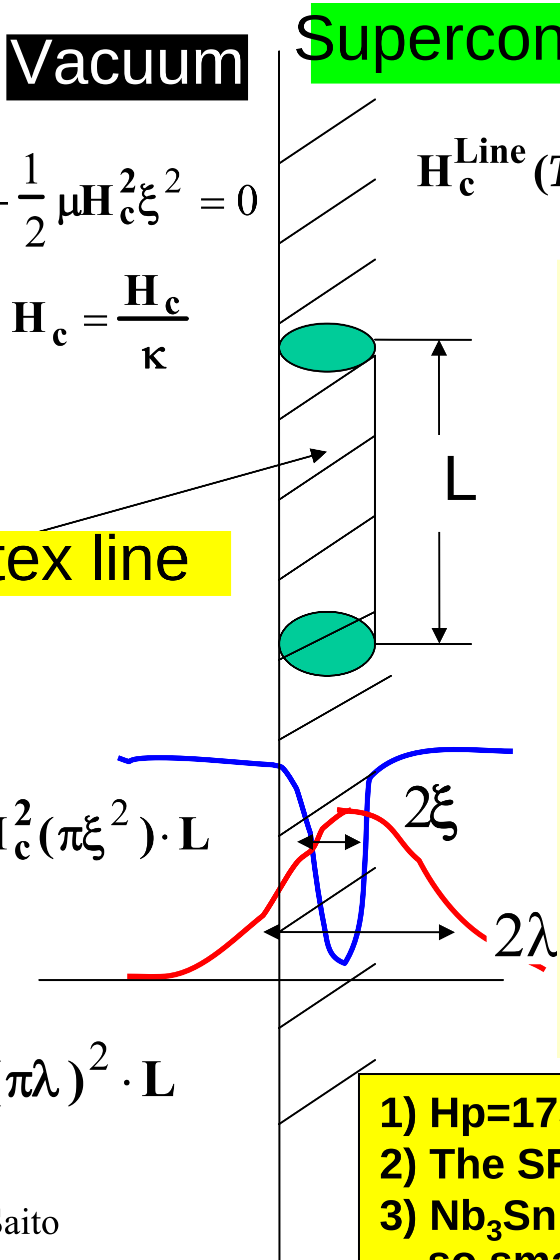

$$\frac{1}{2}\mu H^2\lambda^2 - \frac{1}{2}\mu H_c^2\xi^2 = 0$$

$$H_c^{Line} = \frac{\xi}{\lambda} H_c = \frac{H_c}{\kappa}$$

$$-\frac{1}{2}\mu H_c^2(\pi\xi^2)\cdot L$$

$$\frac{1}{2}\mu H^2(\pi\lambda)^2\cdot L$$

Effective field strength

$$H_c^{Line}(T) = \frac{\xi(T)}{\lambda(T)}\cdot\sqrt{2}H_c(T) = \frac{\sqrt{2}H_c(T)}{\kappa(T)} = \sqrt{2}\frac{H_c(0)}{\kappa(0)}\cdot\left[1-\left(\frac{T}{T_c}\right)^4\right]$$

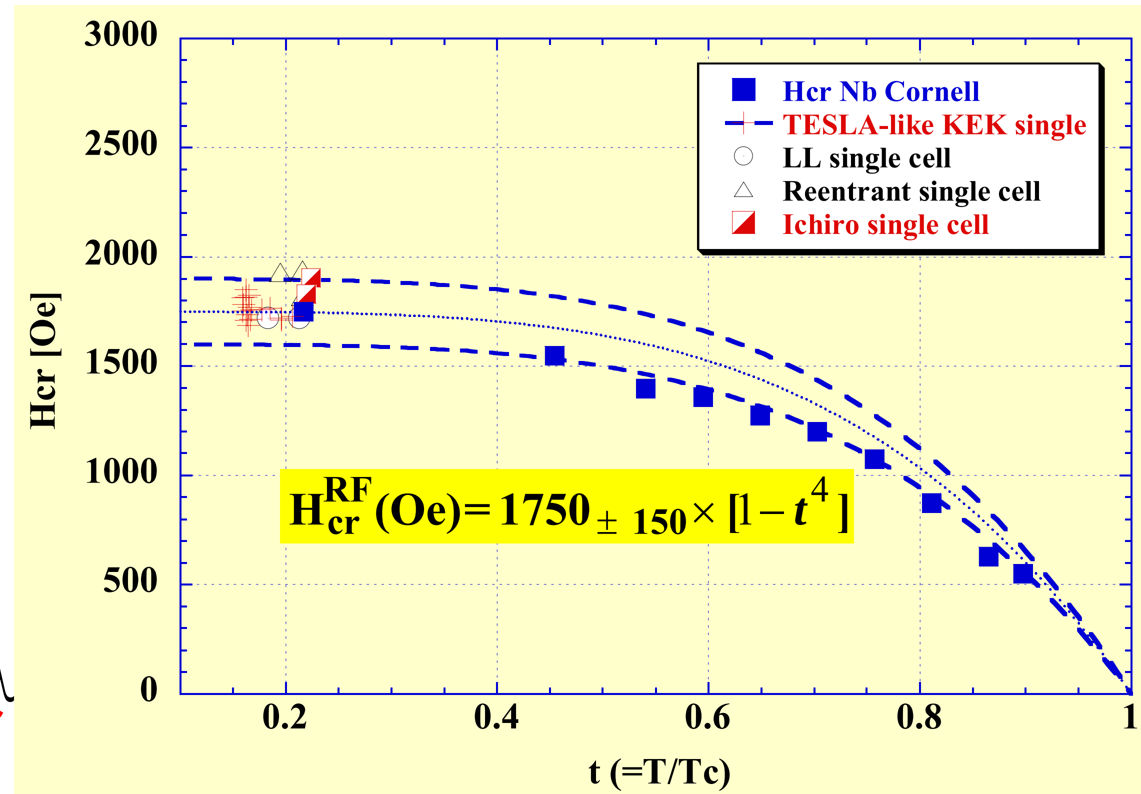

1) Hp=1750±100 Oe with Nb cavity → Eacc ~ 40MV/m
2) The SRF technology is meeting the theoretical limit.
3) Nb_3Sn cavity has a very larger k(0), therefore the critical field i so small.

K.Saito

Checking of the model for other materials

The model looks good for the type-II material cavity !

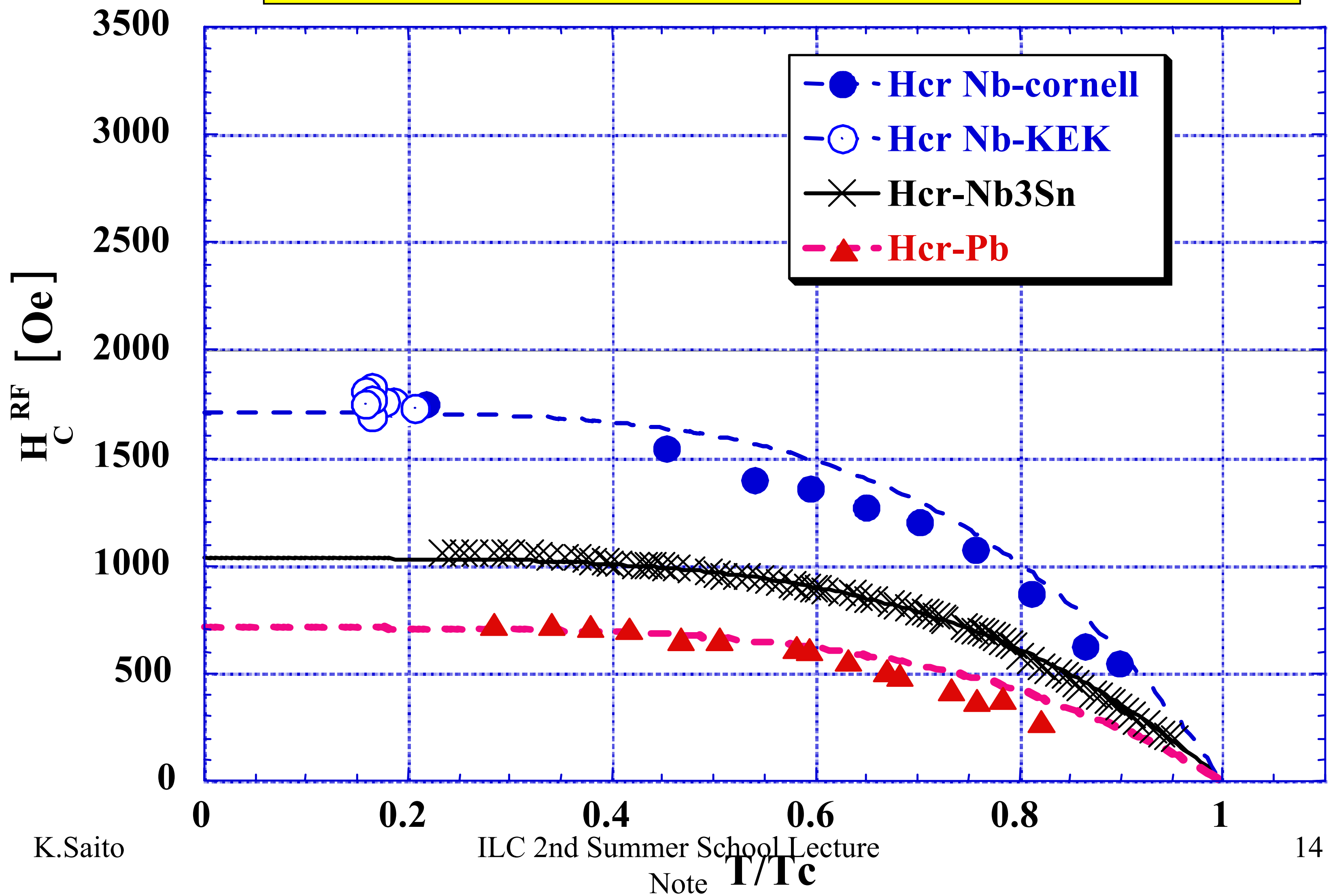

What material is best ?

Material point of view:

- Smaller heat loading for refrigerator → Higher T_C
- High gradient

  $H_{RF} > H_C^{RF}$, then normal conducting

$$H_c^{RF} = \sqrt{2} \cdot \frac{H_c}{\kappa}, \ \kappa : \text{G - L parameter}$$

The material with higher Hc and smaller κ-value

If Hc is high enough, Type-I material is better because of the smaller κ-value.

- Good formability

Materials	Tc [K]	Hc, Hc1 [Gauss]	Type	Fabrication
Pb	7.2	803	I	Electroplating
Nb	9.25	1900, 1700	II	Deep drawing, film
Nb_3Sn	18.2	5350, 300	II	Film
MgB_2	39	4290, 300	II	Film

Niobium has higher Tc, Hc and enough formability.

Now, niobium is widely used for RF sc cavity production.

Note

1.2 Surface Impedance of SRF Cavity

Normal Conducting Case

Maxwell Equations for conductor (ε, μ, ρ = 0)

$$\nabla \cdot \vec{B} = 0,\ \nabla \times \vec{E} + \mu \frac{\partial \vec{H}}{\partial t} = 0$$

$$\nabla \cdot \vec{D} = 0,\ \nabla \times \vec{H} - \varepsilon \frac{\partial \vec{E}}{\partial t} - \sigma \vec{E} = 0$$

$$\vec{J} = \sigma \vec{E} \quad \text{(Ohm's Law)}$$

$$\vec{E}(\vec{x},t) = \vec{E}_{\ell}(\vec{x},t) + \vec{E}_{t}(\vec{x},t),$$

$$\vec{H}(\vec{x},t) = \vec{H}_{\ell}(\vec{x},t) + \vec{H}_{t}(\vec{x},t)$$

From Maxwell Equation,

$$\frac{\partial \vec{H}_{\ell}}{\partial t} = 0,\quad \vec{E}_{\ell}(x,t) = \vec{E}_{\ell}(0) \cdot e^{-\frac{\sigma t}{\varepsilon}}$$

For the transvers,

$$\text{Plane wave}: \vec{E}_{t}(\vec{x},t) = \vec{E}_{t}(0) \cdot \exp(i\vec{k} \cdot \vec{x} - \omega t)$$

$$\vec{H}_{t}(x,t) = \frac{1}{\mu\omega}[\vec{k} \times \vec{E}_{t}(\vec{x},t)],$$

$$[\ k^2 - (\varepsilon\mu\omega^2 + i\mu\omega\sigma)\ ]\begin{Bmatrix} \vec{E}_{t}(\vec{x},t) \\ \vec{H}_{t}(\vec{x},t) \end{Bmatrix} = 0$$

Normal Conducting Case, continued

$$k^2 - (\varepsilon\mu\omega^2 + i\mu\omega\sigma) = 0,$$

$$k = \alpha + i\beta,$$

$$\begin{Bmatrix} \alpha \\ \beta \end{Bmatrix} = \sqrt{\varepsilon\mu} \cdot \omega \left[\frac{\sqrt{1 + \left(\frac{\sigma}{\omega\varepsilon} \right)^2} \pm 1}{2} \right]^{\frac{1}{2}}$$

For good electric conductor

$$\frac{\sigma}{\omega\varepsilon} \gg 1$$

$$k \approx (1+i)\sqrt{\frac{\mu\sigma\omega}{2}}$$

$$\delta = \frac{1}{\beta} = \sqrt{\frac{2}{\mu\sigma\omega}}$$: Skin depth

Surface Impedance for normal conducting case

$$Z \equiv R_s + iX_s \equiv \left. \frac{E_t}{H_t} \right|_{Surface} = \frac{\mu\omega}{k}$$

$$\mathbf{R_s} = \sqrt{\frac{\mu\omega}{2\sigma}} = \frac{1}{\sigma}\sqrt{\frac{\mu\sigma\omega}{2}} = \frac{1}{\sigma\delta}$$

$$P_{loss} = \frac{1}{2} R_S \cdot \int_S H_S^2 \, dS$$

Surface resistance in superconductor (Two Fluid model)

General equation: $m\dfrac{\partial \mathbf{v}}{\partial t} = q(\mathbf{E} + \mathbf{v}\times\mathbf{B}) - m\nu\mathbf{v}$

Two-fluid model by Gorter and Casimir in 1933

$\mathbf{J} = \mathbf{J}_s + \mathbf{J}_\mathbf{n}$, $\mathbf{J}_s = n_s q_s \mathbf{v}$, $\mathbf{J}_\mathbf{n} = n_n q_n \mathbf{v}$

Maxwell equation: neglecting the Lorentz term, $\mathbf{v}\times\mathbf{B} \ll 1$

$$m_s\frac{\partial \mathbf{v}_s}{\partial t} = q_s\mathbf{E}\ ,\ \ m_s = 2m_e\ ,\ q_s = -2e$$

$$m_e\frac{\partial \mathbf{v}_n}{\partial t} = q_n\mathbf{E} - m_e\nu\mathbf{v}_n\ ,\quad q_n = -e$$

$$\mathbf{E} = \mathbf{E}_0 e^{i\omega t} \Rightarrow \mathbf{J}_s = \frac{n_s q_s^2}{i\omega m_s}\mathbf{E}\ ,\ \ \mathbf{J}_n = \frac{n_n q_n^2}{i(\omega - i\nu)m_e}\mathbf{E}$$

$$\mathbf{J} = \left(\frac{n_s q_s^2}{i\omega m_s} + \frac{n_n e^2}{i(\omega - i\nu)m_e}\right)\mathbf{E}$$

$$\nu \gg \omega \Rightarrow \mathbf{J} = \left(\frac{n_n e^2}{\nu m_e} - i\frac{n_s q_s^2}{\omega m_s}\right)\mathbf{E} = \sigma E\ ;\ \ \sigma = \sigma_\mathrm{n} - i\sigma_s \ \Rightarrow \mathrm{R}_s = \sqrt{\frac{\mu\omega}{2\sigma}}$$

Surface resistance in superconductor

$$\sigma_n = \frac{n_n \cdot e^2 \cdot l}{m \cdot v_F} = \frac{e^2 \cdot l}{m \cdot v_F} \cdot n_s(T=0) \cdot e^{-\frac{\Delta}{k_B \cdot T}}$$

$$R_S = \frac{1}{2} \cdot (2\pi)^2 \cdot \mu^2 \cdot f^2 \cdot \lambda_L^3 \cdot l \cdot \frac{n_s(0)}{m v_F} \cdot e^{-\frac{\Delta}{k_B T}}$$

$$= A \cdot f^2 \cdot e^{-\frac{\Delta}{k_B T}}$$

BCS Theory

$$R_S^{BCS}(T,\omega) = A(\lambda, \xi, \ell, T_c) \cdot \exp\left(-\frac{\Delta}{k_B T}\right)$$

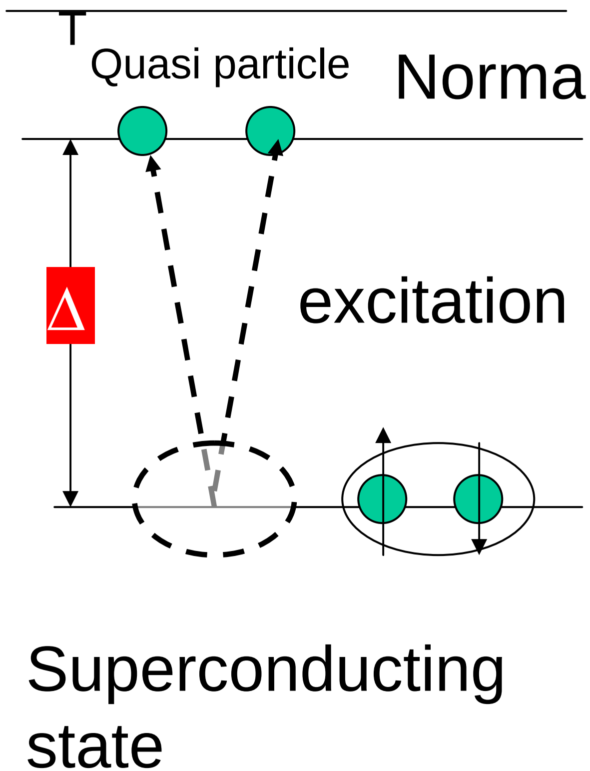

Example of the Surface Resistance of SRF niobium cavity

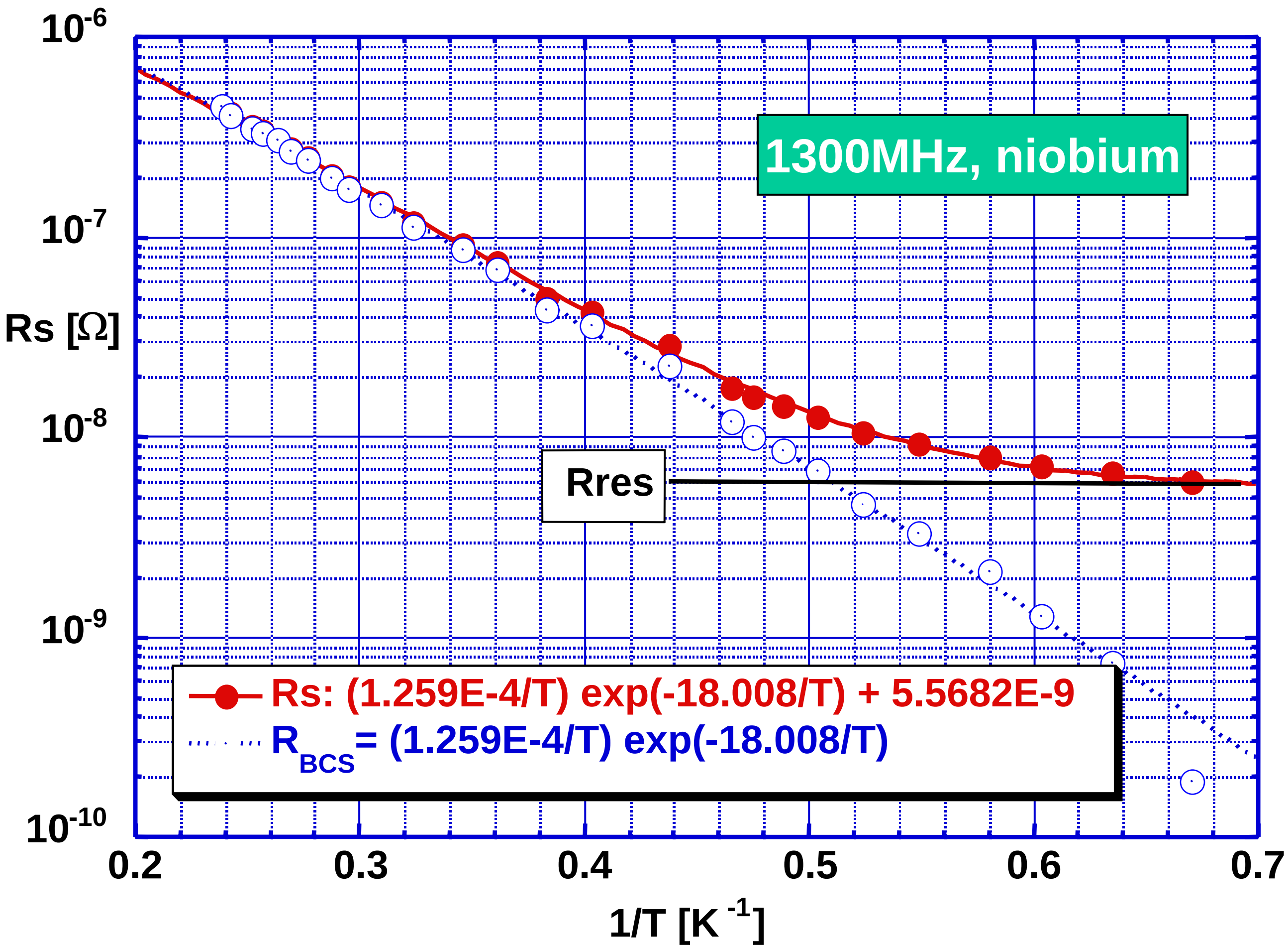

$$\frac{\Delta}{k_B} = 18.008 \Rightarrow \frac{2\Delta}{k_B T_c} = \frac{2 \cdot 18.008}{9.25} = 3.89$$

$$\frac{2\Delta}{k_B T_c} = 3.52 \ \textbf{(BCS theory)}$$

Residual surface resistance depends on residual magnetic field, surface contamination, and so on.

R_{BCS} ~ 8nΩ,
Well fits to the theoretical prediction.

$$R_S(T) = R_S^{BCS}(T) + R_{res}$$

BCS Surface Resistance at 4.25 and 2K

Used J. Halbritter's Code

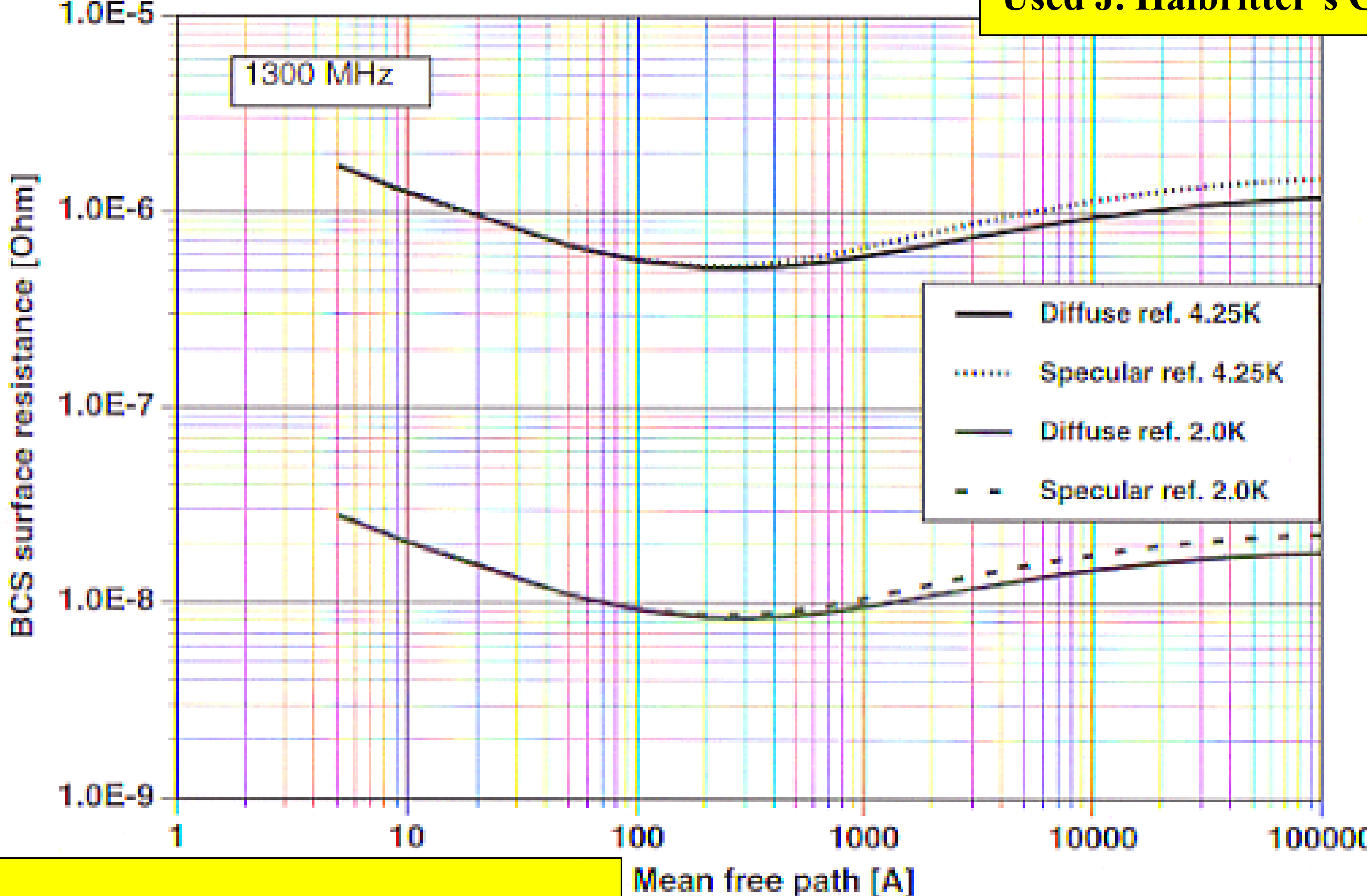

R_{BCS} ~ 8nΩ @ 2K, 1300MHz

$\ell \propto RRR$

Why minimum around $\ell \approx 300$ Å

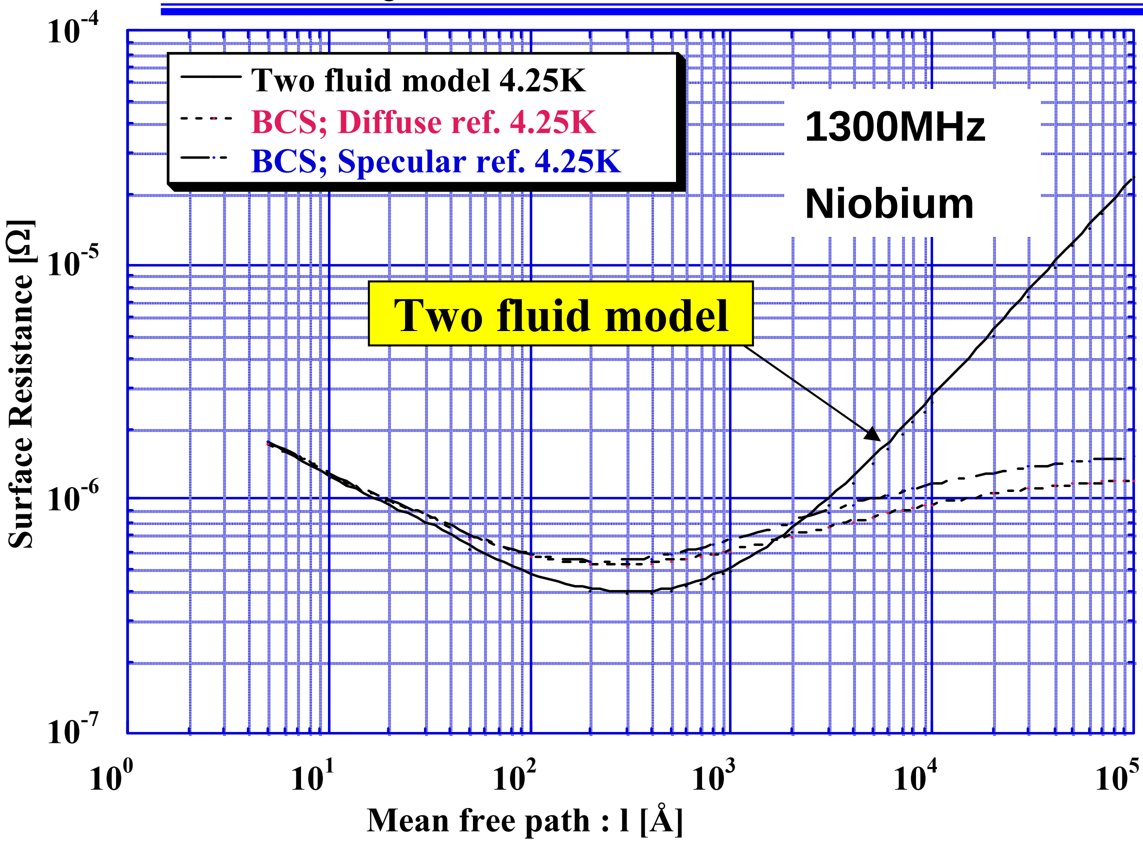

Strange behavior on mean free path(ℓ)

R_s minimum @ ℓ~300 Å

London penetration depth λ : $\lambda(\ell) = \lambda_{\ell=\infty} \cdot \sqrt{1 + \frac{\xi_o}{\ell}}$,

$R_S(TF\ model) \propto (1 + \frac{\xi_o}{\ell})^{\frac{3}{2}} \cdot \ell$, $\ell << 1,\ R_S \to \frac{\xi_o^{\frac{3}{2}}}{\sqrt{\ell}}$, $\ell >> 1,\ R_s \to \ell$

Surface heating in SRF cavity

What happens when microwave is input a cavity?

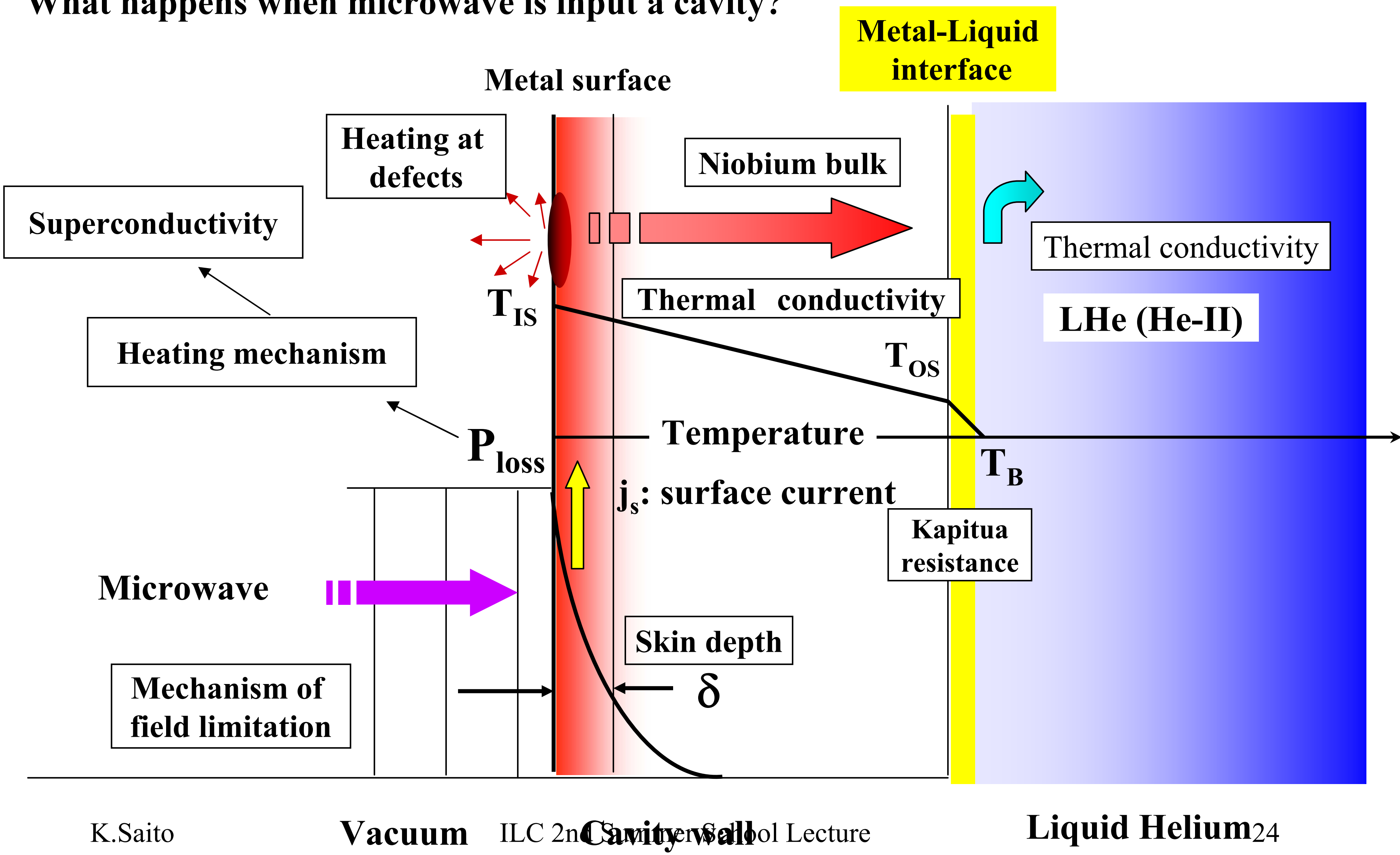

Thermal conductivity

Normal conductor : $\kappa_{en} = \frac{1}{W_{en}} = \left[\frac{\rho}{L_O T} + aT^2 \right]^{-1}$

$\rho = \frac{\rho_{300K}}{RRR}$ e-impurities scatt.

e-lattices scatt.

Wiedemann-Franz low:

$\kappa_e = \frac{\pi^2 n k_B^2 \tau}{3m} \cdot T, \quad \frac{\kappa_e}{\sigma} = \frac{\pi^2}{3} \left(\frac{k_B}{e} \right)^2 \cdot T = L_O T$

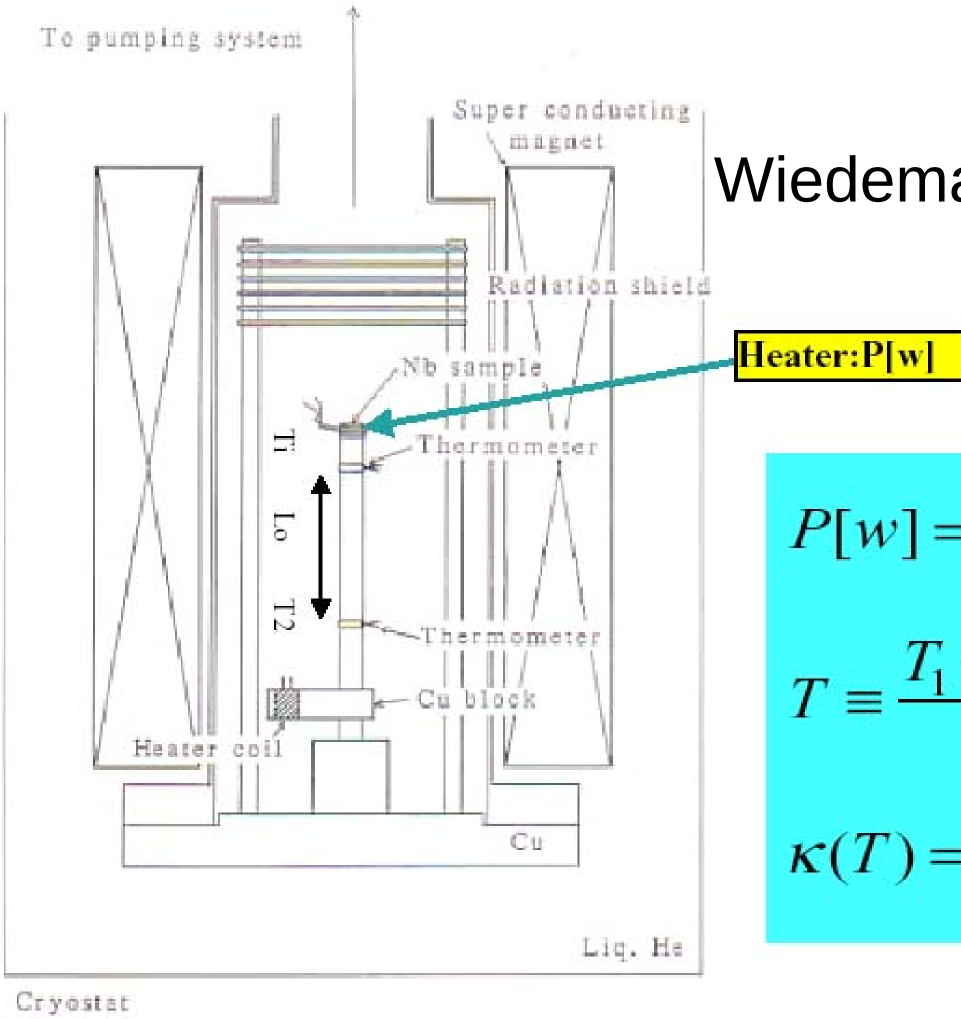

$$P[w] = S(m^2) \cdot \kappa(T) \cdot \frac{T_1(K) - T_2(K)}{L_O(m)}$$

$$T \equiv \frac{T_1 + T_2}{2}, \; S\text{: area of cross-section}$$

$$\kappa(T) = \frac{P}{S} \cdot \frac{L_O}{T_1 - T_2} \qquad \left[\frac{w}{m \cdot K}\right]$$

Thermal conductivity of Nb material at low temperature

Boltzmann statistics：Existing probability at energy Δ, and Temp. T

$$\exp\left(-\frac{\Delta}{k_B \cdot T}\right)$$

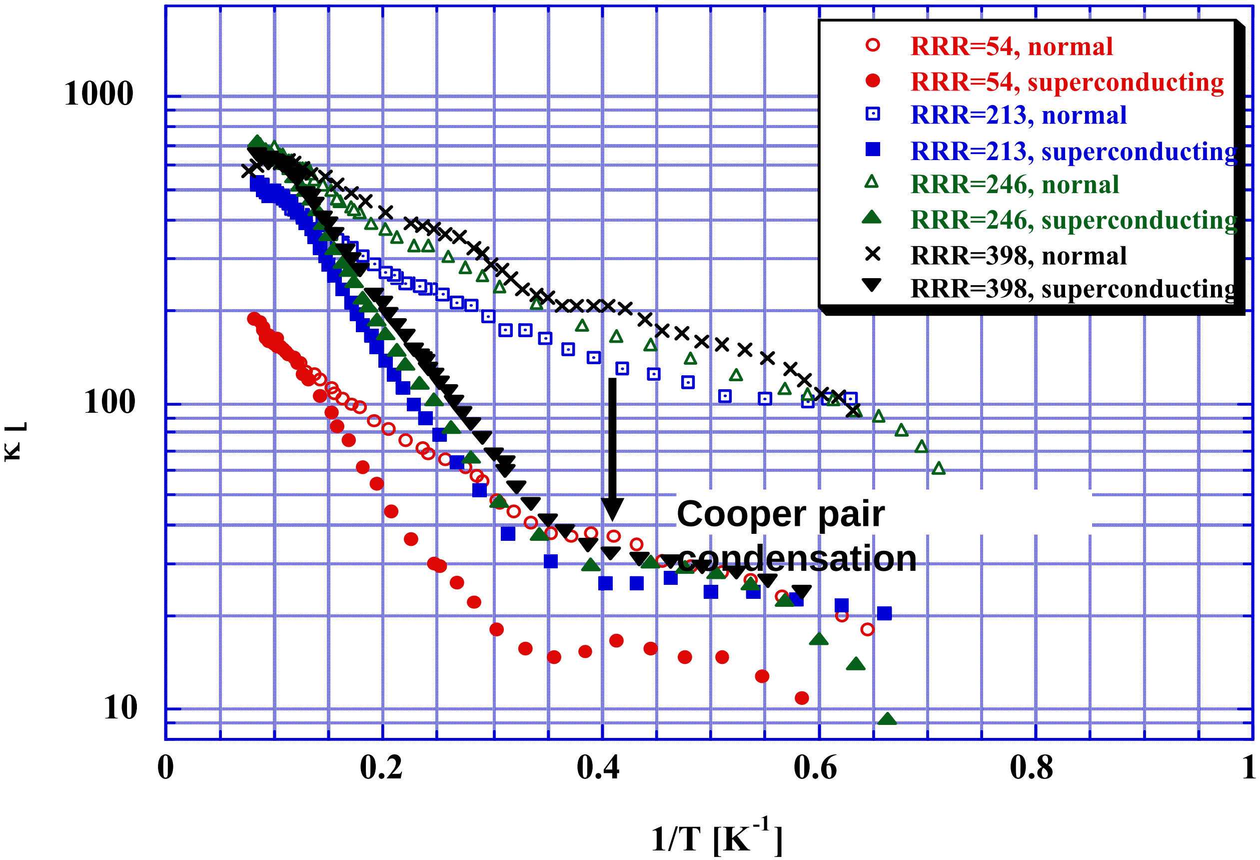

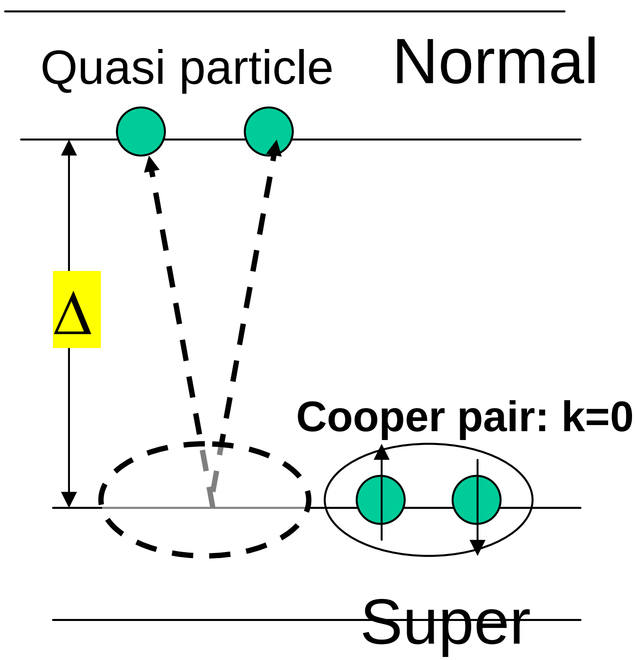

Thermal conductivity comparison with NC and SC

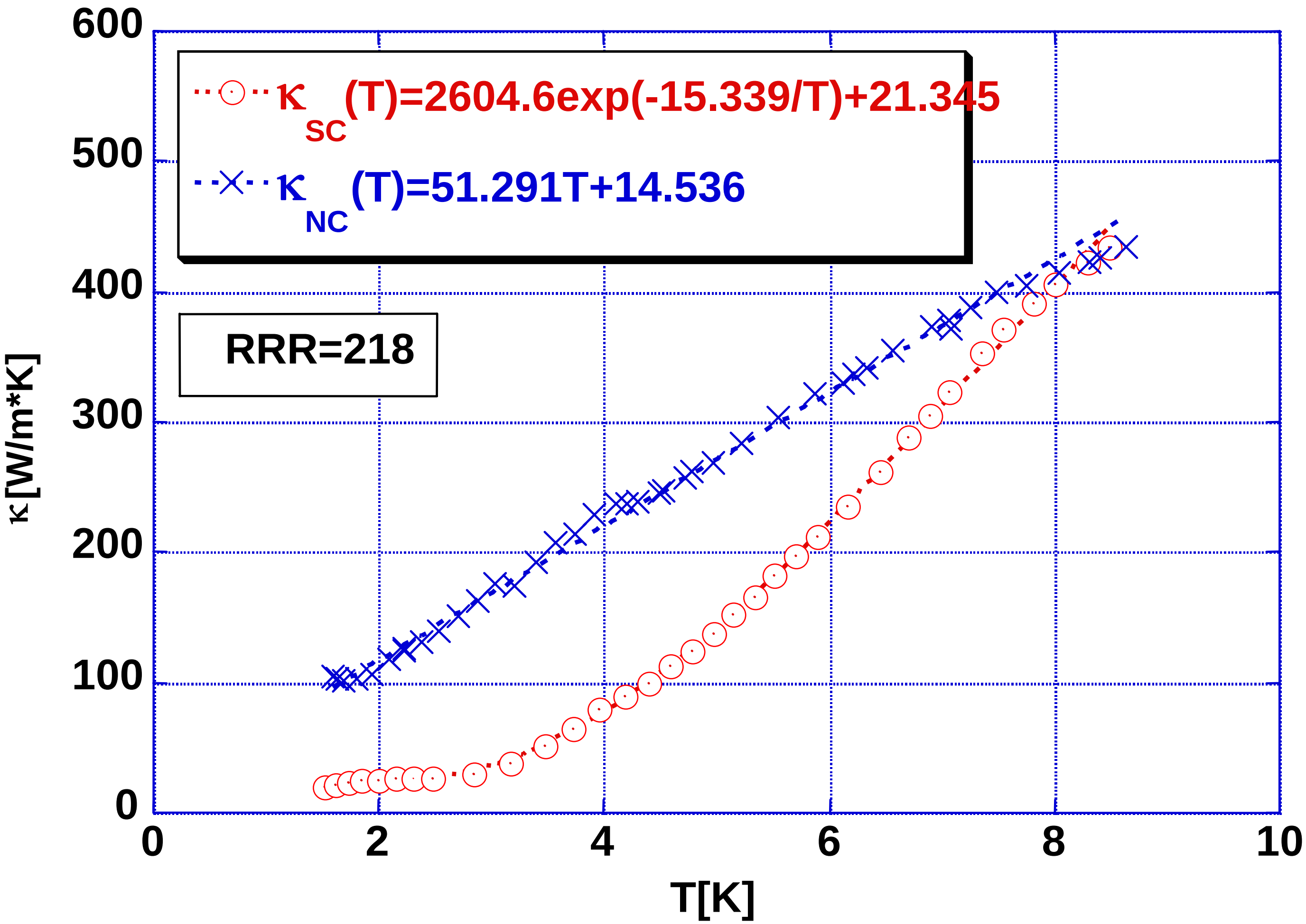

$$\frac{\Delta}{k_B} = 15.339$$

$$\Downarrow$$

$$\frac{2\Delta}{k_B T_c} = \frac{2 \times 15.339}{k_B\, 9.25}$$

$$2\Delta = 3.317 k_B T_c$$

BCS theory

$$2\Delta = 3.52 k_B T_c$$

Calculation of thermal conductivity based on Quantum mechanics

$$\kappa_s(T) = R(y)\cdot\left[\frac{\rho_{295K}}{L\cdot RRR\cdot T} + a\cdot T^2\right]^{-1} + \left[\frac{1}{D\cdot \exp(y)\cdot T^2} + \frac{1}{BlT^3}\right]^{-1}$$

e - impurities scatt. **e - phonons scatt.** **lattice - phonnons scatt.** **lattice - grain boundaries scatt.**

$L = 2.05E-8,\ RRR = 200,\ \rho_{295K} = 14.5E-8\ \Omega m,\ a = 7.52E-7$

$-y = \alpha\cdot\frac{T_c}{T},\ \alpha = 1.53,\ T_c = 9.25K,\ T \le 0.6\cdot T_c$

$D = 4.27E-3,\ B = 4.34E3,\ l = 50\mu m$

$$R(y) = \frac{\kappa_{es}}{\kappa_{en}} = \frac{2F_1(-y) + 2y\ln(1+e^{-y}) + \dfrac{y^2}{(1+e^y)}}{2F_1(0)},$$

$$F_n(-y) = \int_0^\infty \frac{z^n}{1+e^{z+y}}dz$$

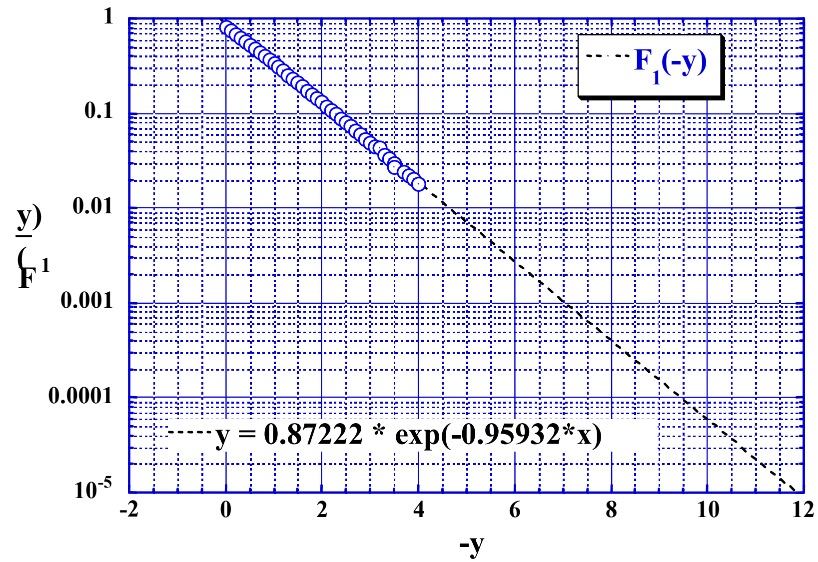

Calculated $\kappa_{sc}(T)$

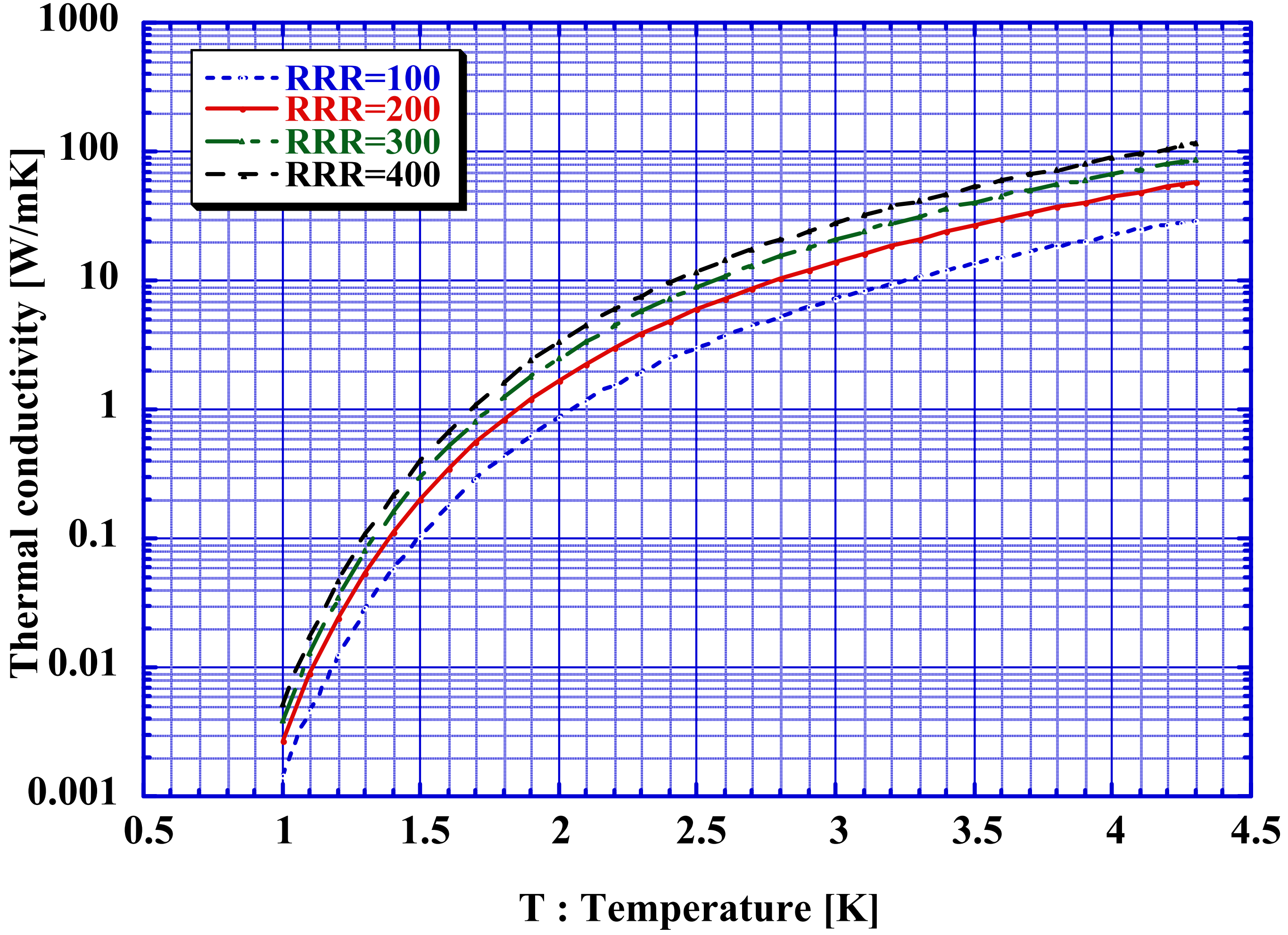

Thermal conductivity of niobium in superconductivity @ 2K is 1/15 that of stainless at R.T. (15W/(m•K)) and 1/6800 of pure cooper at 4.2K

Linear relationship between κ_{sc} (2K, 4.25K) and RRR

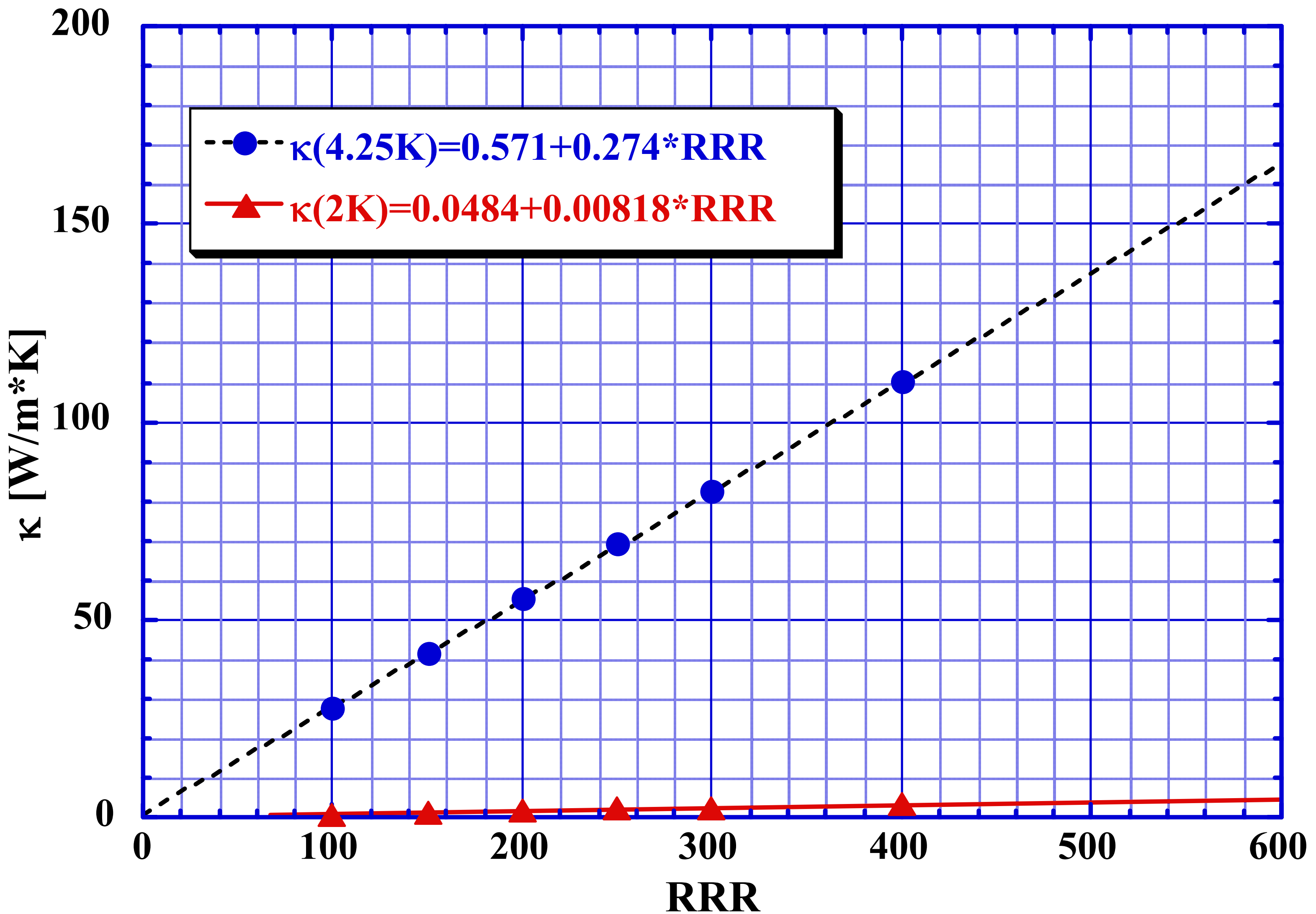

Effect of Various Scattering Mechanisms on Electric Resistivity

High purity + Homogeneity

High RRR material

Vacuum annealing

Nb

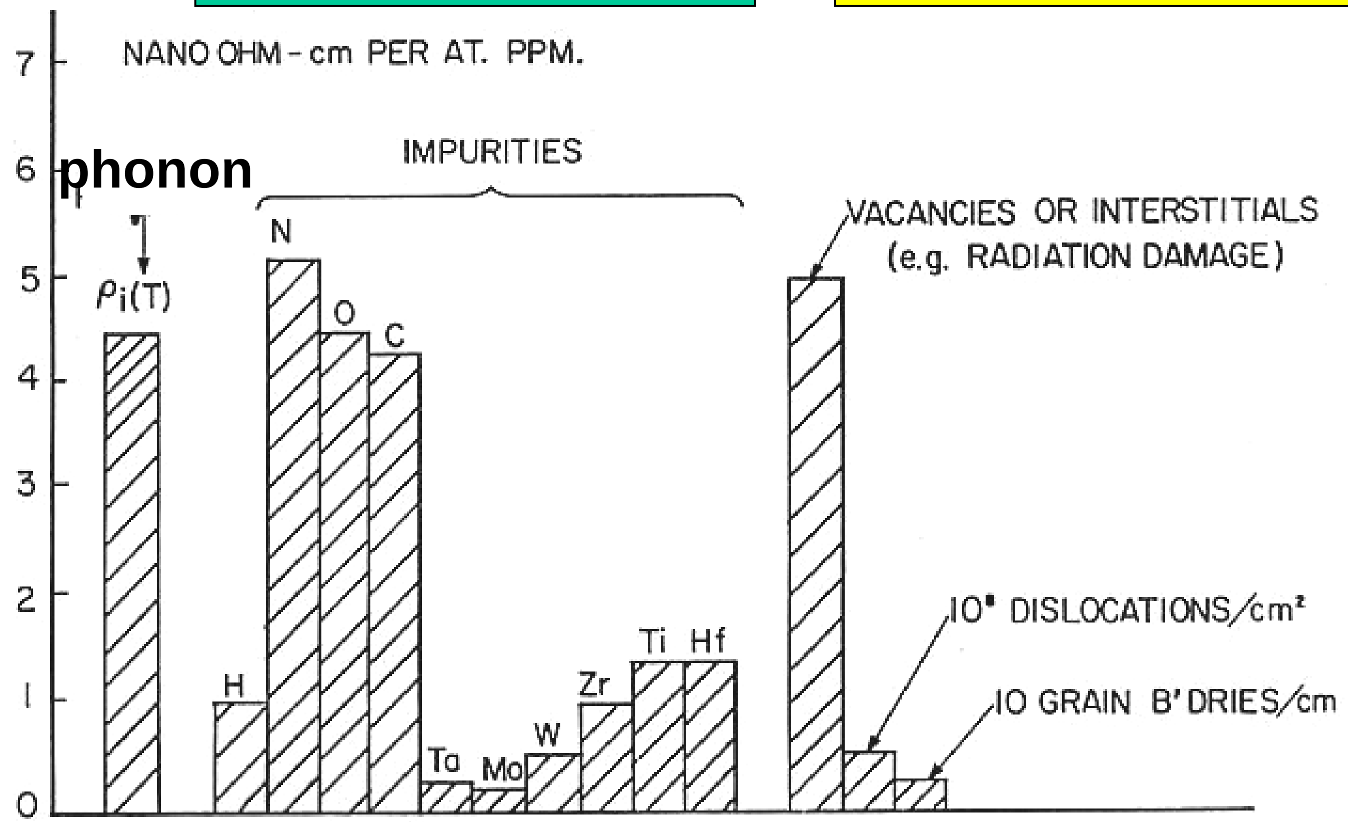

$$\text{E-Resistivity} = \sum (\text{mechanism})_i$$

$$= \text{e-phonon scat.} + \text{e-imprity scat.} + \text{e-inhomogenety scat.} + \cdots$$

RRR measurement

$$RRR \equiv \frac{R_{300K}}{R_{9.5K}}$$

Very simple measurement!!

RRR is linearly proportional to thermal conductivity.

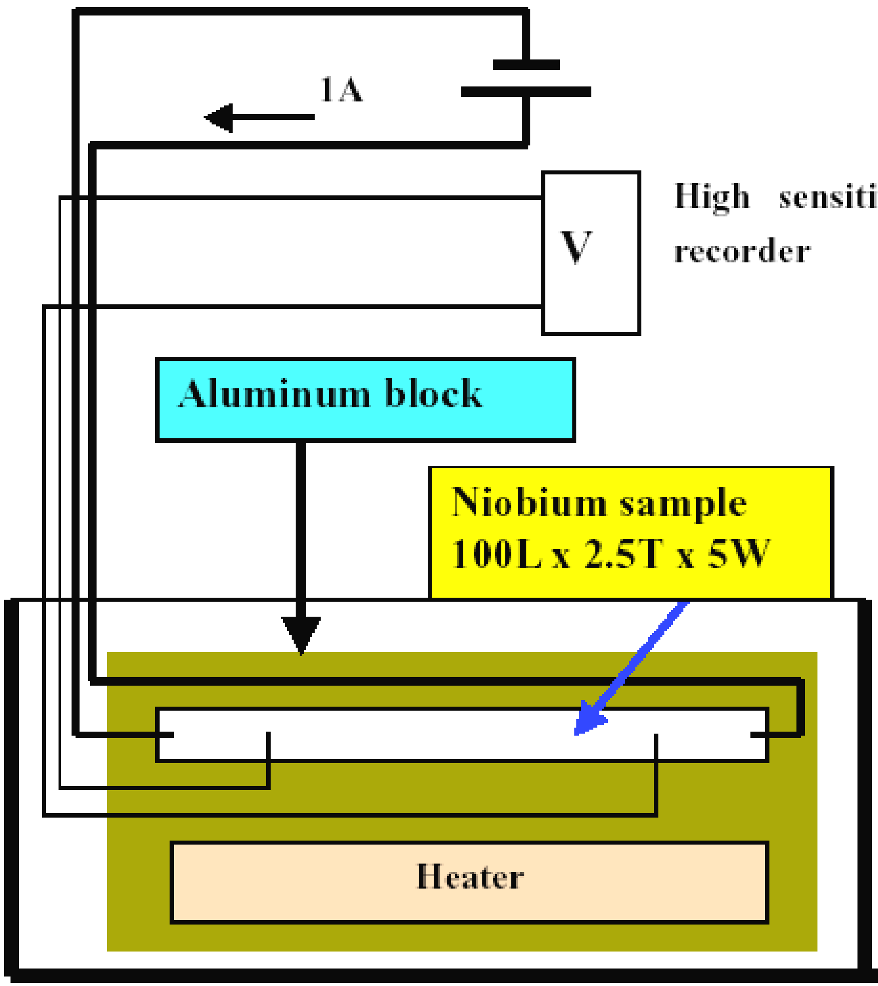

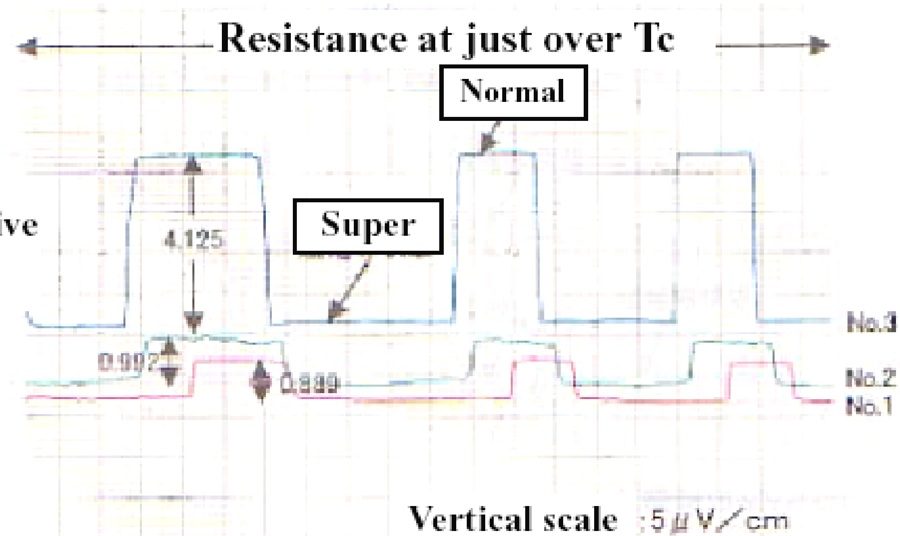

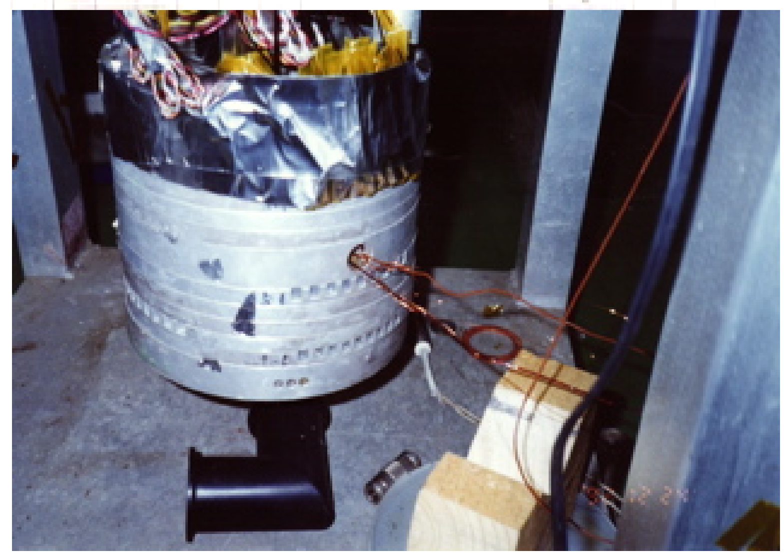

History of RRR improvement in a Nb production Company

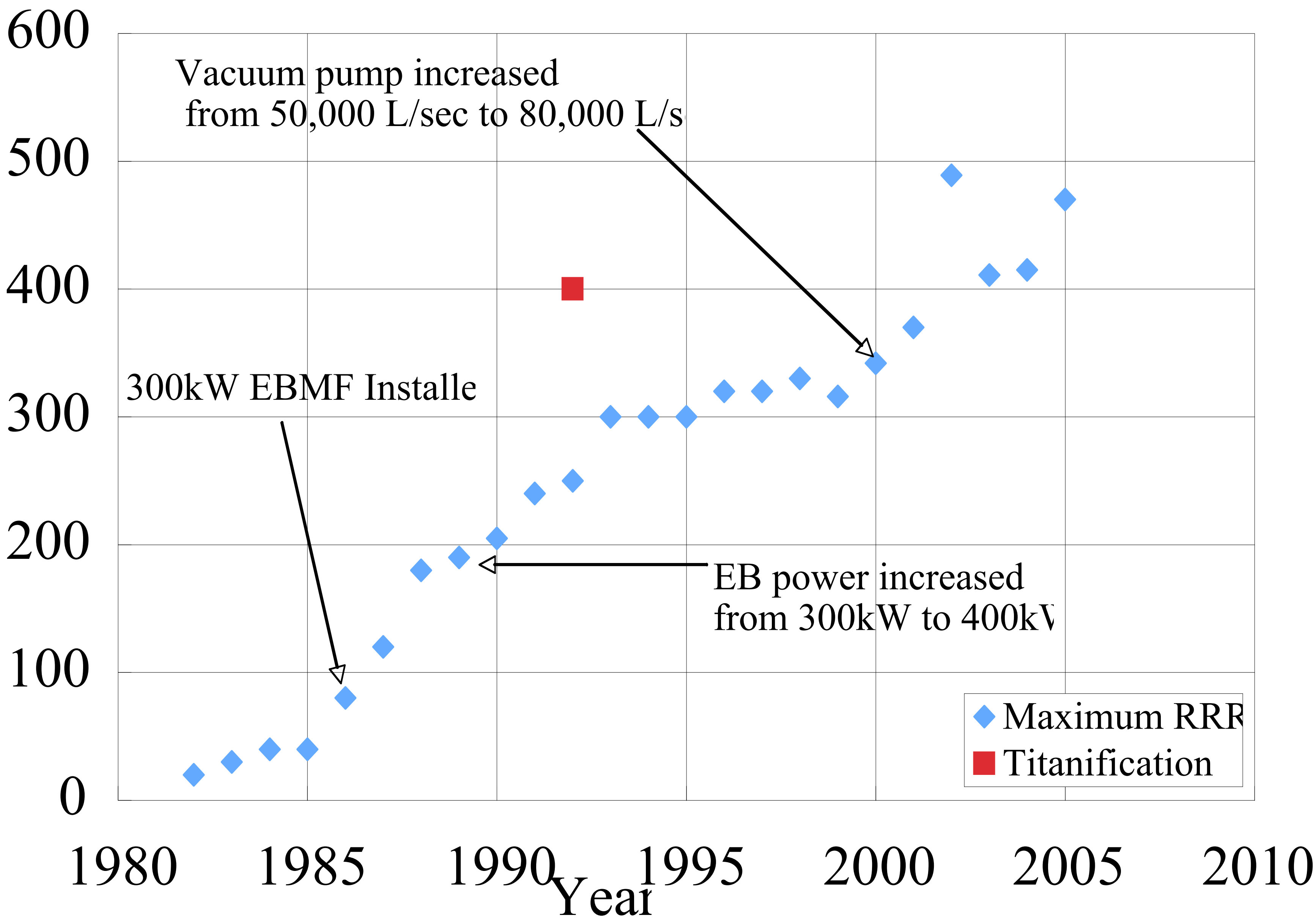

2. Niobium Material

2.1 Niobium Mien
2.2 High Purity Niobium Production

2.1 Niobium Miens

Niobium mine:Carbonatite

Big three mines in the world
Brazil：Araxa'(アラシャ）
Catalao（カタラウン）
Canada：St.Honore
（サン・オノレ）

図１　世界のニオブ埋蔵地（■）とニオブ製品を生産する主要な鉱山（★）

金属　Vol.72 (2002) No.3

Niobium is 33rd abundant metal element in the earth.

A Niobium Mien

Process of Niobium Refining

CBMM

Nb Ore
Pyrochlore

→ Crashing → Concentration
Float-selection

Refining

S

Burning @ 700,1100^{O}C
(Evaporate S)

Pb

Be

Melting
(Isolation)

Fe, P

Fero-niobium

ATR
Aluminum Termitt Reduction

EBM

CBMM Nb Production Facilities

By A.Ono, CBMM

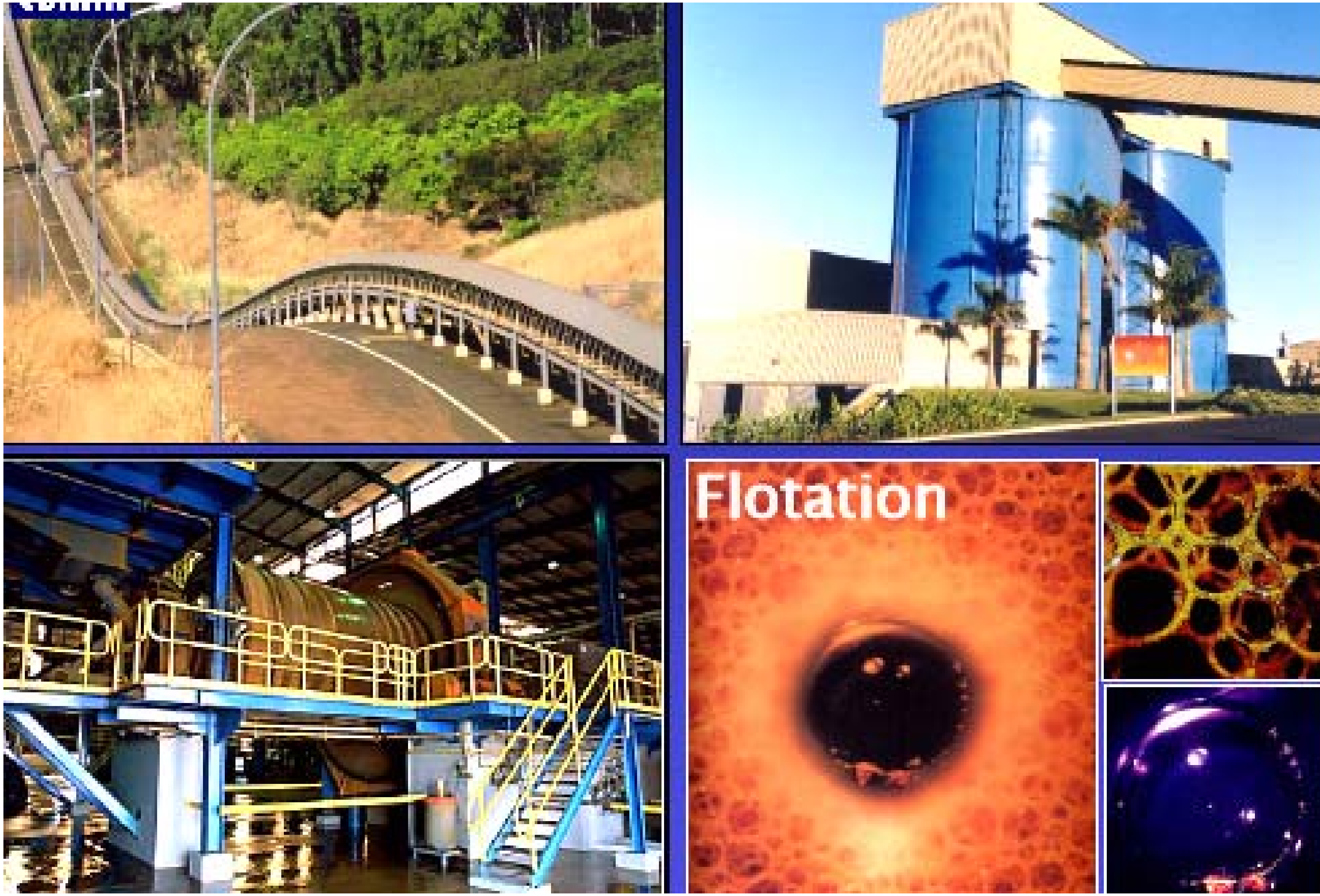

CBMM

Nb Ore

After concentrated (55%)

Pellets

Fero-niobium

Aluminum Termitte Reduction

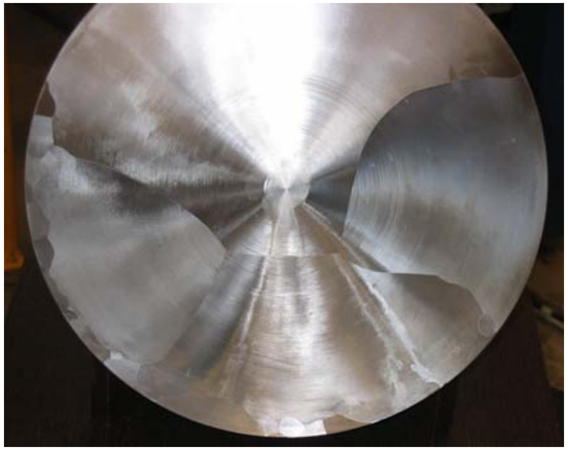

Large Grain Nb Ingot

2.1 High Purity Nb production

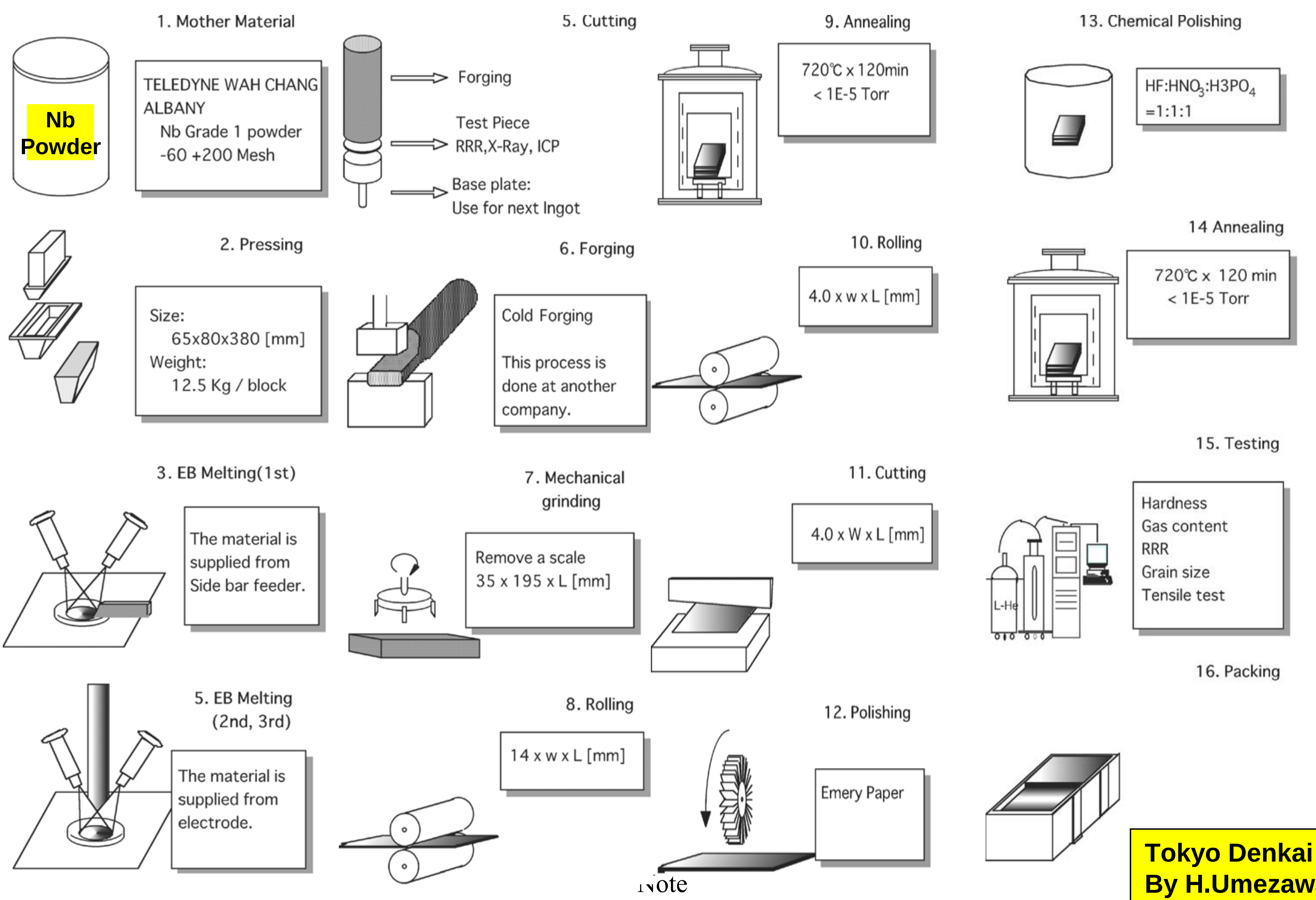

Original material for high pure niobium

Tokyo Denkai

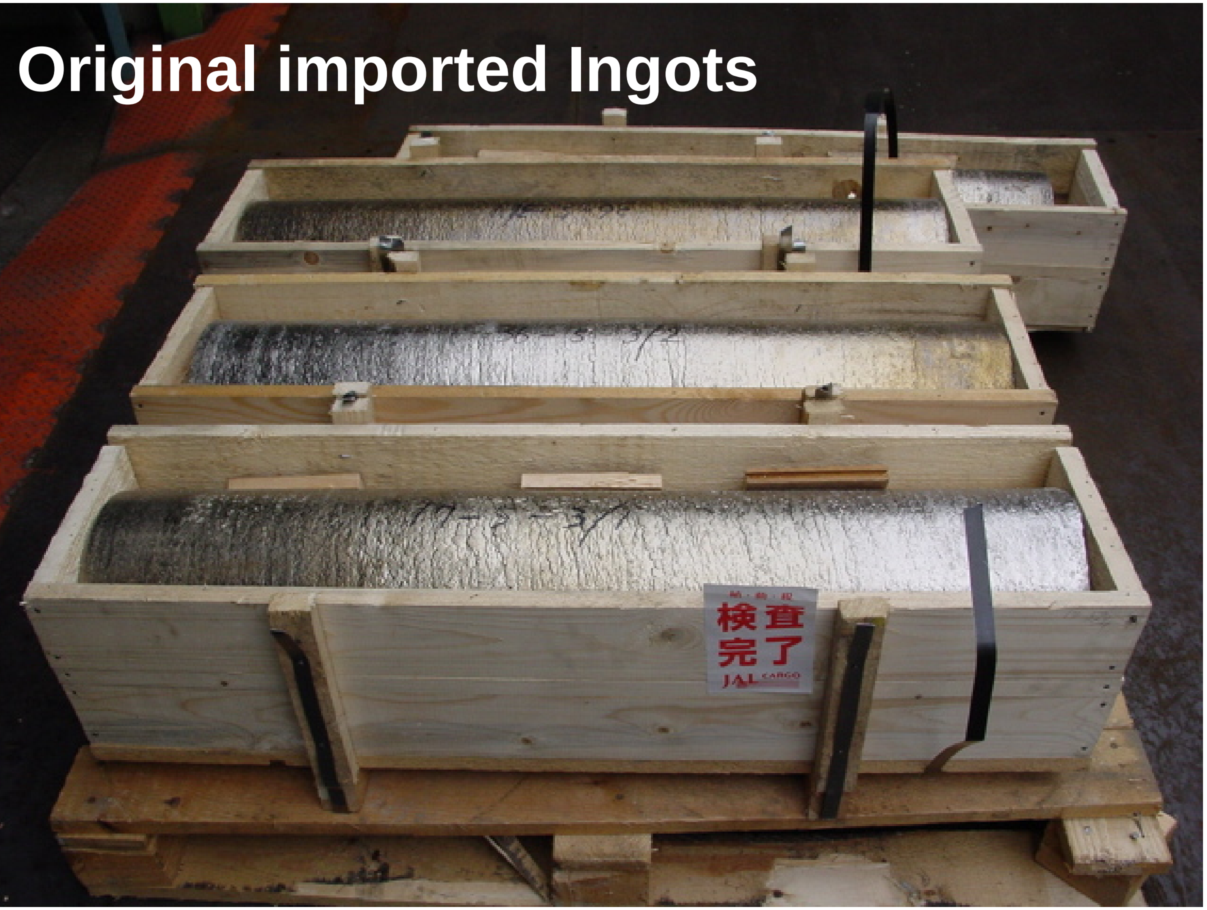

Electron Beam Melting

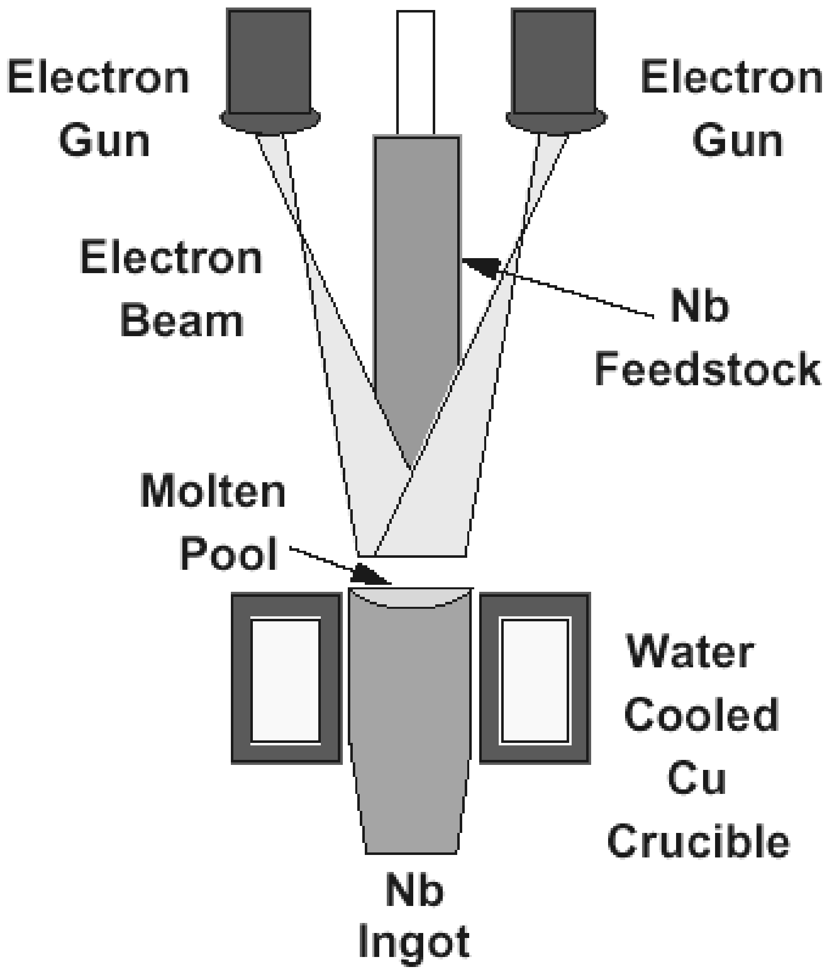

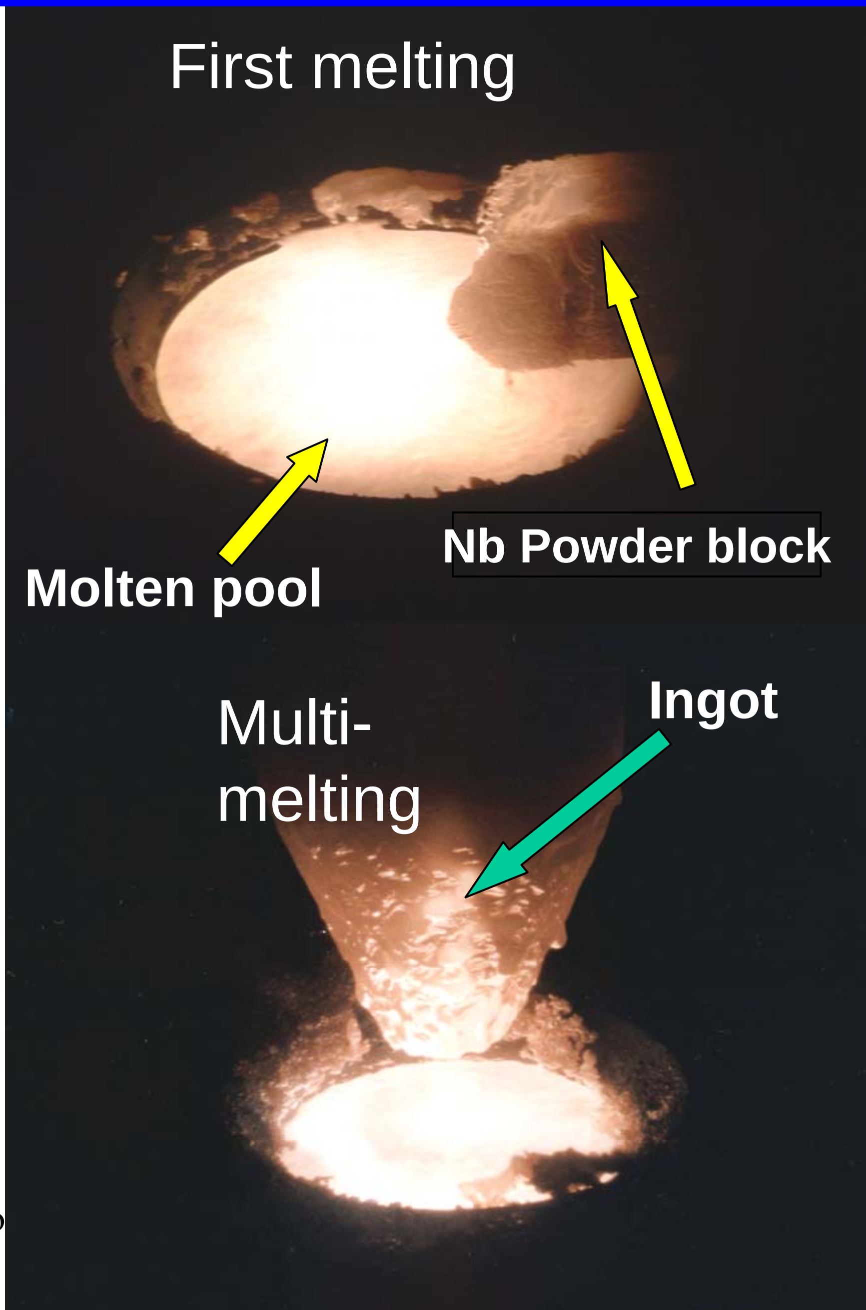

Scho

Note

EBM furnace and Nb Ingots

400kw EBM furnace

Tokyo Denkai

Nb Ingots after multi-melted

Vapor Presser for various metals

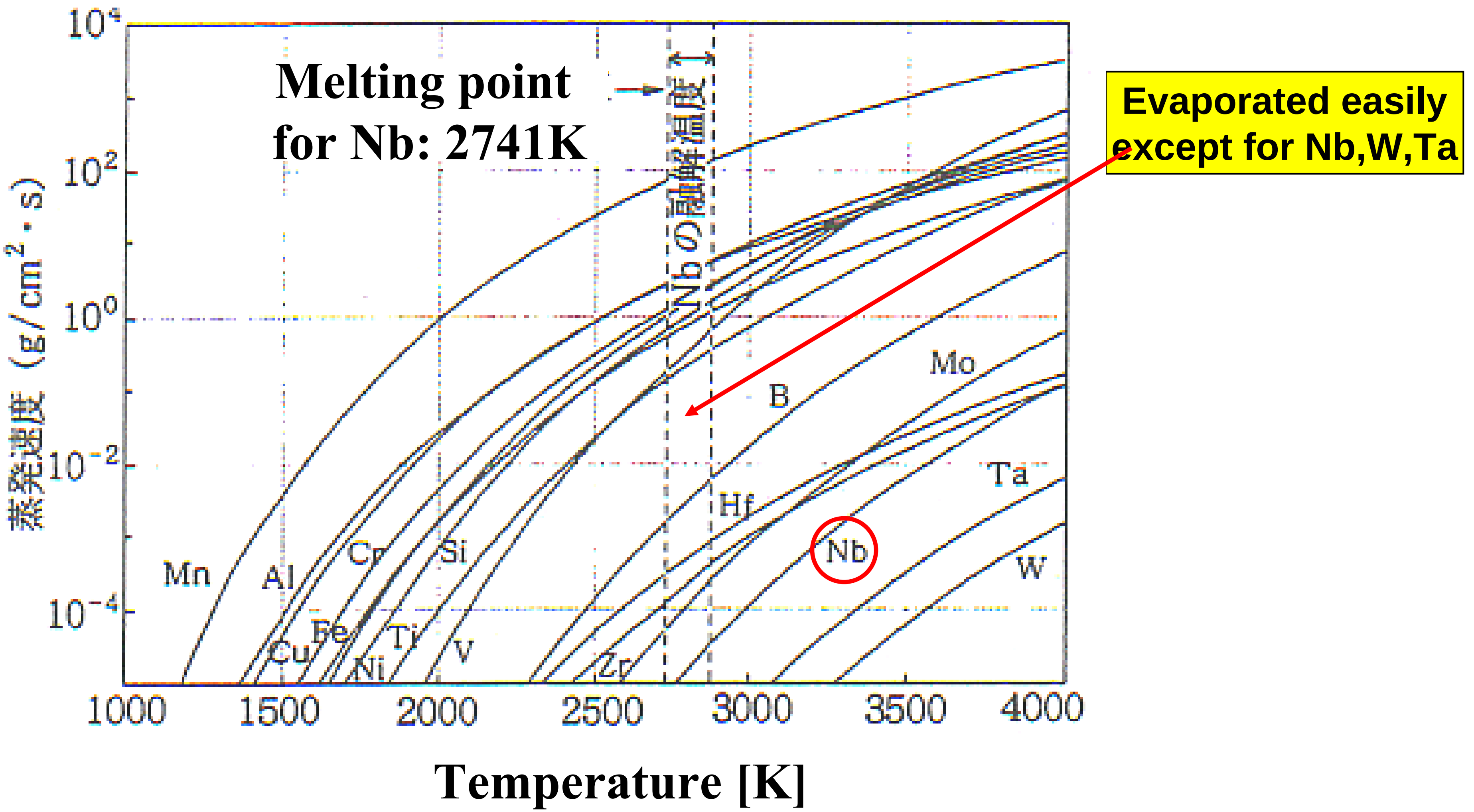

Note

Keys for High purity Nb Ingot production

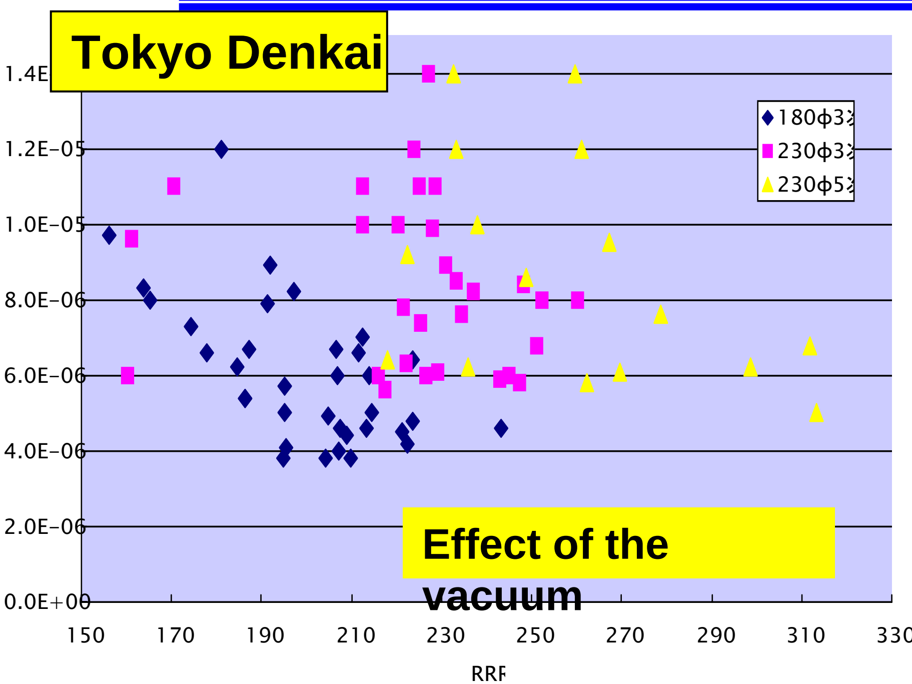

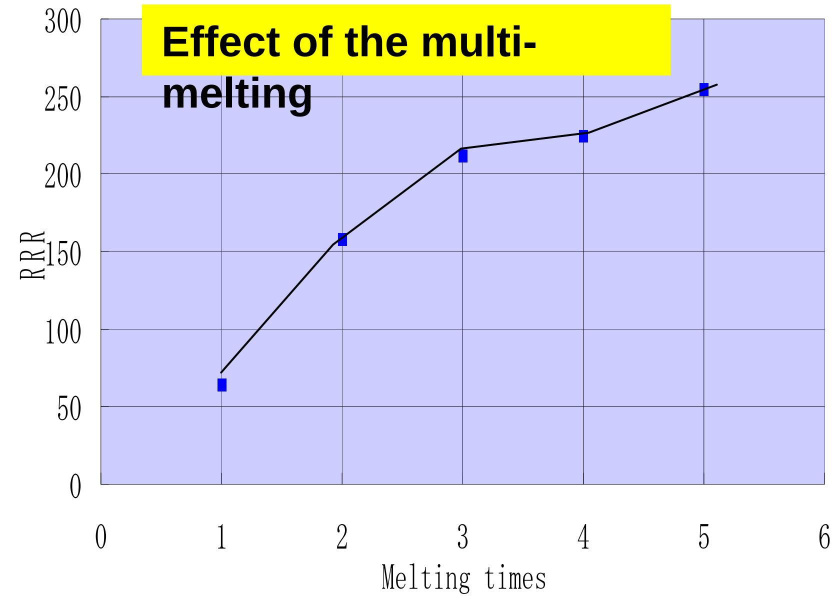

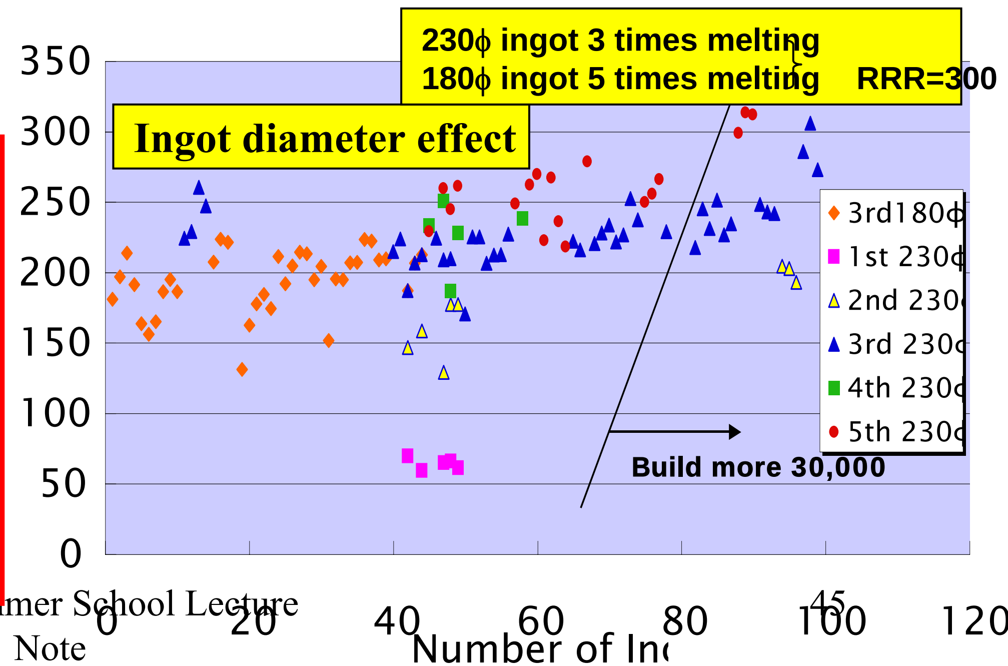

Three keys:

1) **High Vacuum,**
2) **2) Multi-melting,**
3) **Large molten pool surface**
   (Large Ingot diameter)

Impurities

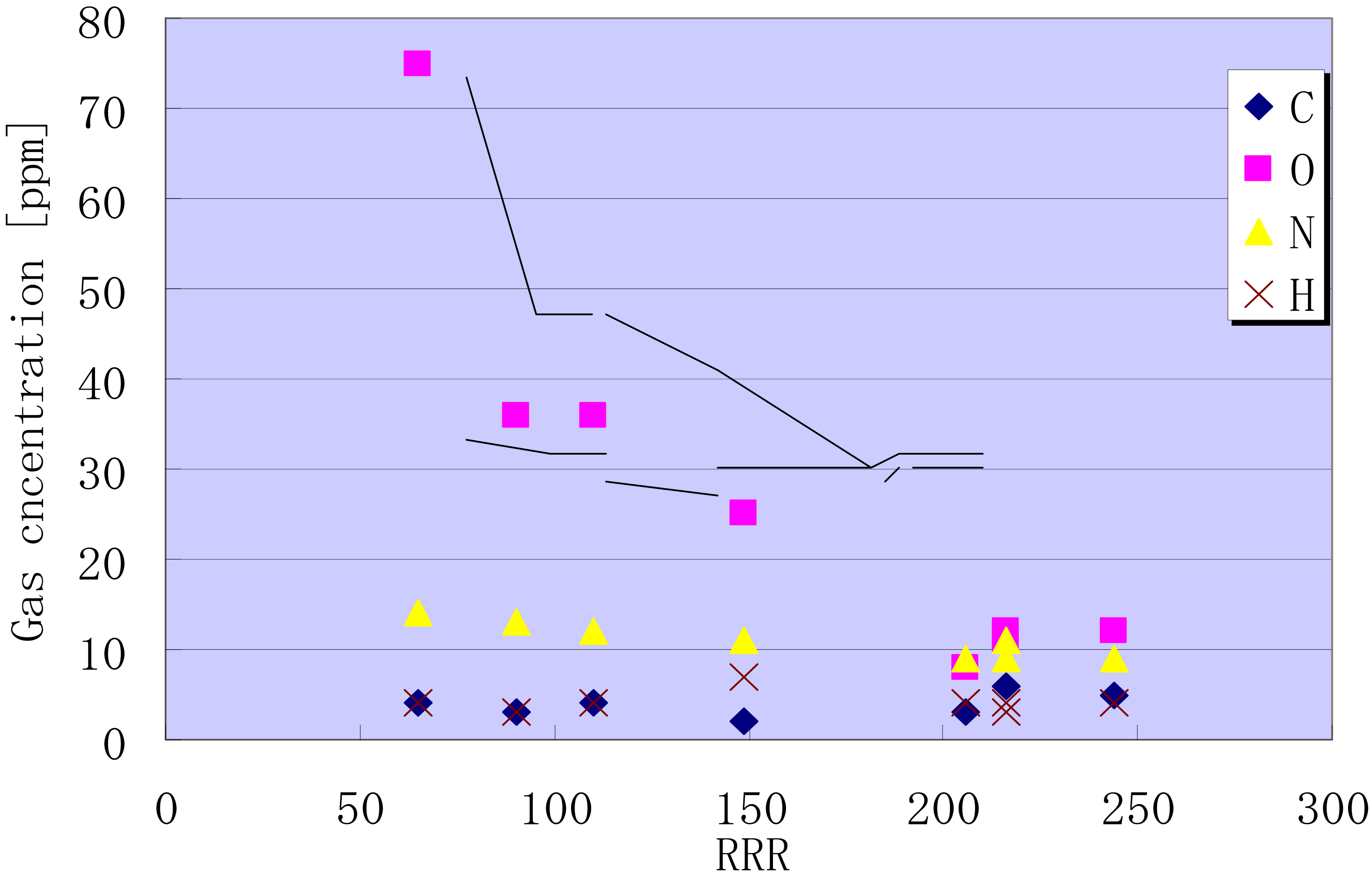

80
70
60
50
40
30
20
10
0
Gas cncentration [ppm]
0
50
100
150
200
250
300
RRR
C
O
N
H

Gas analysis in niobium

Tokyo Denkai

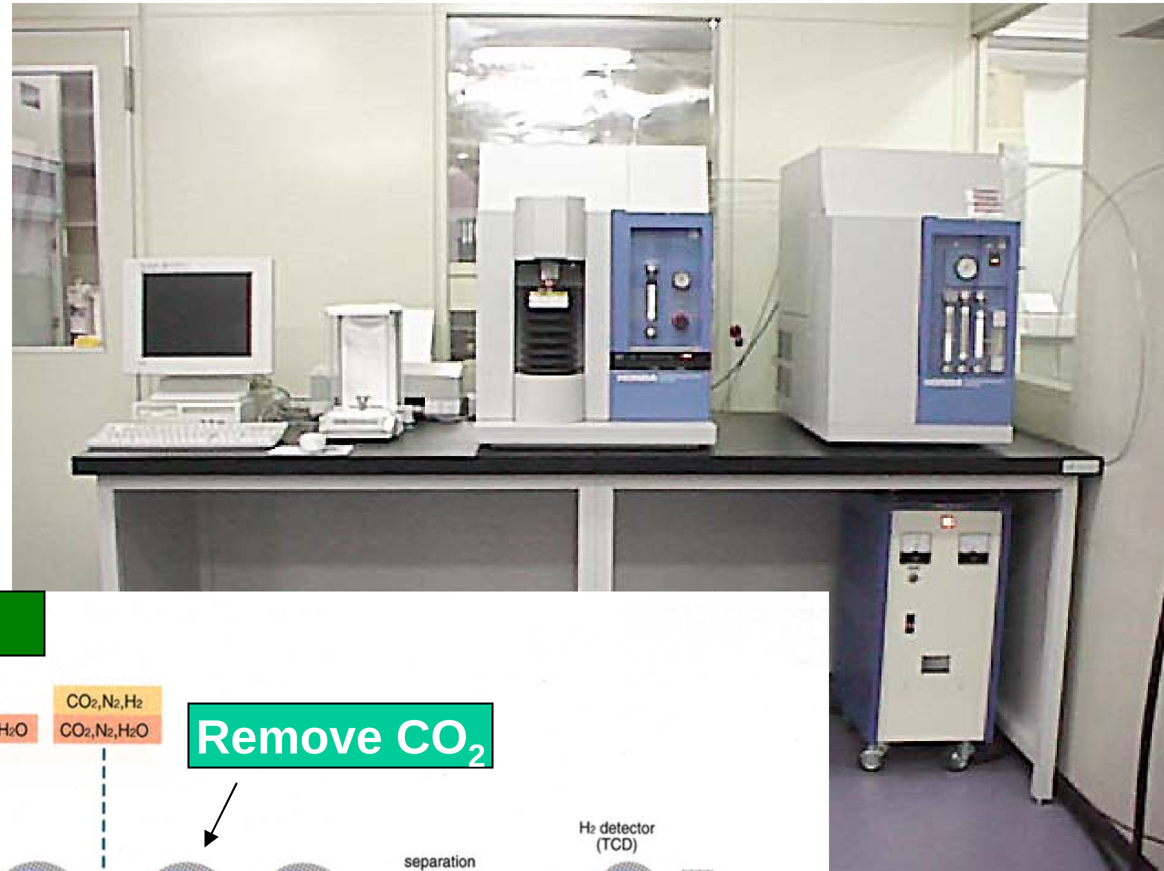

Case of N

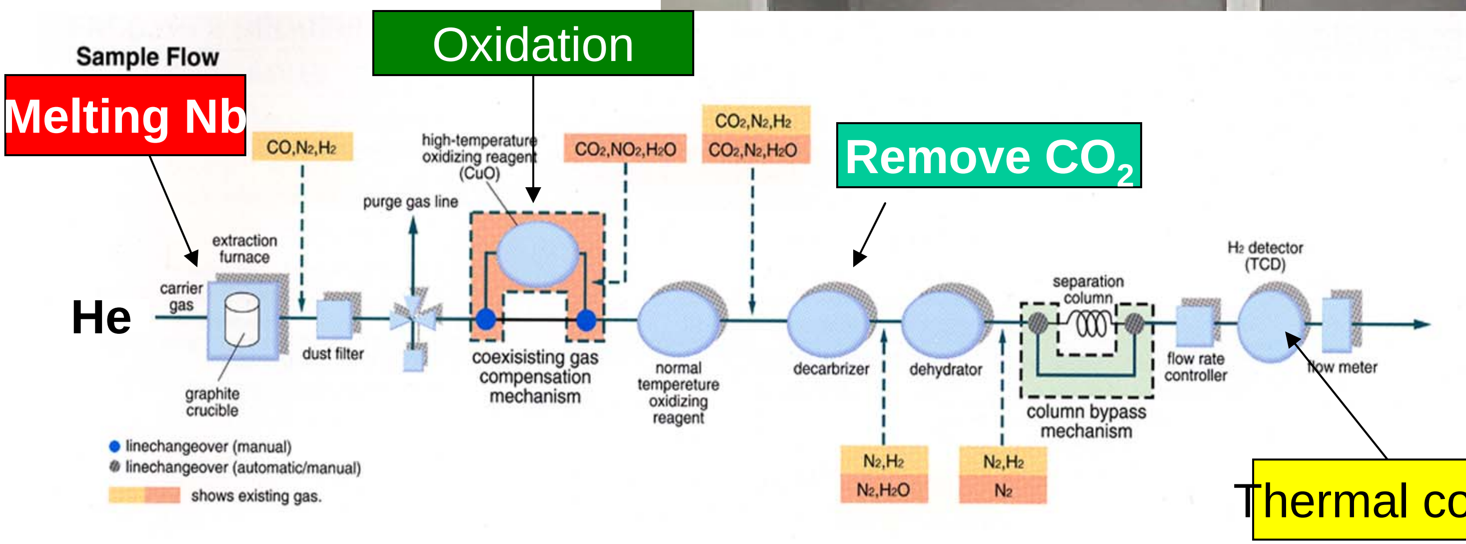

Gas analysis (Hydrogen, Oxygen, Nitrogen) ：HORIBA

Regression Analysis Result

Umezawa's result.

$$\frac{1}{RRR} = \frac{O}{5800} + \frac{N}{2273} + \frac{H}{16322} + \frac{C}{8911} + \frac{Ta}{604690} + \frac{1}{1249}$$

K.K.Schulze: J. Metals, 33(1981), 33-41

$$\frac{1}{RRR} = \frac{O}{5000} + \frac{N}{3900} + \frac{H}{1550} + \frac{C}{4100} + \frac{Ta}{550000} + \ldots$$

Correlation between theoretical RRR and measured RRR

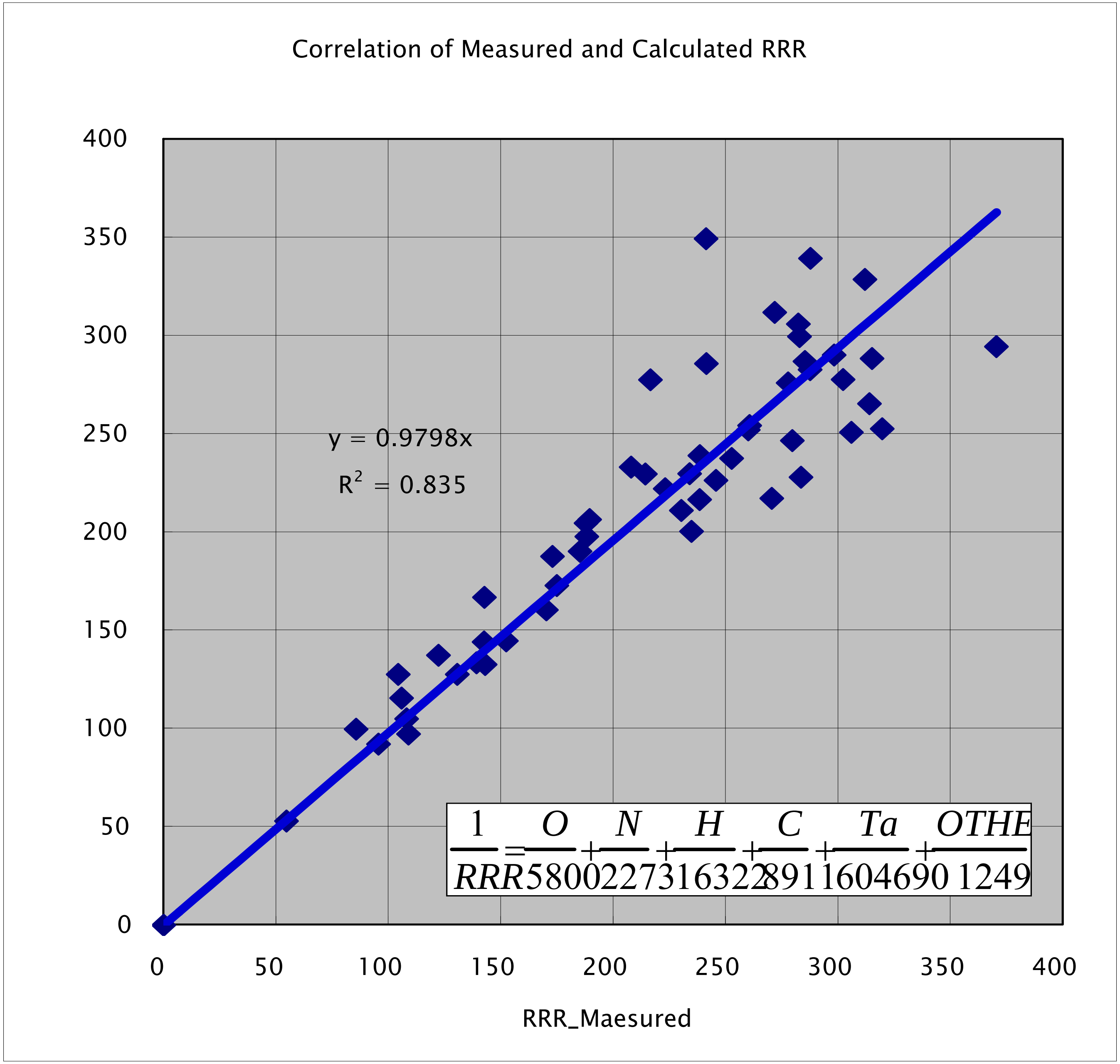

Rolling

Tokyo Denkai

Intermediate rolling

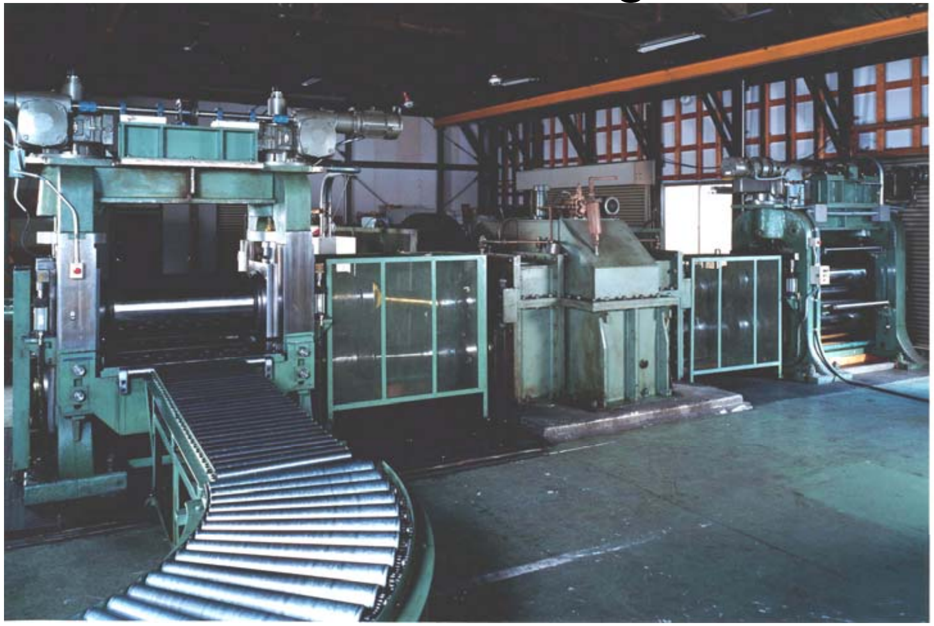

Cleanroom

Final rolling

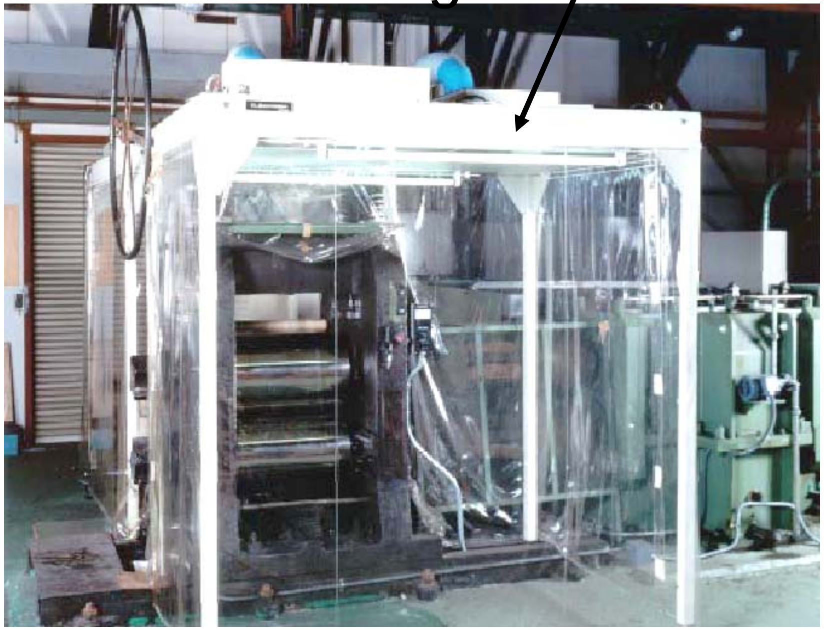

Careful control against dust

Vacuum annealing system

Tokyo Denkai
1400^{o}C Max,
~1x10^{-6} Torr
Effective working zone
1000ϕ x 1800L
Ta heater

Metallurgy of Nb

Remained roll rolled structure

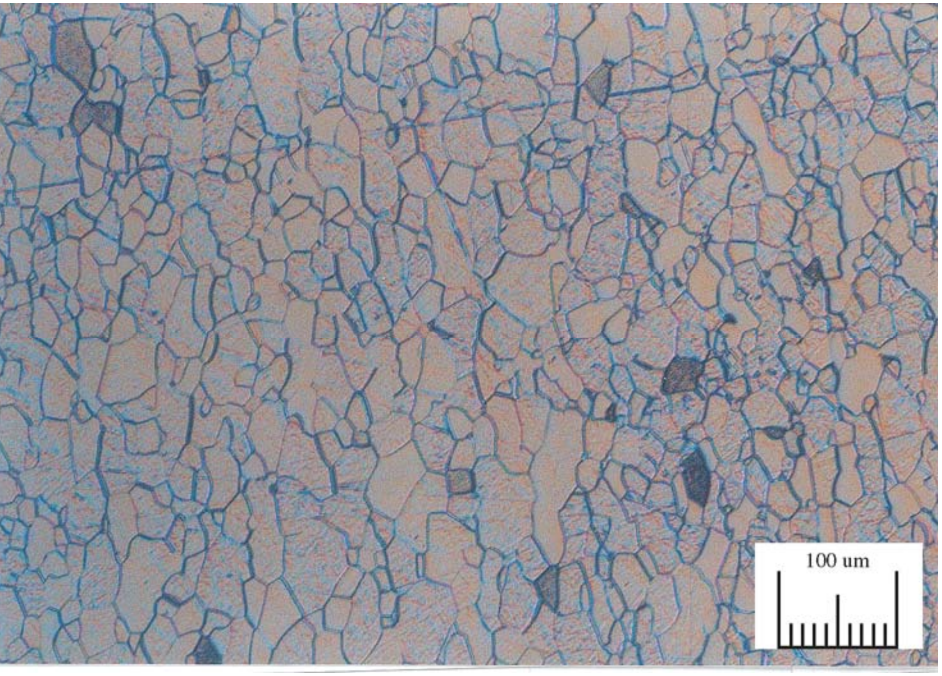

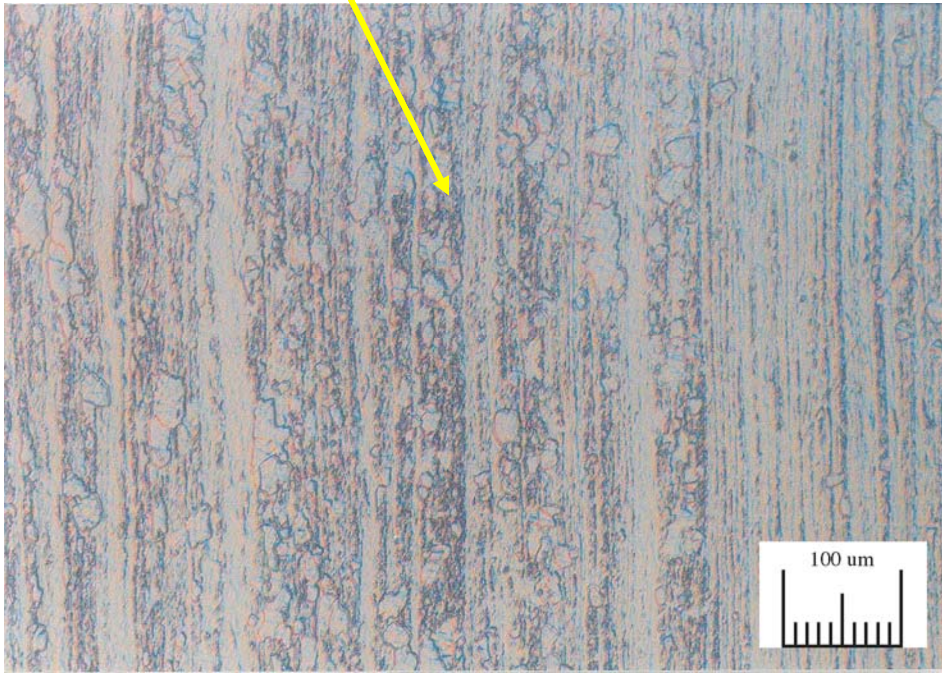

Well annealed

None annealed

Annealing Temp. and Mechanical Properties

TRISTAN

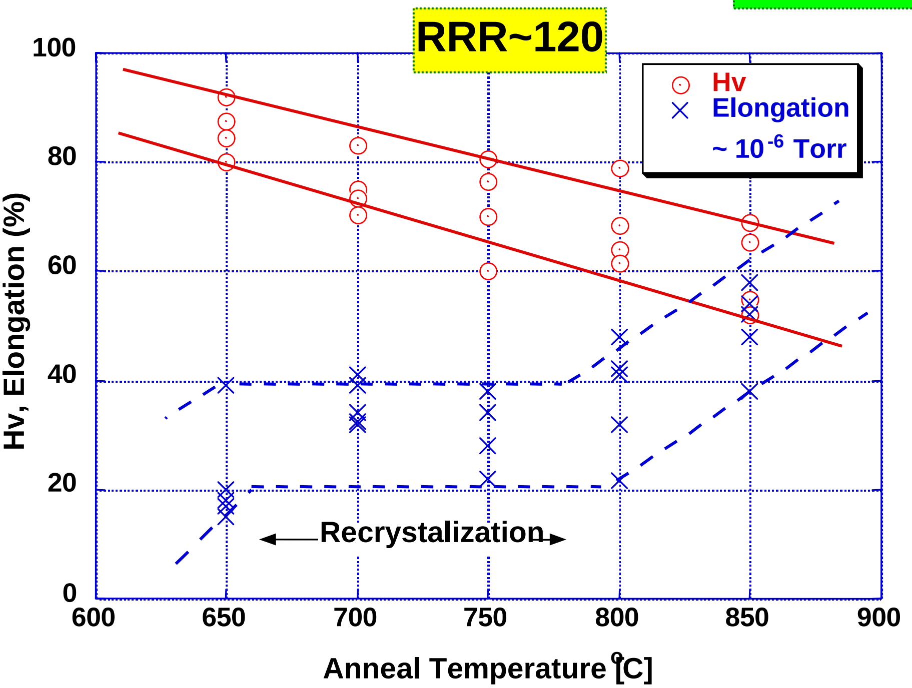

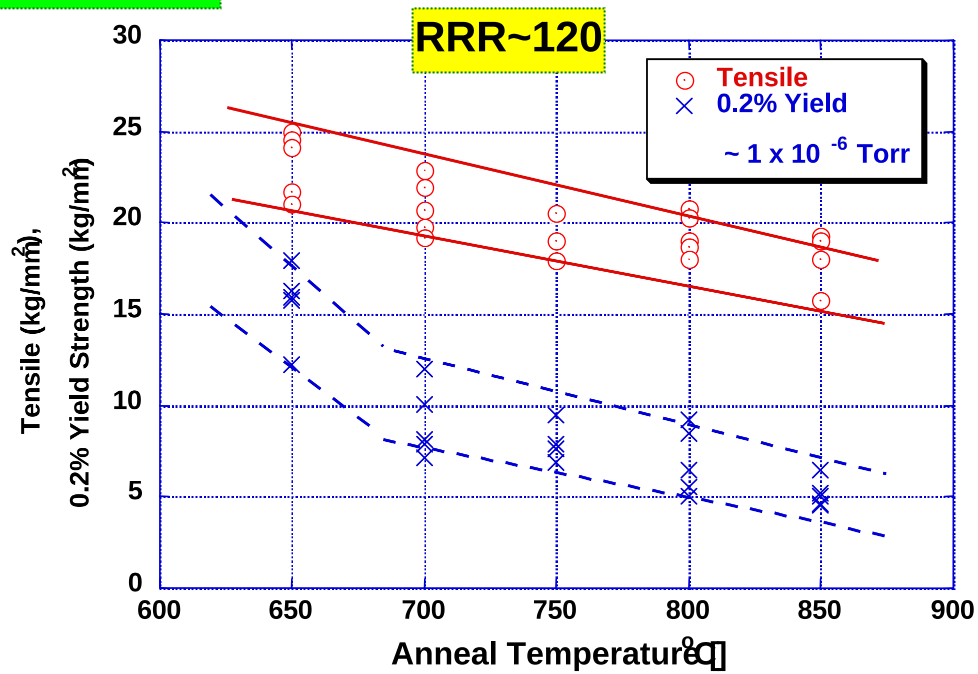

Re-crystallization Temperature : 680 ~ 780°C
Vacuum Pressure : ~10^{-6} Torr

High Pure Niobium Sheets

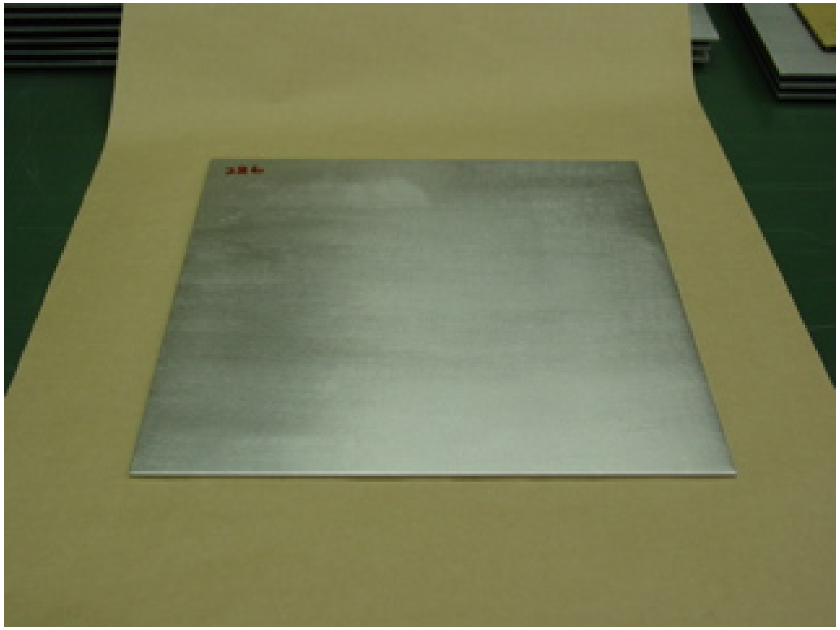

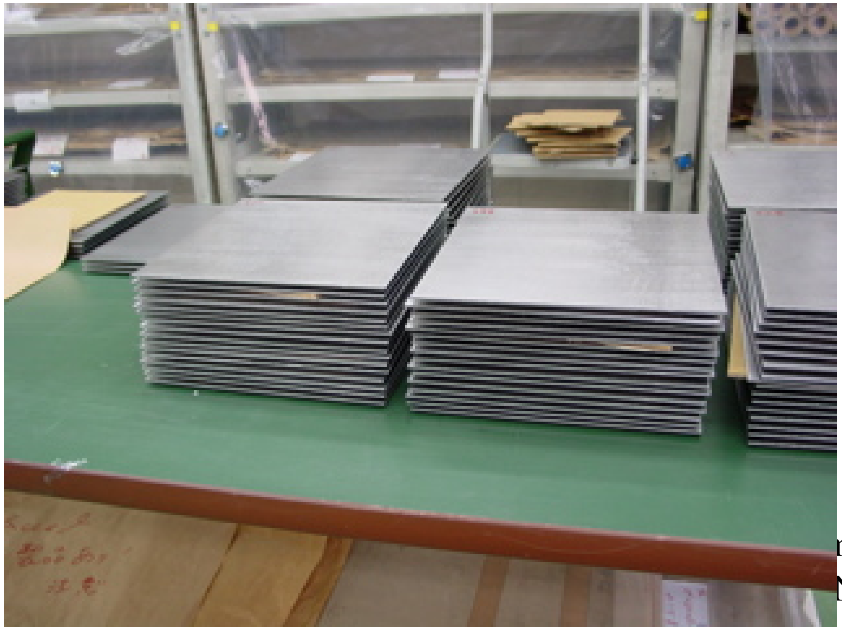

Tokyo Denkai

Improvement of RRR at Tokyo Denkai

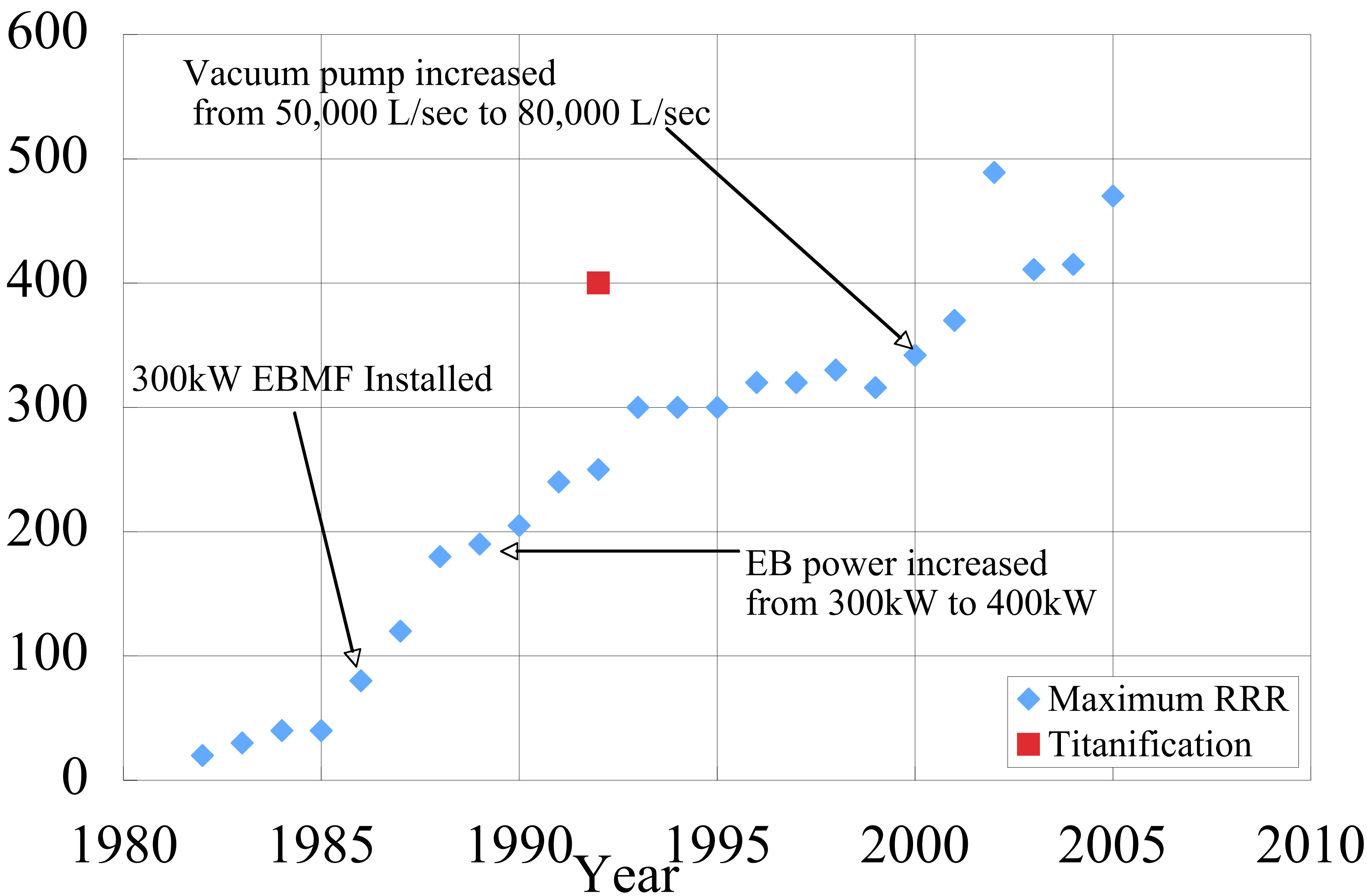

Other metal analysis :ICP-OES Analysis

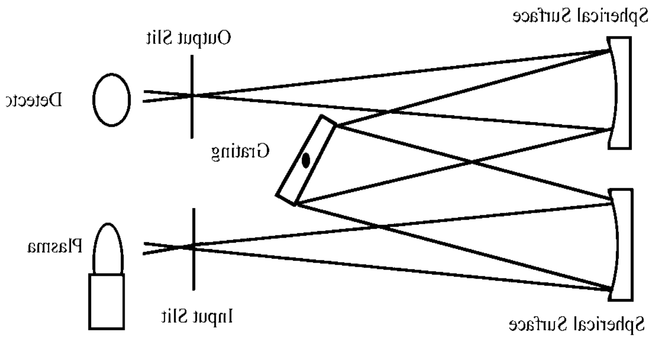

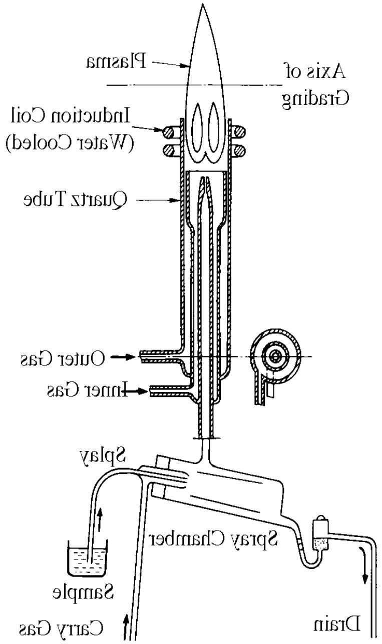

Tokyo Denka

RRR measurement

Tokyo Denkai

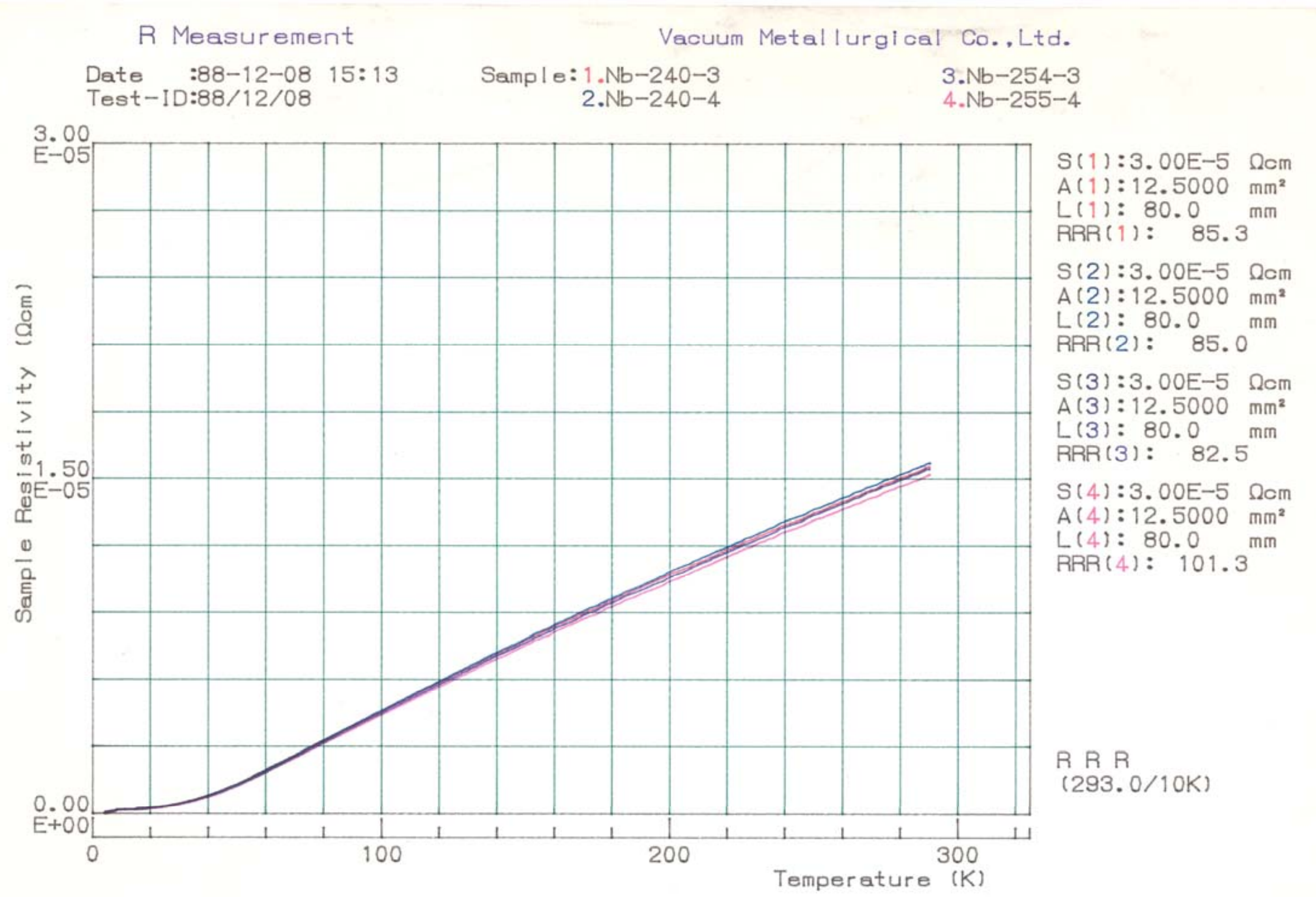

K.Saito

Tensile Test Machine

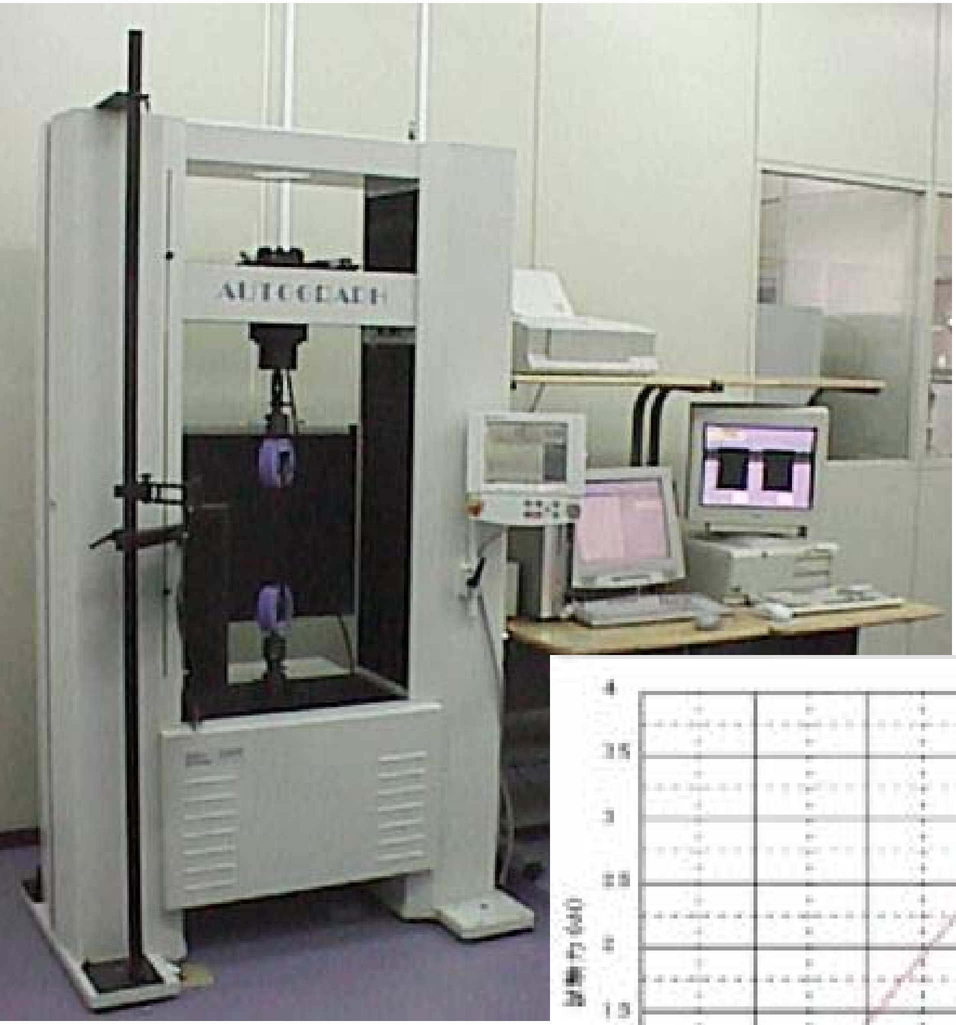

Tokyo Denkai

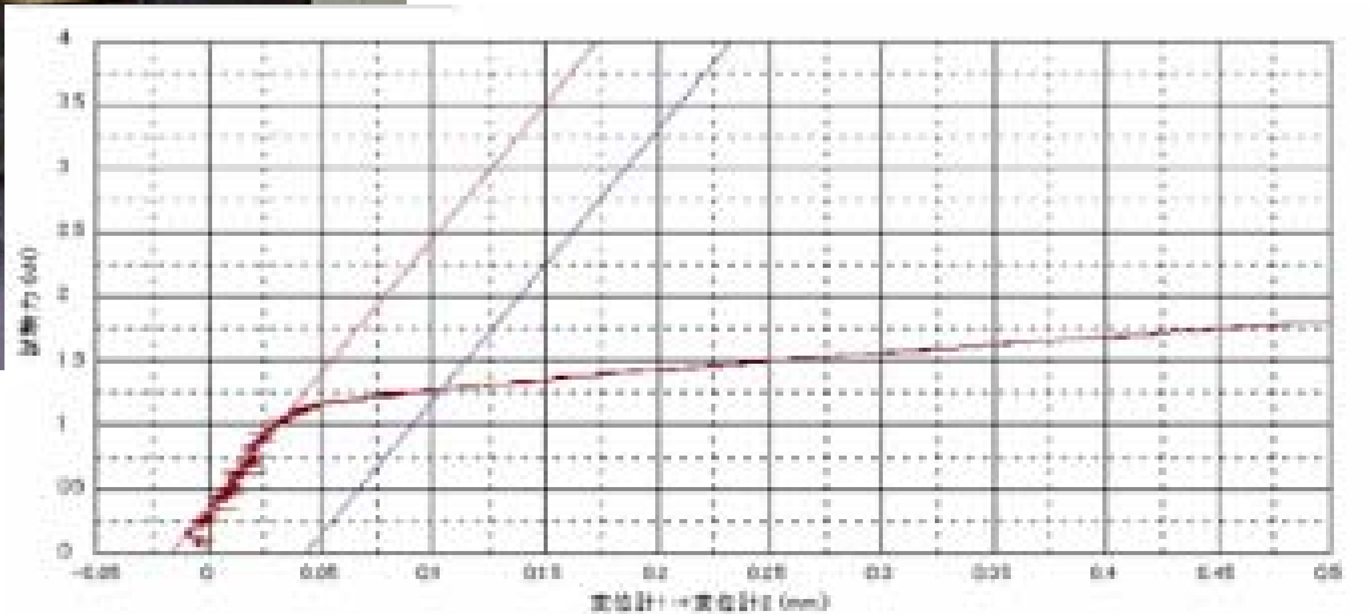

K.Saito

Material R&D for ILC

Large grain niobium cavity R&D in Jlab

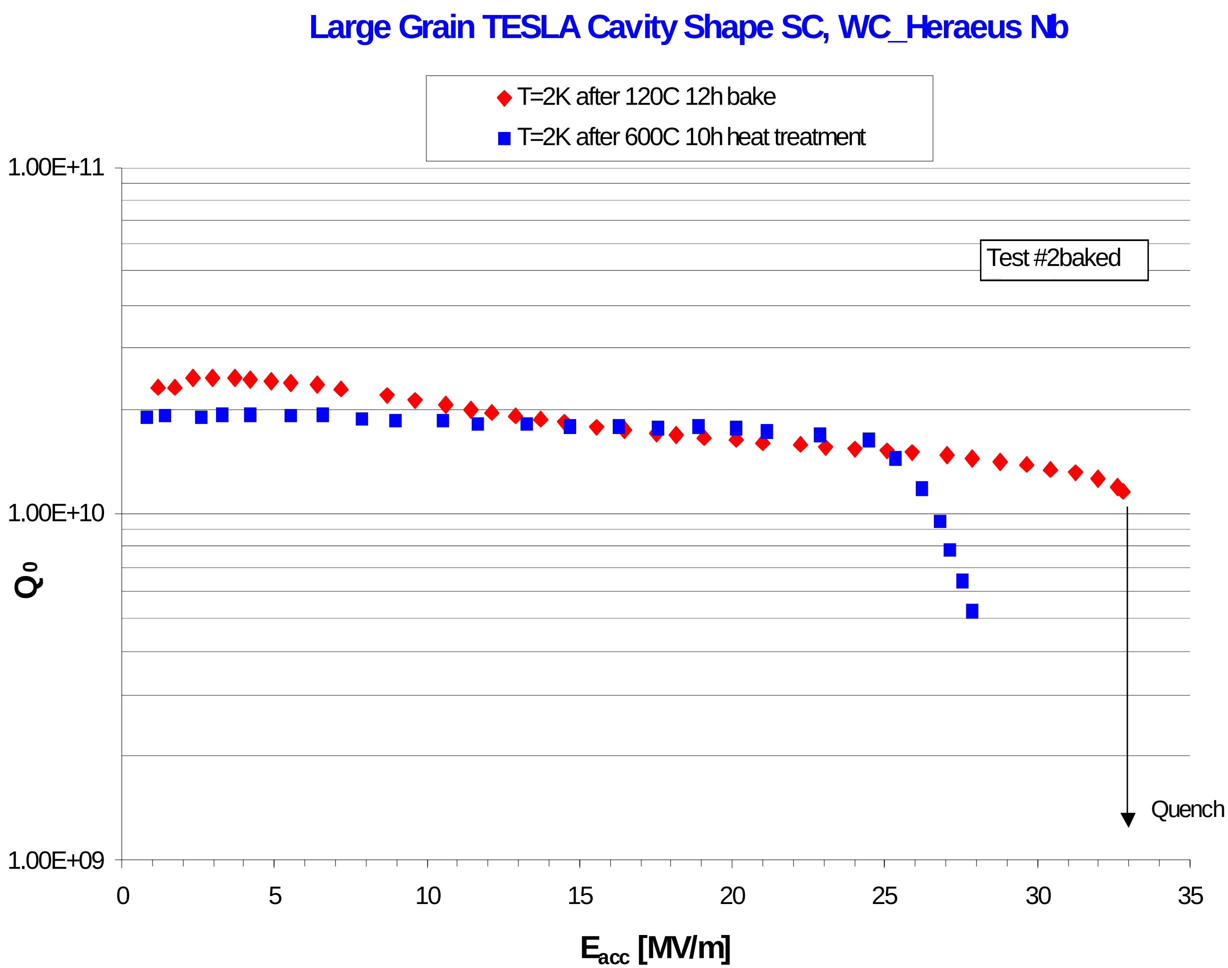

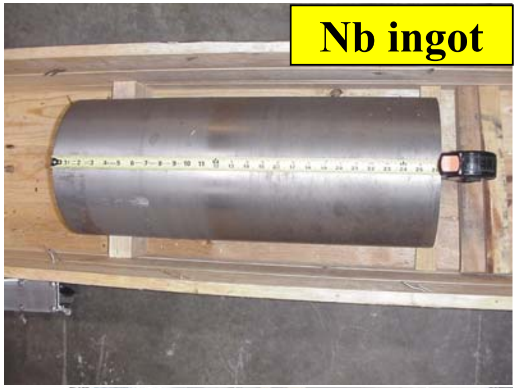

Large grain Nb sheet production can bring a cost down.
BCP could produce 35MV/m gradient and it brings further cost down.

Single Crystal / Large Grain Nb Production

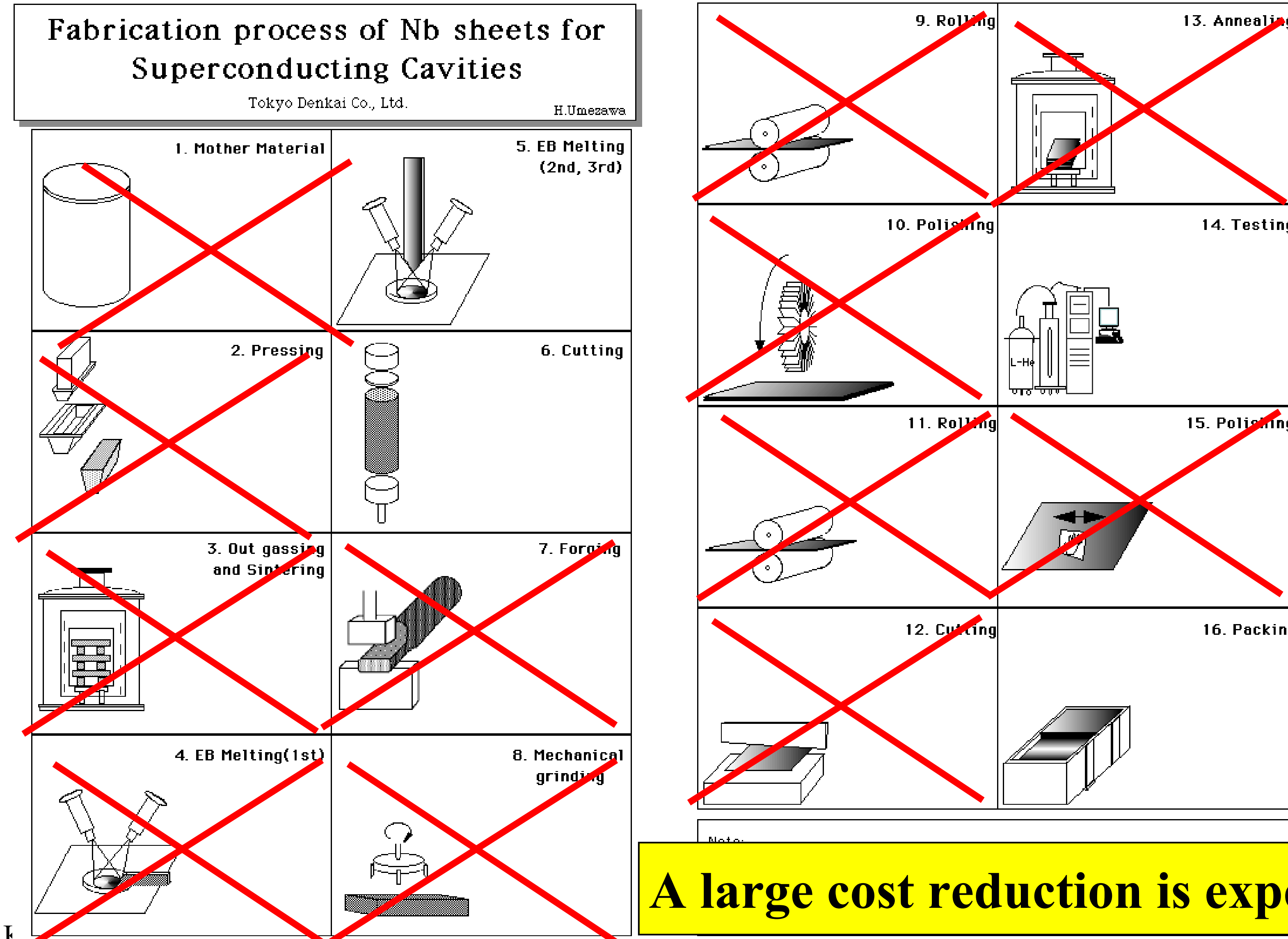

A large cost reduction is expected !

3. SRF RF Cavity Design

3.1 Single Cell Cavity Design
3.2 Criteria General for Cavity Shape
3.3 Criteria for Multi-cell Structures

What is RF cavity ?

Principle of RF acceleration
TM-mode : Ez≠0, Bz=0,   frequency: f
TM_{010} - mode, π -mode, Standing Wave
V(electron velocity)⌒C(light velocity)
L(cell length) = λ/2 ; λ(wave length)=C/f
If the velocity is low like protons,
β=V/C < 1, then L=βλ/2

RF Cavity: accelerates charged particles by the electric field synchronized with RF frequency.

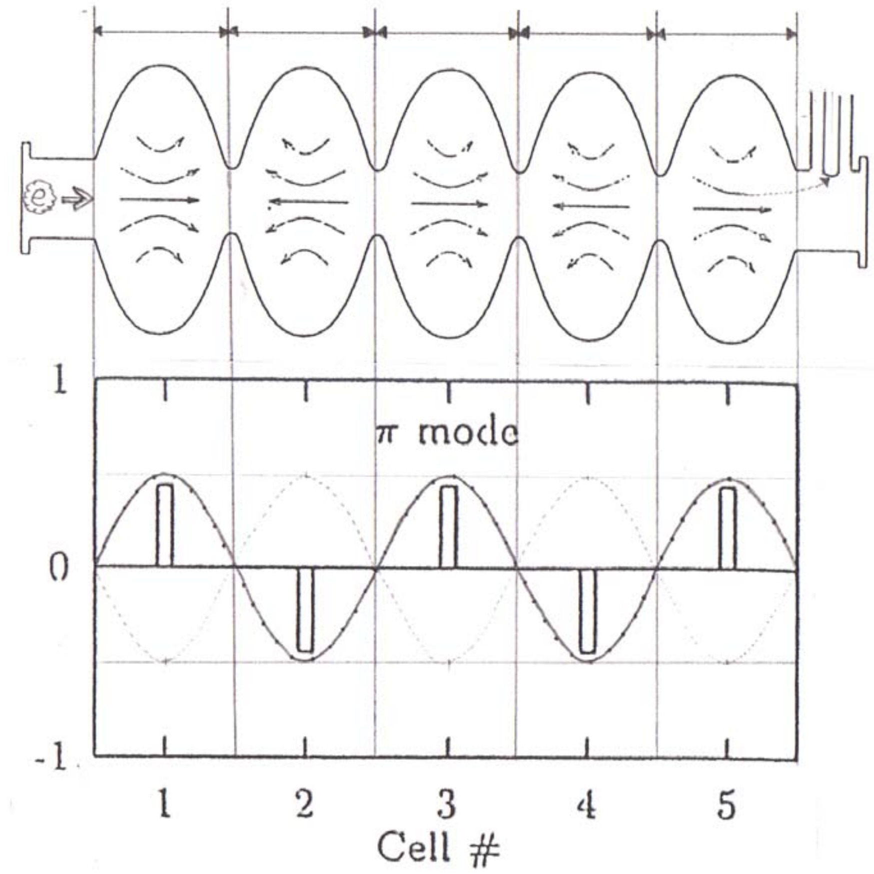

Equivalent circuit

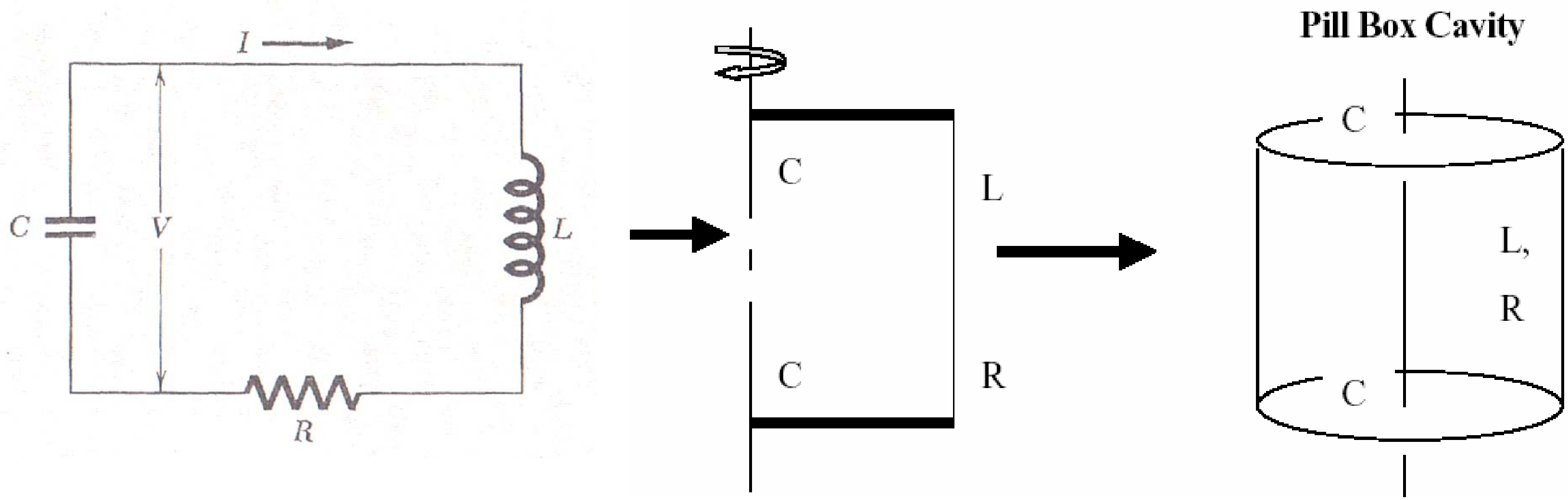

$$I = -\frac{dQ}{dt}, \quad Q = CV, \quad V = L\frac{dI}{dt} + RI$$

$$\frac{d^2V}{dt} + \left(\frac{R}{L}\right)\frac{dV}{dt} + \left(\frac{1}{LC}\right) = 0, \quad V(t) = V_O \exp(-\alpha + i\omega)t$$

$$(-\alpha + i\omega)^2 + (-\alpha + i\omega)\left(\frac{R}{L}\right) + \left(\frac{1}{LC}\right) = 0,$$

$$\alpha = \frac{R}{2L}, \quad \omega^2 = \frac{1}{LC} - \frac{R^2}{4L^2}$$

$$R << L, \quad \omega_O^2 = \frac{1}{LC} \Rightarrow f = \frac{1}{2\pi\sqrt{LC}}$$

Q-value of the circuit

$$Q \equiv \omega \cdot \frac{stored\ energy}{power\ loss / sec} = \omega \cdot \frac{P}{dP/dt} = \omega \cdot \frac{L}{R}$$

$$= \frac{\omega}{2\alpha}$$

Simple Circuit Model of RF Cavity
- Oscillation in the LCR Circuit -

$$\propto \exp(-\frac{\omega}{2Q}t)$$

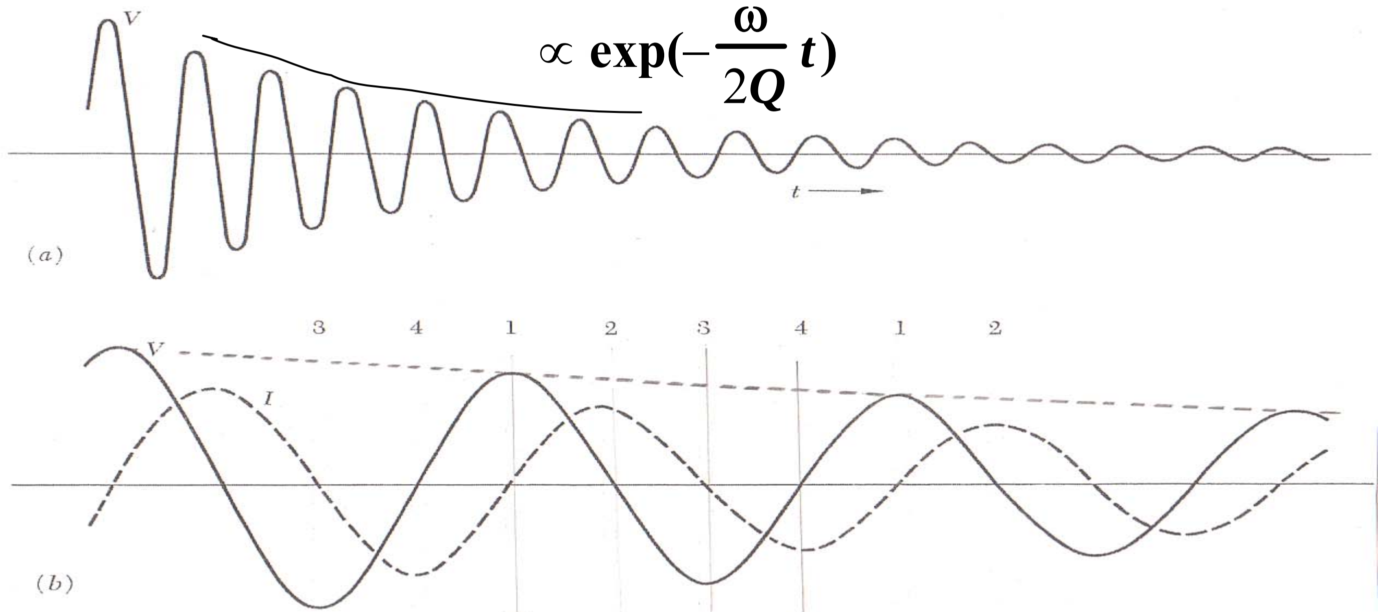

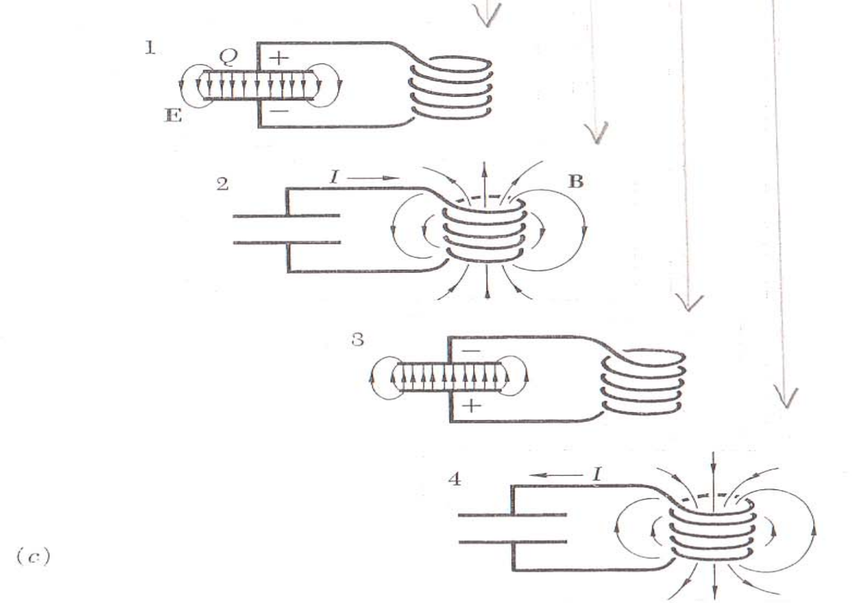

(*a*) The damped sinusoidal oscillation of voltage in the *RLC* circuit.
(*b*) A portion of (*a*) with the time scale expanded and the graph of the current *I* included.
(*c*) The periodic transfer of energy from electric field to magnetic field, and back again. Each picture represents the condition at times marked by the corresponding number in (*b*).

Electro-magnetic field in a waveguide

Maxwell equations in a waveguide

$$\nabla\times\mathbf{E}=i\frac{\omega}{c}\mathbf{B},\ \nabla\cdot\mathbf{B}=0,\ \nabla\times\mathbf{B}=-i\mu\varepsilon\frac{\omega}{c}\mathbf{E},\ \nabla\cdot\mathbf{E}=0,\ \rho=0,\ \mathbf{j}=0$$

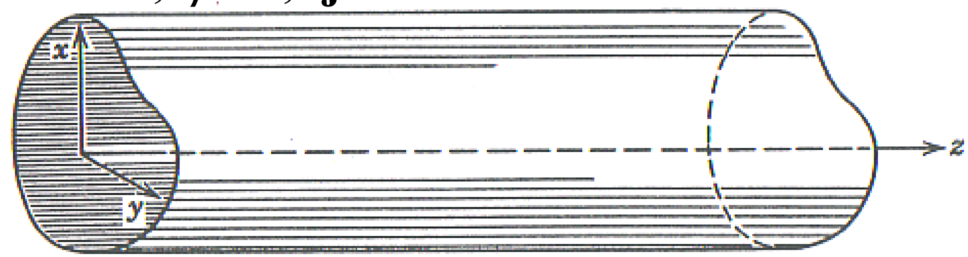

$$\left(\nabla^2+\mu\varepsilon\frac{\omega^2}{c^2}\right)\left\{\frac{\mathbf{E}}{\mathbf{B}}\right\}=0,$$

$$\mathbf{E}(x,y,z,t)=\mathbf{E}(x,y)\exp(\pm ikz-i\omega t),\ k\text{: wavevector},$$

$$\mathbf{B}(x,y,x,t)=\mathbf{B}(x,y)\exp(\pm ikz-i\omega t),$$

$$\left[\nabla_t^2+(\varepsilon\mu\frac{\omega^2}{c^2}-k^2\right]\left\{\frac{\mathbf{E}}{\mathbf{B}}\right\}=0,\ \ \nabla_t^2\equiv\nabla^2-\frac{\partial^2}{\partial^2 z},\ \ \mathbf{E}=E_z\mathbf{e}_z+\mathbf{E}_t,\ \ \mathbf{B}=B_z\mathbf{e}_z+\mathbf{B}_t$$

$$\mathbf{B}_t=\frac{1}{\left(\varepsilon\mu\frac{\omega^2}{c^2}-k^2\right)}\left[\nabla_t\left(\frac{\partial B_z}{\partial z}\right)+i\varepsilon\mu\frac{\omega}{c}\mathbf{e}_z\times\nabla_t E_z\right],$$

$$\mathbf{E}_t=\frac{1}{\left(\varepsilon\mu\frac{\omega^2}{c^2}-k^2\right)}\left[\nabla_t\left(\frac{\partial E_z}{\partial z}\right)-i\frac{\omega}{c}\mathbf{e}_z\times\nabla_t B_z\right]$$

TM- mode Assign

TM-mode : $\mathbf{B_z} = 0,\ \boldsymbol{E_z} \neq 0$ → Can accelerate beam Beam

$$\mathbf{B}_t = \frac{i\varepsilon\mu\frac{\omega}{c}}{\left(\varepsilon\mu\frac{\omega^2}{c^2} - k^2\right)}\left[\mathbf{e}_z \times \nabla_t E_z\right],$$

$$\mathbf{E}_t = \frac{1}{\left(\varepsilon\mu\frac{\omega^2}{c^2} - k^2\right)}\nabla_t\left(\frac{\partial E_z}{\partial z}\right),$$

$$\left[\nabla_t^2 E_z + (\varepsilon\mu\frac{\omega^2}{c^2} - k^2)\right]E_z = 0,$$

→ **Solve the eigenvalue problem, get k and Ez**

Boundary condition $E_z|_S = 0$ **(** $\because$ $\mathbf{n}\times\mathbf{E} = 0$ **on the surface of perfect conducto**

$\frac{\partial B_z}{\partial n}|_S = 0$ **(** $\because$ $\mathbf{n}\cdot\mathbf{B} = 0$ **on the surface,**

but automatically satisfied by the TM mode condition)

TE-mode Assign

TE-mode : $\boldsymbol{E_z} = 0\,,\ \boldsymbol{B_z} \neq 0$ ⇒ **Can not accelerate**

$$\mathbf{B}_t = \frac{i\varepsilon\mu\frac{\omega}{c}}{(\varepsilon\mu\frac{\omega^2}{c^2} - k^2)} \nabla_t \left(\frac{\partial B_z}{\partial z} \right),$$

$$\mathbf{E}_t = \frac{-i\frac{\omega}{c}}{\left(\varepsilon\mu\frac{\omega^2}{c^2} - k^2 \right)} \mathbf{e}_z \times \nabla_t B_z,$$

$$\left[\nabla_t^2 B_z + (\varepsilon\mu\frac{\omega^2}{c^2} - k^2) \right] B_z = 0,$$

Boundary condition $E_z|_S = 0$ **(** $\because\ \mathbf{n} \times \mathbf{E} = 0$ **on the surface of perfect conductor**

but automatically satisfied by the TE-mode condition)

$$\frac{\partial B_z}{\partial n}\Big|_S = 0 \ (\because\ \mathbf{n} \cdot \mathbf{B} = 0 \text{ on the surface})$$

Eigevalue problem

$$\psi(x,y) = E_z(x,y) \text{ for TM- mode or } B_z(x,y) \text{ for TE- mode}$$

$$\left(\vec{\nabla}_t^2 + \gamma^2\right)\psi = 0, \quad \psi\big|_S = 0 \text{ (for TM - mode) or } \frac{\partial}{\partial n}\psi\big|_S = 0 \text{ (for TE - mode)}$$

$$\gamma^2 = \varepsilon\mu\frac{\omega^2}{c^2} - k^2 \geq 0$$

From the boundary condition,

$$\gamma^2 = \gamma_\lambda^2, \ \psi = \psi_\lambda \quad (\lambda = 1, 2, \cdots)$$

$$\Rightarrow \quad k_\lambda^2 = \varepsilon\mu\frac{\omega^2}{c^2} - \gamma_\lambda^2$$

If $\omega < c\frac{\gamma_\lambda}{\sqrt{\varepsilon\mu}}$, then k_λ is an imaginal number. The wave is damped in the waveguic

$$\omega_\lambda = c\frac{\gamma_\lambda}{\sqrt{\varepsilon\mu}} \cdots \text{cutoff frequency}$$

When $\omega \geq \omega_\lambda$, wave number k_λ is a real number,

then the wave can propagate into the waveguide.

TM-mode in a Pill Box Cavity

TM-modes

$$\mathbf{E}(x,y,z,t)=\mathbf{E}(x,y)\exp(ikz-i\omega t)$$

When shorted at $z=0$ and $z=d$, then the wave makes a standing wave.

$$\therefore\ \mathbf{E}(x,y,z,t)=\left[\mathbf{A}(x,y)\cos(kz)+\mathbf{B}(x,y)\sin(kz)\right]\exp(-i\omega t)$$

If the cavity is made from perfect conductor, $\mathrm{E}_{\mathrm{t}}=0\ at\ z=0$ and d.

$$\therefore\ \mathbf{E}(x,y,z)=\mathbf{B}(x,y)\sin(kz)\ \text{and}\ \sin(kd)=0\Rightarrow kd=p\pi(p=0,1,2,\cdots)\Rightarrow k=\frac{p\pi}{d}$$

$$\mathbf{E}_z(x,y,z)=\Psi(x,y,z)\mathbf{e}_z=\left[\mathbf{A}_z(x,y)\cos(kz)+\mathbf{B}_z(x,y)\sin(kz)\right]\mathbf{e}_z$$

$$\mathbf{E}_t(x,y,z,)=\frac{1}{\gamma^2}\nabla_t\left(\frac{\partial\Psi}{\partial z}\right),\ \text{and the boundary condition: } \mathrm{E}_{\mathrm{t}}=0 \text{ at } z=0.$$

$$\Rightarrow\Psi=B_z(x,y)\cos(kz)=B_z(x,y)\cos(\frac{p\pi}{d}z)$$

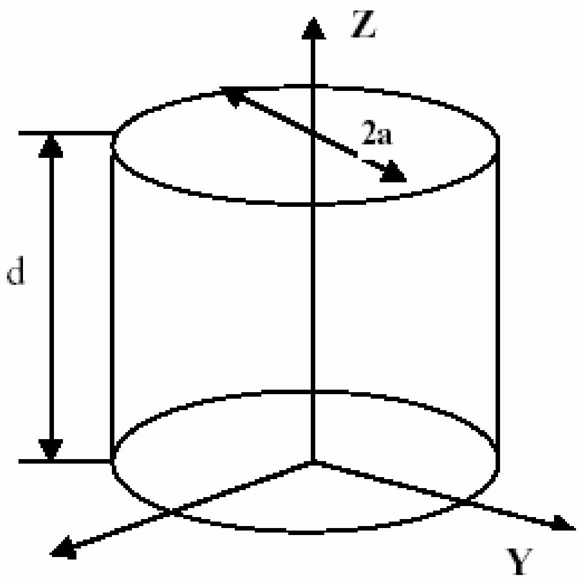

Now one can solve the eigenvalue problem.

$$\left(\nabla_{\mathrm{t}}^2+\gamma^2\right)\Psi=0,\ \gamma^2=\varepsilon\mu\frac{\omega^2}{c^2}-k^2=\varepsilon\mu\frac{\omega^2}{c^2}-\left(\frac{p\pi}{d}\right)^2$$

Cylindorical cordinate (r,θ,z), $\Psi\rightarrow\Psi{=}B_z(r,\theta)$

$$\left(\nabla_t^2+\gamma^2\right)\Psi=\left(\frac{\partial^2}{\partial^2 r}+\frac{1}{r}\frac{\partial}{\partial r}+\frac{1}{r^2}\frac{\partial^2}{\partial^2\theta}\right)\Psi+\gamma^2\Psi=0$$

$$\Psi(r,\theta)=R(r)\cdot\Theta(\theta)$$

$$r^2 \frac{\partial^2 R(r)}{\partial^2 r} + \frac{r}{R(r)} \frac{\partial R(r)}{\partial r} + \gamma^2 r^2 = -\frac{1}{\Theta(\theta)} \frac{\partial^2 \Theta(\theta)}{\partial^2 \theta}$$

$$-\frac{1}{\Theta(\theta)} \frac{\partial^2 \Theta(\theta)}{\partial^2 \theta} = m^2 \Rightarrow \Theta(\theta) = \Theta_0 \exp(\pm im\theta), m = 0, 1, 2, \cdots$$

Θ is for a single-value function at θ=0 ~ 2π.

ρ=γr,

$$\frac{\partial^2 R}{\partial^2 \rho} + \frac{1}{\rho} \frac{\partial R}{\partial \rho} + (1 - \frac{m^2}{\rho^2}) R = 0 \Rightarrow R : mthBesselfunction(J_m)$$

For no divergence at ρ=0 $\Rightarrow R(\rho) = J_m(\rho)$

Boundary condition: $E_z(r, \theta) = 0$ at $r = a \Rightarrow J_m(\gamma a) = 0 \Rightarrow \gamma a = \rho_{m,n}$: nth solution of J_m

$\rho_{m,n}$	n=1	n=2	n=3
m=0	$\rho_{0,1} = 2.405$	$\rho_{0,2} = 5.520$	$\rho_{0,3} = 8.654$
m=1	$\rho_{1,1} = 3.832$	$\rho_{1,2} = 7.016$	$\rho_{1,3} = 10.173$
m=2	$\rho_{2,1} = 5.136$	$\rho_{2,2} = 8.417$	$\rho_{2,3} = 11.620$

$$\gamma_{m,n} = \frac{\rho_{m,n}}{a}, \quad \text{thus } \Psi(r, \theta) = J_m(\frac{\rho_{m,n}}{a} \cdot r) \cdot \exp(\pm im\theta),$$

Resonance frequency ($\text{TM}_{m,n,p}$ – mode)

$$\omega_{m,n,p} = \frac{c}{\sqrt{\varepsilon\mu}} \sqrt{\frac{\rho_{m,n}}{a^2} + \frac{p^2 \pi^2}{d^2}}$$

For E_t and B_t, calculate

$$\mathbf{B}_t = \frac{i\varepsilon\mu\frac{\omega}{c}}{\left(\varepsilon\mu\frac{\omega^2}{c^2} - k^2\right)}\left[\mathbf{e}_z \times \nabla_t E_z\right],$$

$$\mathbf{E}_t = \frac{1}{\left(\varepsilon\mu\frac{\omega^2}{c^2} - k^2\right)}\nabla_t\left(\frac{\partial E_z}{\partial z}\right),$$

$TM_{m,n,p}$ − mode

$$E_z = E_o \cos(kz) J_m(\frac{\rho_{m,n}}{a} r)\exp(-im\theta), \qquad B_z = 0$$

$$E_r = \frac{iE_0 p\pi}{\gamma_{m,n,p}}\cos(\frac{p\pi}{d}z)\frac{\partial J_m(\rho)}{\partial\rho}\exp(-im\theta), \qquad B_r = -\frac{E_0 m\varepsilon\mu\omega_{m,n,p}}{}\cos(kz)J_m(\frac{\rho_{m,n}}{a}r)\exp(-im\theta)$$

$$E_\theta = \frac{E_0 mp\pi}{\gamma_{m,n,p}^2 dc}\cos(\frac{p\pi}{d}z)J_m(\frac{\rho_{m,n}}{a}r)\exp(-im\theta), \quad B_\theta = \frac{iE_0\varepsilon\mu\omega_{m,n,p}}{\gamma_{m,n,p}c}\cos(kz)\exp(-im\theta)\frac{\partial J_m(\rho)}{\partial\rho}$$

Design of TM_{010}-mode single cell cavity

$$E_z = E_0 J_0\left(\frac{\rho_{0,1}}{a} r\right) = E_0 J_0\left(\frac{2.405}{a} r\right), \quad B_z = 0$$

$$E_r = 0, \qquad B_r = 0$$

$$E_\theta = 0, \qquad B_\theta = -\frac{iE_0 \varepsilon\mu\omega_{0,1,0}}{\gamma_{0,1,0} c} J_1\left(\frac{2.405}{a} r\right)$$

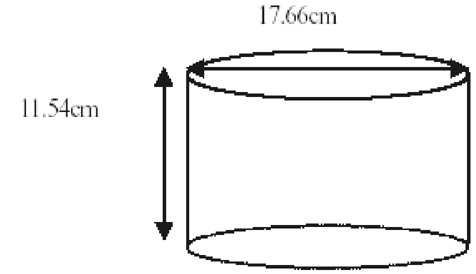

Here, remember $\frac{\partial J_m}{\partial \rho} = mJ_{m-1} - J_{m+1}$

$$\gamma_{0,1,0} = \frac{2.405}{a}, \quad \omega_{0,1,0} = \frac{2.405}{\sqrt{\varepsilon\mu}} \cdot \frac{c}{a}$$

Example of cavity design: 1300MHz,

pill-box type single cell cavity

$$\omega_{0,1,0} = \frac{2.405}{\sqrt{\mu\varepsilon}} \cdot \frac{c}{a} = 2\pi f, \quad a = \frac{2.405 \cdot c}{2\pi f \sqrt{\mu\varepsilon}},$$

c=3.00×10^{10} $cm/\sec$,

$\mu=\mu_o=1$, $\varepsilon=\varepsilon_o=1$ (Gauss unit), a = $\frac{2.405 \times 3.00 \times 10^{10}}{2\pi \times 1.30 \times 10^9} = 8.83c$

$$d = \frac{\lambda}{2} = \frac{c/f}{2} = \frac{3.00 \times 10^{10} / 1.30 \times 10^9}{2} = 11.54cm$$

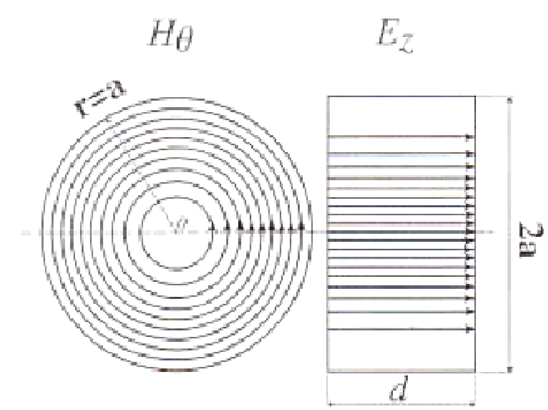

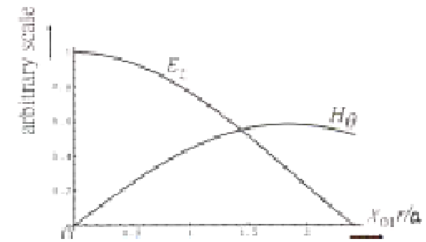

Characteristic parameters of RF cavity

Surface Impedance Z[Ω]: $\boldsymbol{Z} \equiv \dfrac{\mathbf{E}_{//}}{\mathbf{H}_{//}} = \mathbf{R_S} + \boldsymbol{iX}$, $\mathbf{R_S} = \dfrac{1}{\sigma\delta} = \sqrt{\dfrac{\mu\omega}{2\sigma}}$,

Skin depth δ [m] : $\delta = \sqrt{\dfrac{\mathbf{2}}{\mu\omega\sigma}}$

Wall loss P_{loss} [W]: $P_{loss} = \dfrac{1}{2} R_S \int_S H_s^2 ds$ $\left(= \dfrac{\pi R_S E_o^2}{(\mu/\varepsilon)} J_1^2(2.405) \cdot a \cdot (a+d)\right.$ for pill box cavity)

Transit time factor T : $T = \dfrac{\int_0^d E_z e^{i(\omega \times \frac{z}{c})} dz}{\int_0^d E_z dz}$ $\left(= \dfrac{2}{\pi}\right.$ for pill box cavity)

Accelerating Voltage V : $V = \int_0^d E_o(\rho = 0, z)\, e^{i(\omega \cdot \frac{z}{c})} dz$ $(= dE_o T$ for pill box)

Accelerating gradient E_{acc} : $E_{acc} = \dfrac{V}{d}$ $\left(= E_o T = 2\dfrac{E_o}{\pi}\right.$ for pill box cavity)

Stored energy U: $U = \dfrac{1}{2}\mu \int_V H^2 dv = \dfrac{1}{2}\varepsilon \int_V E^2 dv$ $\left(= \dfrac{\pi \varepsilon E_0^2}{2} \cdot J_1^2(2.405) \cdot d \cdot a^2\right.$ for pill box cavity

Unloaded Q - value Q_O: $Q_O = \dfrac{\omega \cdot U}{P_{loss}}$ $\left(= \omega \cdot \dfrac{\mu \cdot a^2 d}{2 \cdot a(a+d)} \cdot \dfrac{1}{R_S}\right.$ for pill box cavity)

Transit time factor

$$E_z(r=0,z,t)=E_0J_0(\frac{p_{0,1}}{a}r)\cdot\exp(-i\omega t)$$

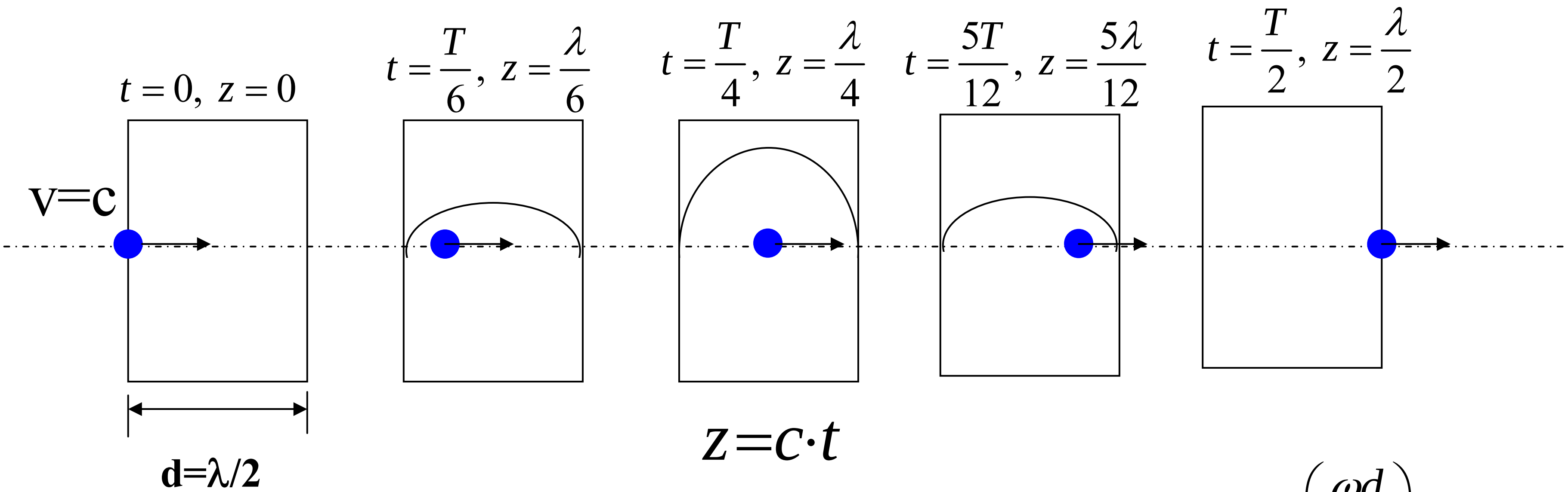

$$V=\left|\int_0^d E_z(r=0,z)e^{i\omega t}dz\right|=\left|\int_0^d E_z(r=0,z)e^{i\omega\frac{z}{c}}dz\right|=E_0\left|\int_0^d e^{i\omega\frac{z}{c}}dz\right|=E_0d\frac{\sin\left(\frac{\omega d}{2c}\right)}{\frac{\omega d}{2c}}=E_0d\cdot T$$

T : Transit time factor

$$T=\frac{2}{\pi}=0.637\ \ \text{(for Pill Box Cavity)}$$

$$Eacc\equiv\frac{V}{d}=E_0T$$

Characteristic parameters of RF cavity

Shunt impedance R_{sh} [Ω]: $R_{sh} = \dfrac{V^2}{P_{loss}}$ $\left(= \dfrac{4(\varepsilon/\mu)d^2}{\pi^3 R_S J_1^2(2.405)a(a+d)}\right.$ **for pill box cavity**

Geometrical factor Γ: $\Gamma = Q_O \cdot R_S = \dfrac{\omega\mu\int_V H^2 dv}{\int_S H_S^2 ds}$ $\left(= \dfrac{\omega\mu d a^2}{2(a^2 + ad)}\right.$ for pill box cavity) $\Rightarrow R_S = \dfrac{\Gamma}{Q_O}$

R/Q : $\left(R/Q\right) = \dfrac{R_{sh}}{Q_O} = \dfrac{V^2}{\omega U}$ Goodness of the cavity shape,No dependent on material

E_{SP}/E_{acc} $\left(= \dfrac{\pi}{2} = 1.57\right.$ for pill box cavity), H_{SP}/E_{acc} $\left(= 30.5 \dfrac{O_e}{MV/m}\right.$ for pill box cavity)

Smaller value is better from field emission problem point of view

Smaller value is better from high gradient point of view

Pill-box cavity maximum Eacc = 1750/30.5 =57.4MV/m

Frequency dependence of the cavity parameters

Characteristic Parameter	ω dependence Normal conducting	ω dependence Super conducting
R_S	$\omega^{\frac{1}{2}}$	ω^{2}
P_{loss}	$\omega^{-\frac{3}{2}}$	No dependence
U	ω^{-3}	ω^{-3}
Q_O	$\omega^{-\frac{1}{2}}$	ω^{-2}
R_{sh}	$\omega^{-\frac{1}{2}}$	ω^{-2}
R_{sh}/L	$\omega^{\frac{1}{2}}$	ω^{-1}
Γ	No dependence	No dependence
R/Q	No dependence	No dependence

Rsh per length linearly increases to $\sqrt{\omega}$, so normal conducting choose higher frequency, for example 11.4GHz @ warm LC.

3.2 Criteria General for Cavity Shape

- Suppressed Multipacting
- Lower Surface Electric field

2001-2004

- Lower Surface Magnetic field
- High Efficient
- High Gradient

} incorporate

Real Cavity Design

1) Need a hole on the cavity for electron to pass the cavity
2) Need RF input port
3) HOM coupler port

Need Beam pipes on both Ends

4) High efficient cavity
5) Better performance
   Smaller Ep/Eacc : Field emission
   Smaller Hp/Eacc : Multipaction

Optimization of cell shape
Multi-cell cavity

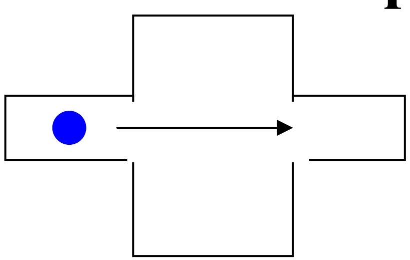

Choose spherical shape to reduce multipacting

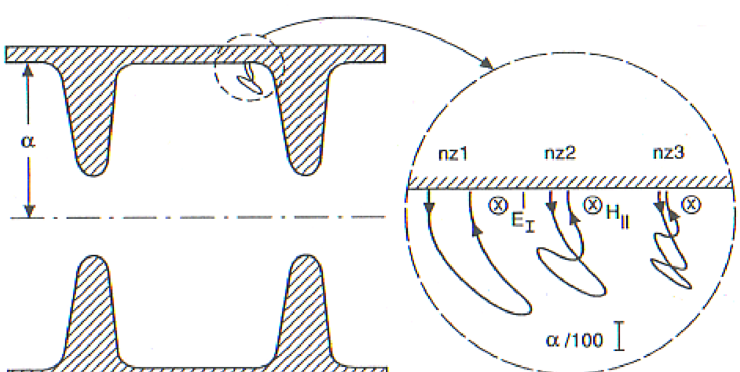

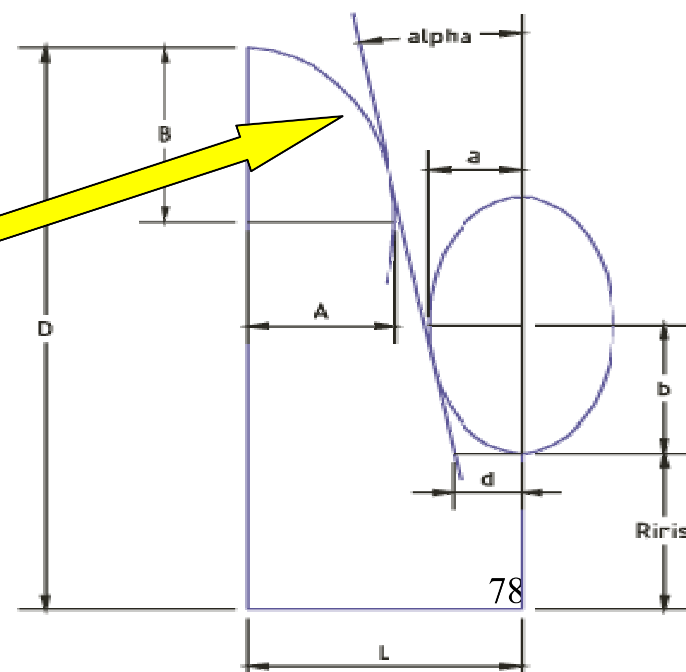

Cavity Design (single cell cavity)

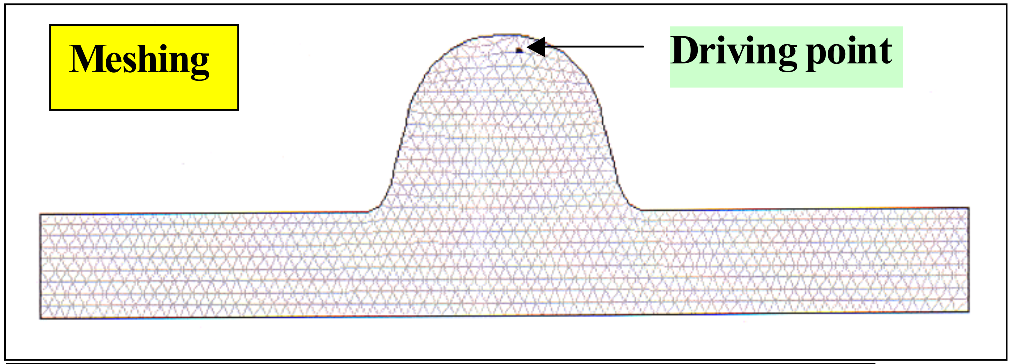

Superfish

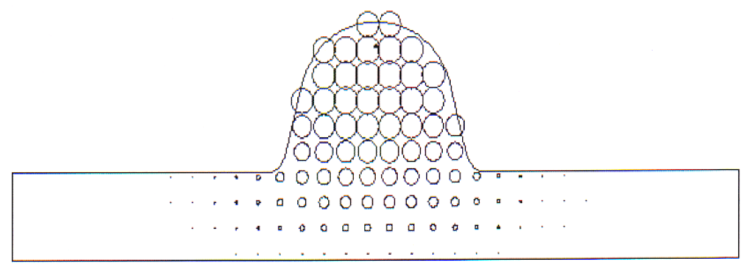

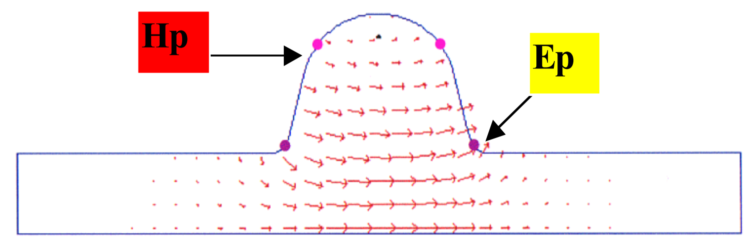

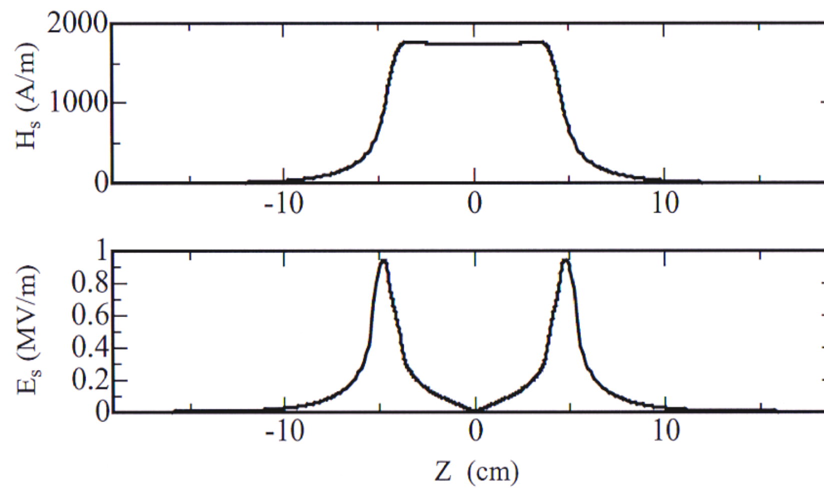

All calculated values below refer to the mesh geometry only.
Field normalization (NORM = 0): EZERO = 1.00000 MV/m
Length used for E0 normalization = 10.76000 cm
Frequency (starting value = 1300.000) = 1293.77430 MHz
Particle rest mass energy = 0.510999 MeV
Beta = 1.0000000
Normalization factor for E0 = 1.000 MV/m = 7048.913
Transit-time factor Abs(T+iS) = 0.5454664
Stored energy = 0.0038869 Joules
Using standard room-temperature copper.
Surface resistance = 9.38405 milliOhm
Normal-conductor resistivity = 1.72410 microOhm-cm
Operating temperature = 20.0000 C
Power dissipation = 1118.1551 W
Q = 28257.6 Shunt impedance = 96.230 MOhm/m
Rs*Q = 265.171 Ohm Z*T*T = 28.632 MOhm/m
r/Q = 109.024 Ohm Wake loss parameter = 0.22157 V/pC
Average magnetic field on the outer wall = 1729.9 A/m, 1.40411 W/cm^2
Maximum H (at Z,R = 3.32643,8.55466) = 1753.44 A/m, 1.44258 W/cm^2
Maximum E (at Z,R = 4.75232,4.24425) = 0.946176 MV/m, 0.02953 Kilp.
Ratio of peak fields Bmax/Emax = 2.3288 mT/(MV/m)
Peak-to-average ratio Emax/E0 = 0.9462

mer S
Note

High Gradient Shapes

Cavity shape designs with low Hp/Eacc

from J.Sekutowicz lecture Not

TTF: TESLA shape
Reentrant (RE): Cornell Univ.
Low Loss(LL): JLAB/DESY
Ichiro-Single（IS）： KEK

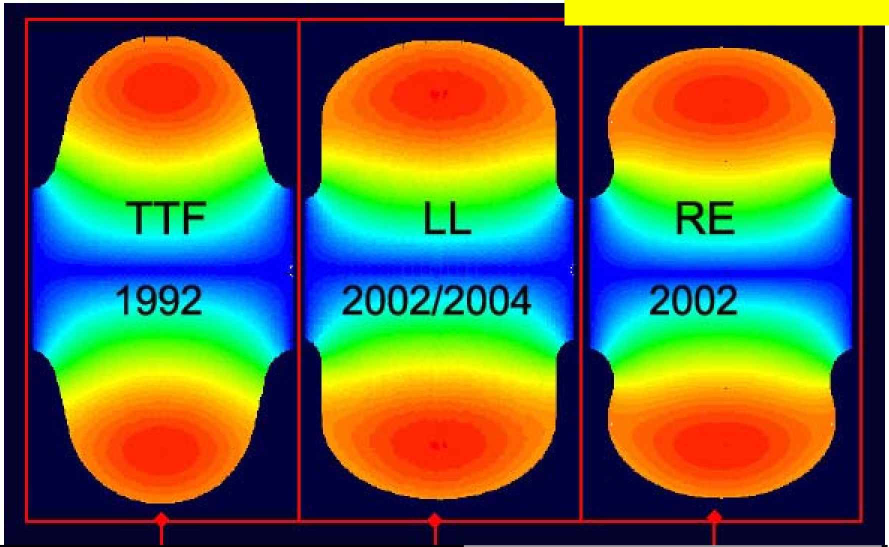

	TESLA	LL	RE	IS
Diameter [mm]	**70**	**60**	**66**	**61**
Ep/Eacc	**2.0**	**2.36**	**2.21**	**2.02**
Hp/Eacc [Oe/MV/m]	**42.6**	**36.1**	**37.6**	**35.6**
R/Q [W]	**113.8**	**133.7**	**126.8**	**138**
G[W]	**271**	**284**	**277**	**285**
Eacc max	**41.1**	**48.5**	**46.5**	**49.2**

Eacc vs. Year

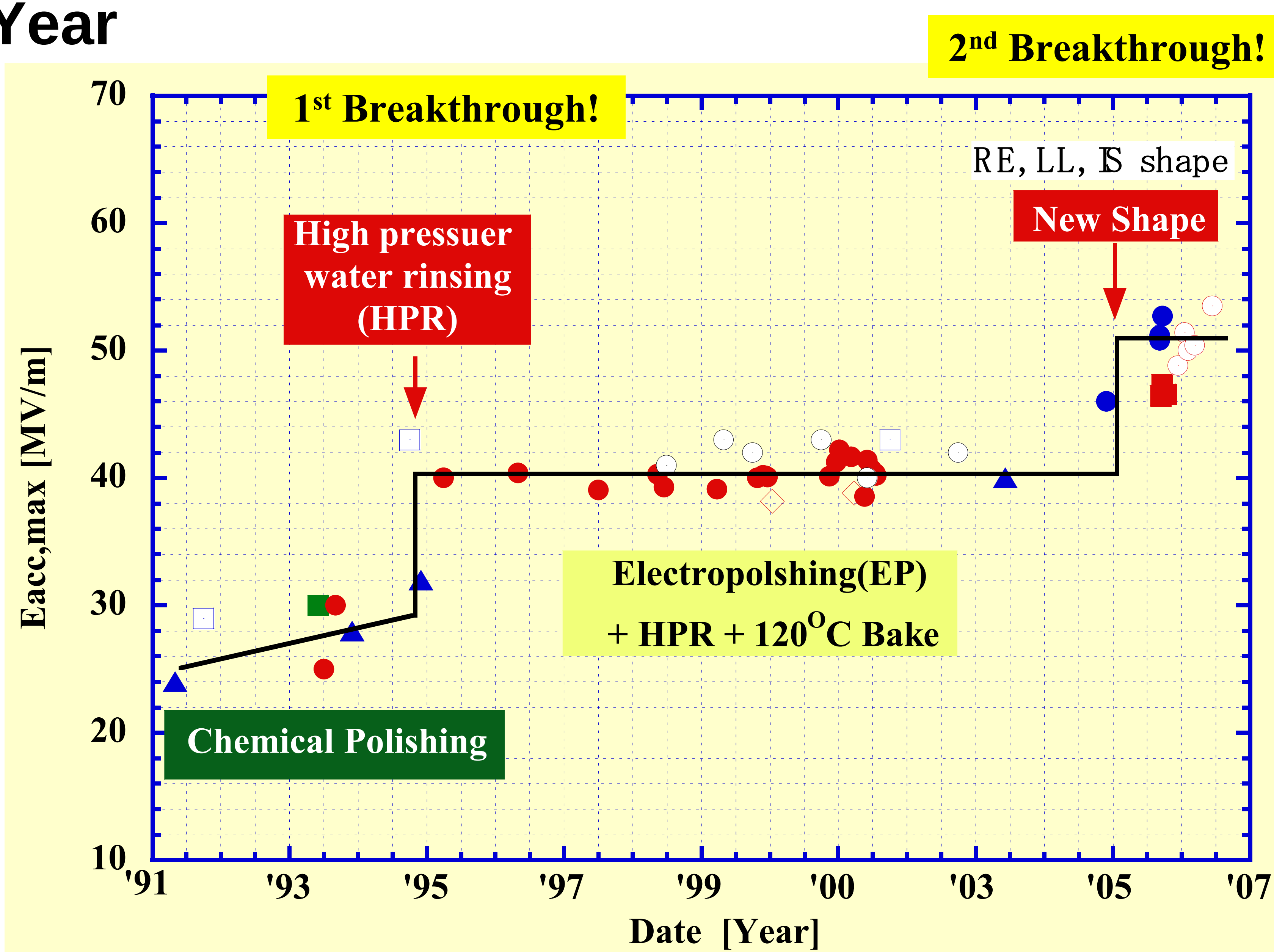

2nd Breakthrough!
1st Breakthrough!
RE, LL, IS shape
New Shape
High pressuer water rinsing (HPR)
Electropolishing(EP) + HPR + 120°C Bake
Chemical Polishing
70
60
50
40
30
20
10
Eacc,max [MV/m]
'91
'93
'95
'97
'99
'00
'03
'05
'07
Date [Year]

3.3 Criteria for Multi-cell Structures

Pros and cons for a multi-cell structure

- *Cost of accelerators is lower (less auxiliaries: LHe vessels, tuners, fundamental power couplers, control electronics)*
- *Higher real-estate gradient (better fill factor)*

- *Field flatness vs. N*
- *HOM trapping vs. N*
- *Power capability of fundamental power couplers vs. N*
- *Chemical treatment and final preparation become more complicated*
- *The worst performing cell limits whole multi-cell structure*

How to decide the number of cells

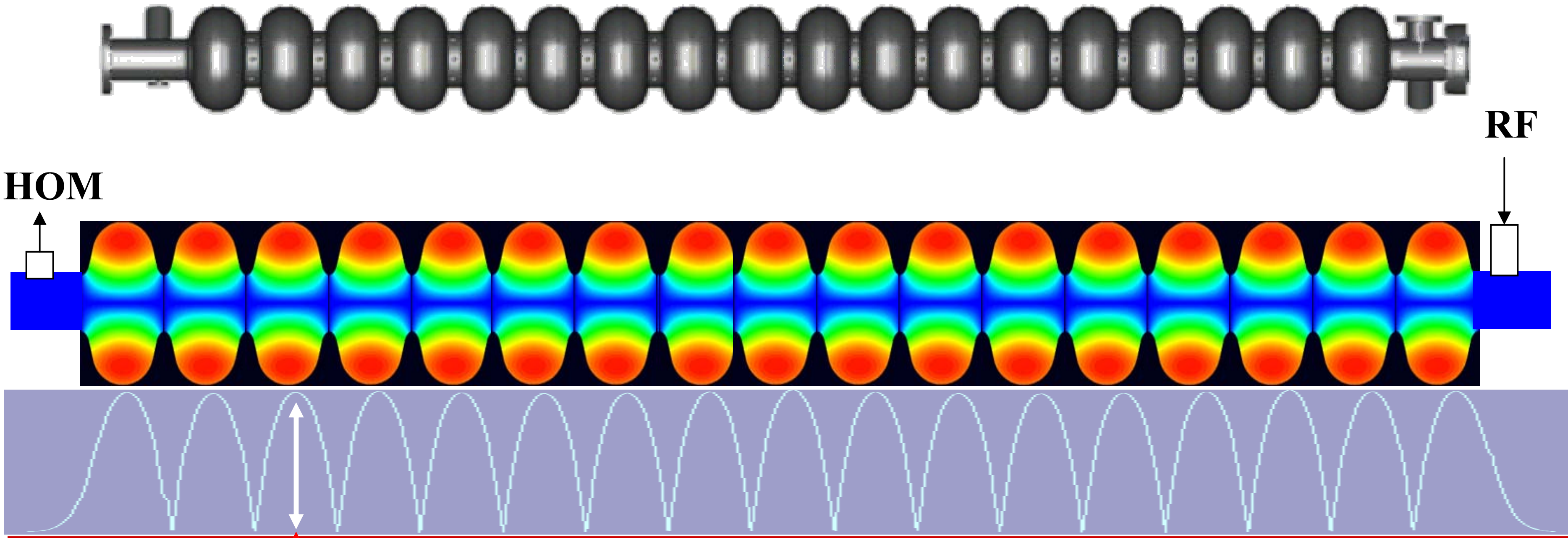

$$\frac{\Delta A_i}{A_i} = a_{ff}\,\frac{\Delta f_i}{f_i} = \frac{N^2}{k_{cc}} \cdot \frac{\Delta f_i}{f_i}$$

Beam pipe has no acceleration beam.
BP reduce the efficiency.
Multi-cell is more efficient.

N: number of cells

Field flatness factor : $a_{ff} = \frac{N^2}{k_{cc}}$

Cell to cell coupling : $k_{cc} = 2 \cdot \frac{f_\pi - f_0}{f_\pi + f_0}$

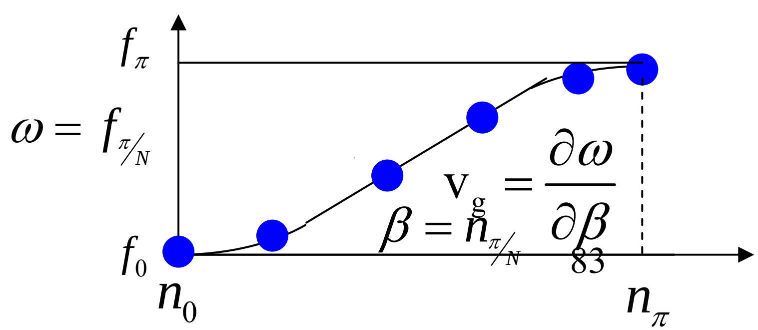

HOM trapping vs. N

No fields at HOM couplers positions, which are always placed at end beam tubes

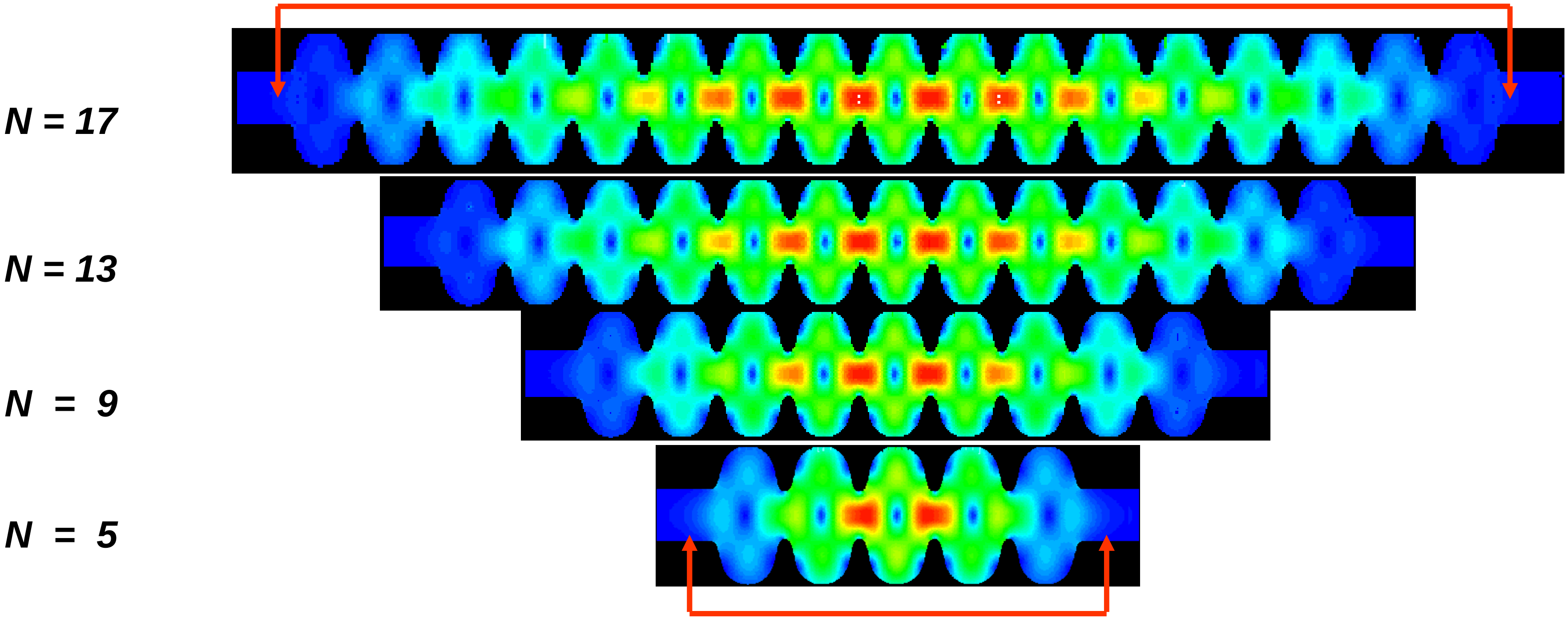

e-m fields at HOM couplers positions

Smaller number of cells is easy to take out HOMs.

HOM Calculation on ICHIRO cavity by SLAC/KEK/DESY collaboration

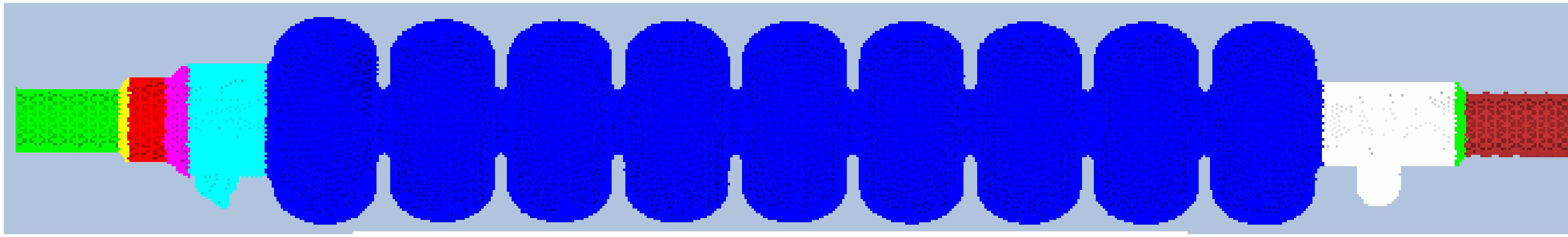

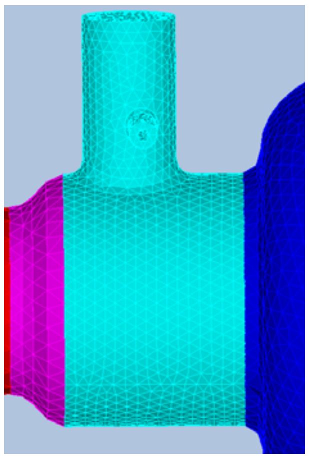

Mesh Info: non-uniform mesh

elements: 343991
coordinates: 66759
BOUNDING BOX:
  min = (-0.116009, -0.100575, 0)
  max= (0.100515, 0.100575, 1.52446)
EDGE LENGTH:
  min = 2.94128e-07
  max = 0.0274961
  average = 0.00882544
  std dev = 0.00274525

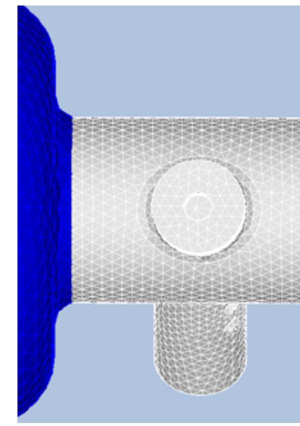

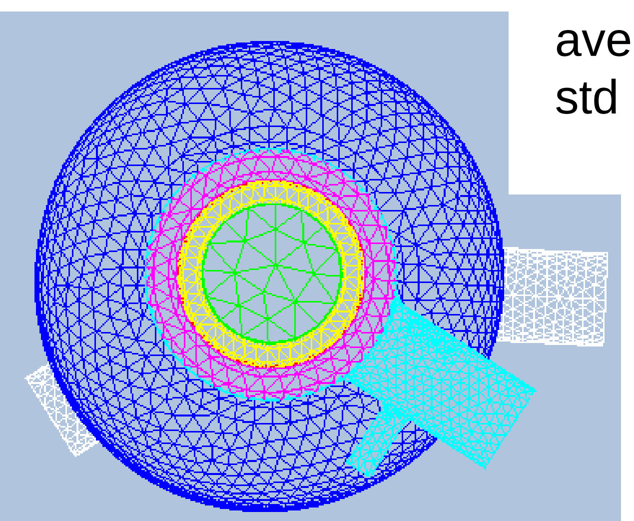

Sample Mesh

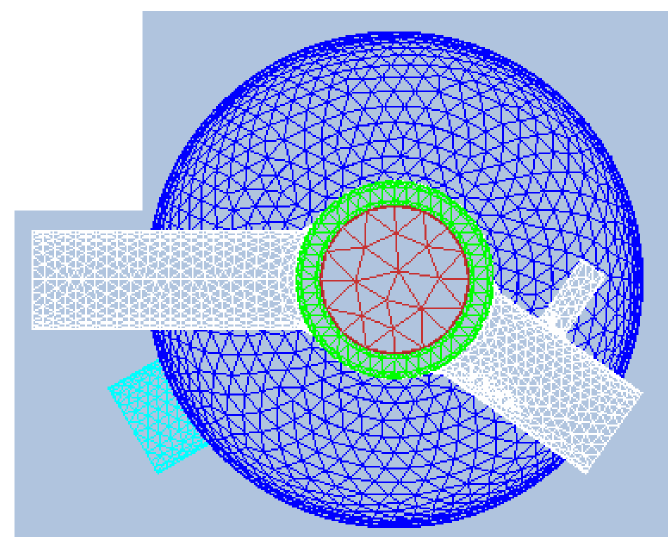

RF Structure Simulation

Currently full 3D analysis is possible using cords Omega or ANALIS, example SLAC, KEK

Element Model (Mesh)

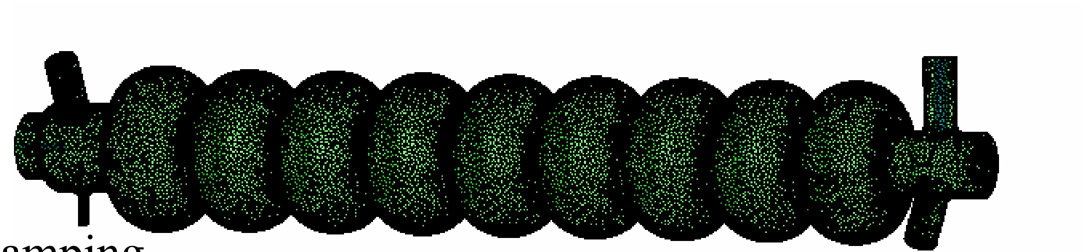

Simulation of Higher Order Mode Damping

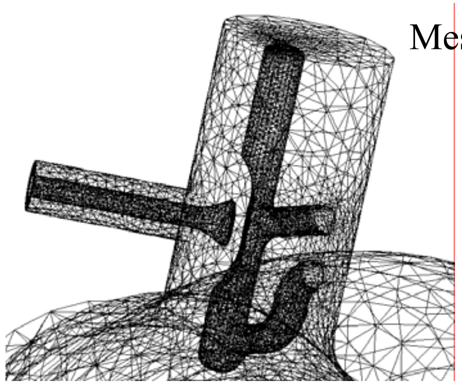

Mesh of HOM Damper

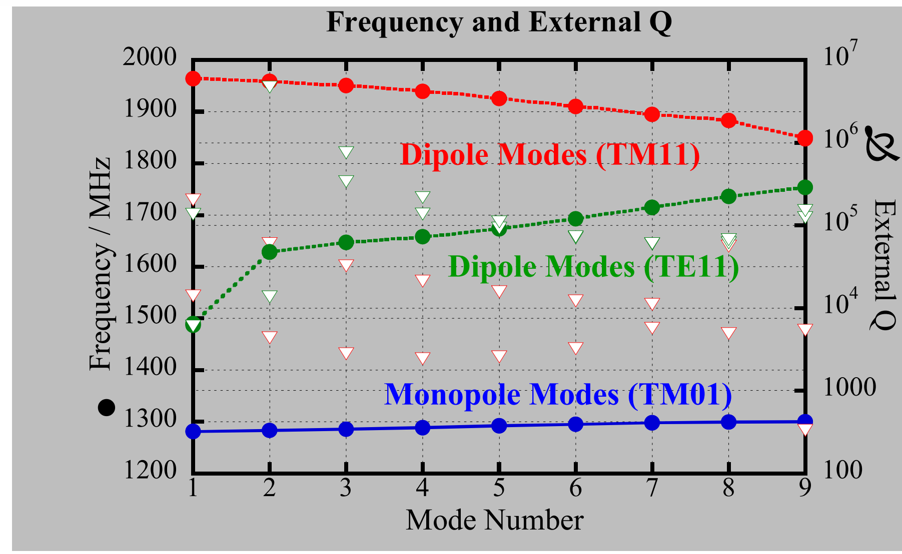

Analysis of Wall Loss in Vertical Testing

Measured Low Q of 1.1×10^{10} at 21 MV/m for 38 W ----- Reproduced by Simulation

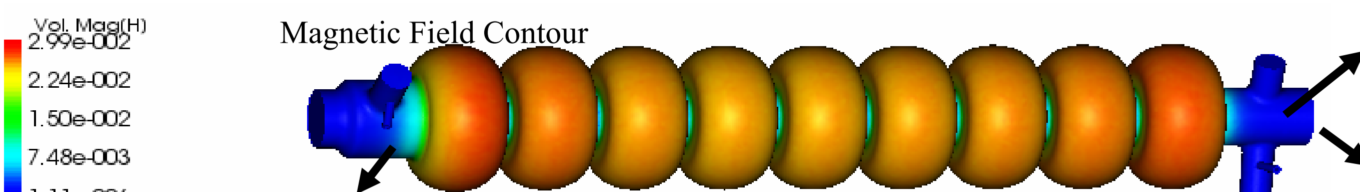

«1 W

15.8 W on SUS 316 Wall

0.7 W on SUS 316L Wall

21.8 W on Niobium Walls

Note

Field distributions in passband modes of 9-cell cavity

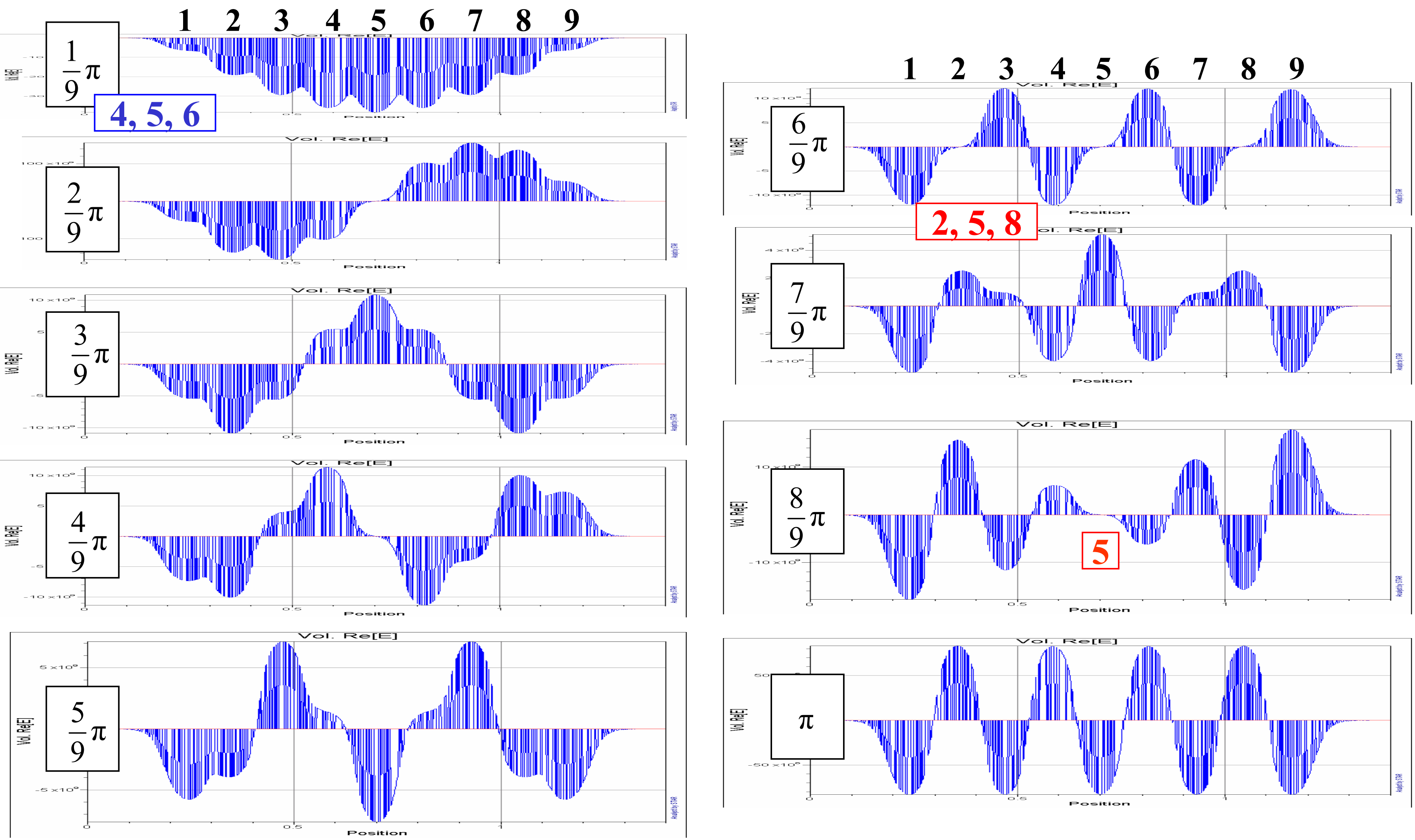

17000 cavities

BCD Cavity shape : TESLA

ACD cavity shape : LL

4. HOM Issues

4.1 HOM
4.2 HOM Coupler

4.1 HOM (Higher Order Mode)

The beam will excite HOM modes if it passes off beam axis of the cavity.

J.Sekutwitz's Slide

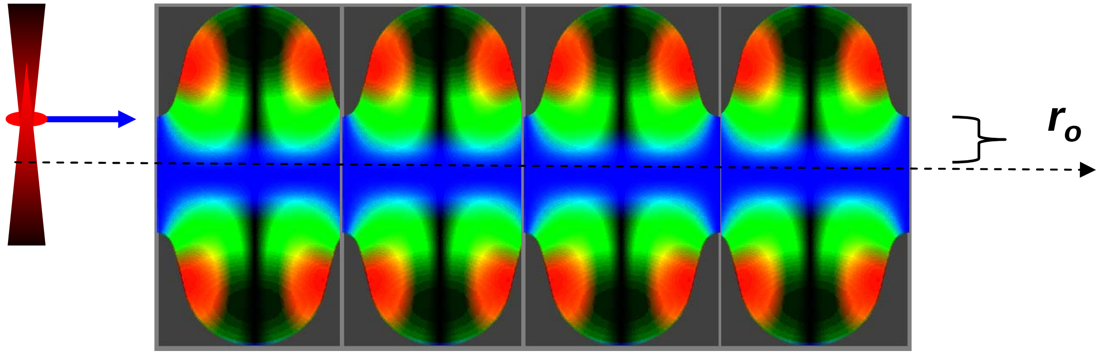

*The amount of induced energy by charge **q** is:*

$$\Delta U_q = k_{/} \cdot q^2 \quad \text{for monopole modes (max. on axis)}$$

$$\Delta U_q = k_{\perp} \cdot q^2 \quad \text{for non monopole modes (off axis)}$$

where $k_{/}$ *and* $k_{\perp}(r)$ *are loss factors for the monopole and transverse modes respectively.*

The induced E-H field is a superposition of cavity eigenmodes having the component of the electric field along the trajectory.

HOM Problem

J.Sekutwitz's Slide

Two kind of phenomena can limit performance of a machine due to the beam induced HOM power*:*

- *Beam Instabilities and/or dilution of emittance*
- *Additional cryogenic power and/or overheating of HOM couplers output lines*

Beam instabilities and/or dilution of emittance

Transverse modes (dipoles) causing emittance growth+ monopoles causing energy spread
This is mainly problem
in linacs*: TESLA or ILC, CEBAF, European XFEL, linacs driving FELs.*

Additional cryogenic power and/or overheating of HOM couplers output lines

Monopoles having high impedance on axis are excited by the beam and store energy which must be coupled out of cavities, since it causes additional cryogenic load, and induces energy spread.
This is mainly problem
in high beam current *machines: B-Factories, Synchrotrons, Electron cooling.*

HOM modes has to be taken out from the cavity through HOM coupler.

Note

Spectra of accelerated beams, which bunches are shorter than 1 mm, extend to hundreds of GHz.

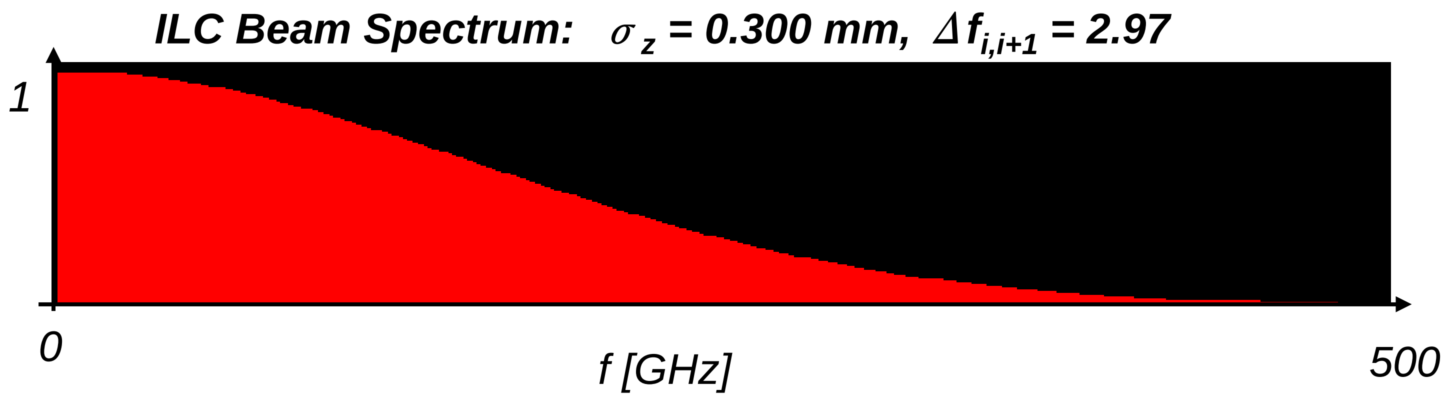

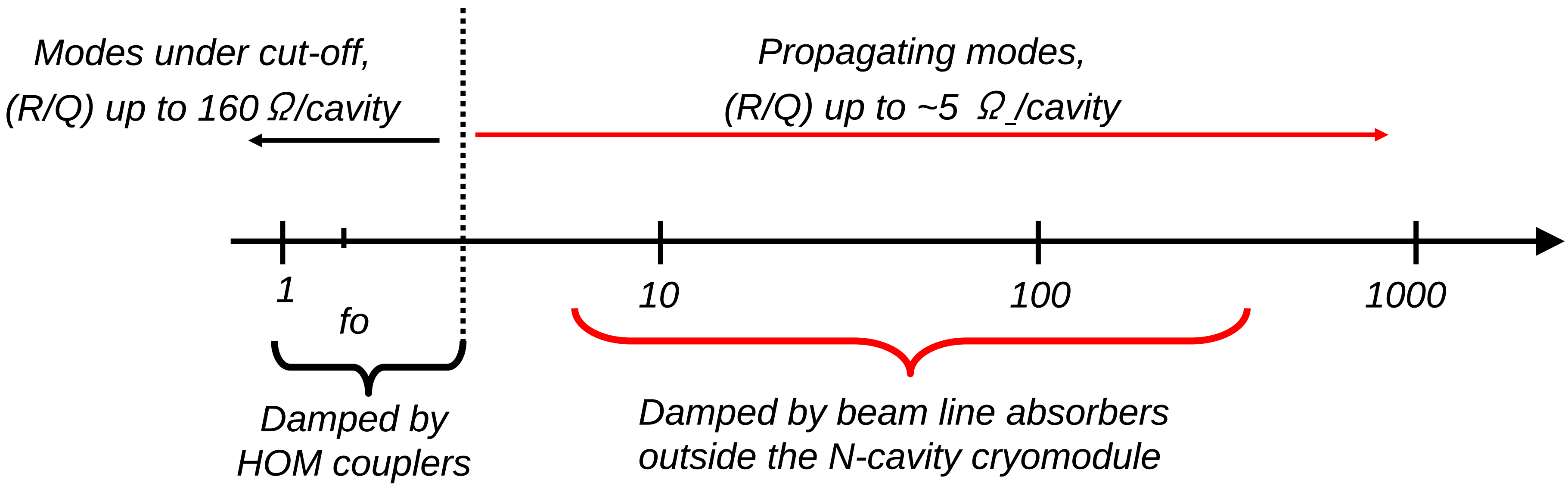

Damping the HOM with higher frequency over than Cut-off frequency

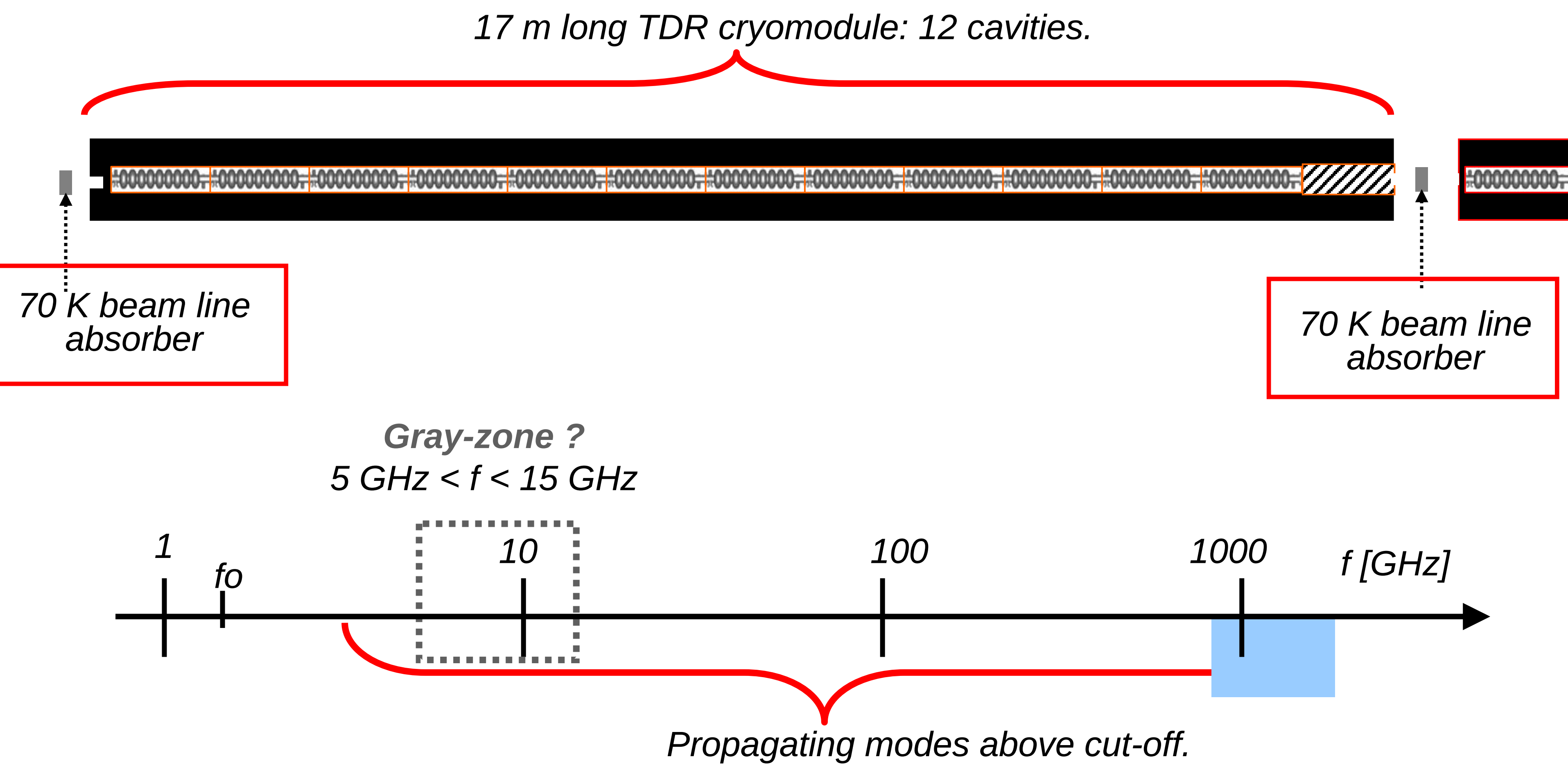

Attention to Trapped modes for damping through HOM coupler

HOM couplers limit RF-performance of sc cavities when they are placed on cells

no E-H fields at HOM couplers positions, which are always placed at end beam tubes

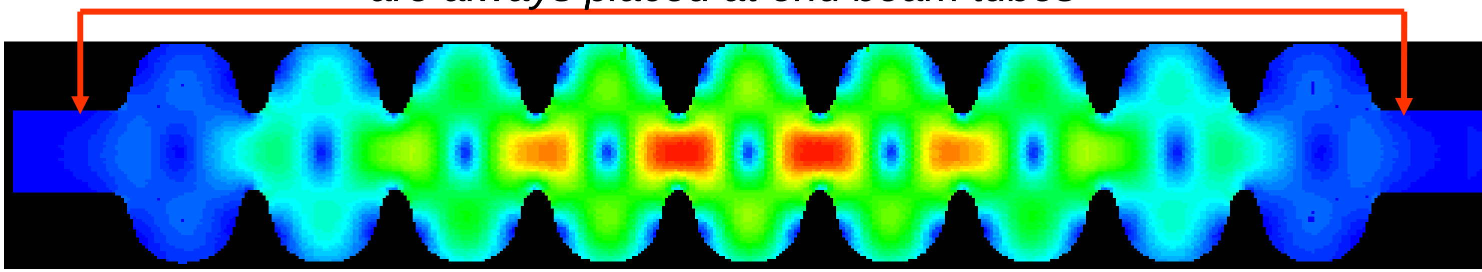

The HOM trapping mechanism is similar to the FM field profile unflatness mechanism:

- *weak coupling HOM cell-to-cell,* $\boldsymbol{k}_{cc,HOM}$
- *difference in HOM frequency of end-cell and inner-cell*

f = 2385 MHz

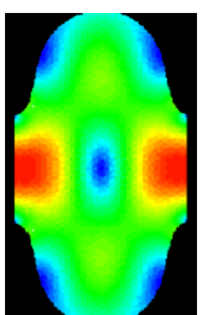

That is why they hardly resonate together

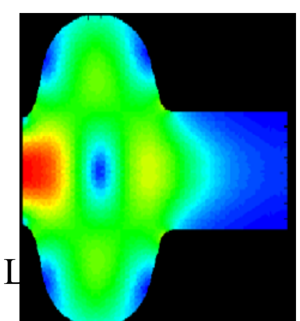

f = 2415 MHz

4.2 HOM Coupler

The TESLA –like HOM couplers are nowadays designed in frequency range: 0.8-3.9 GHz

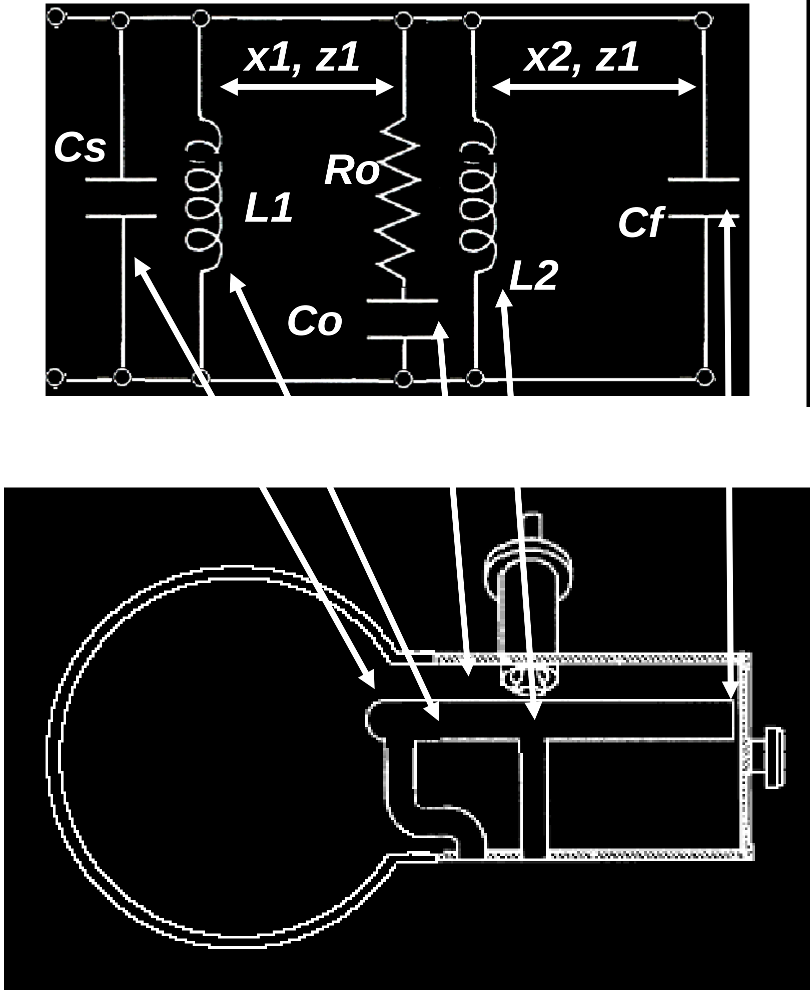

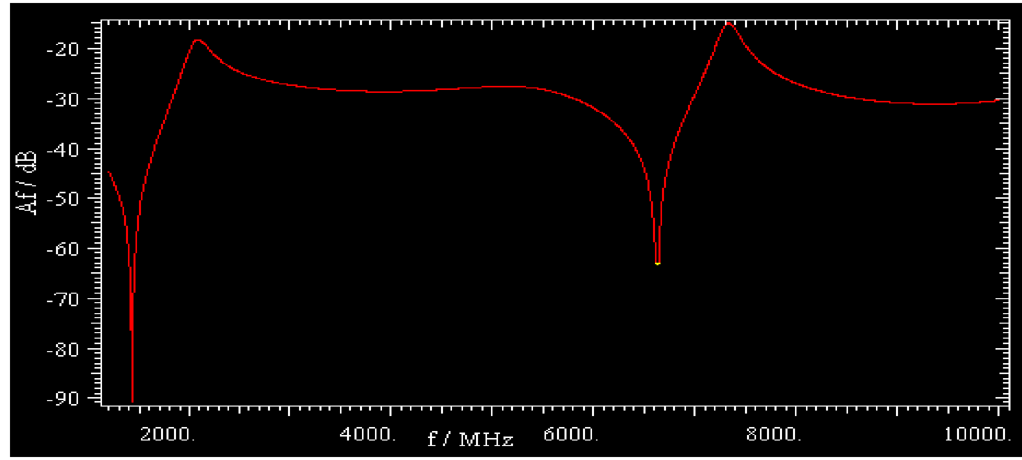

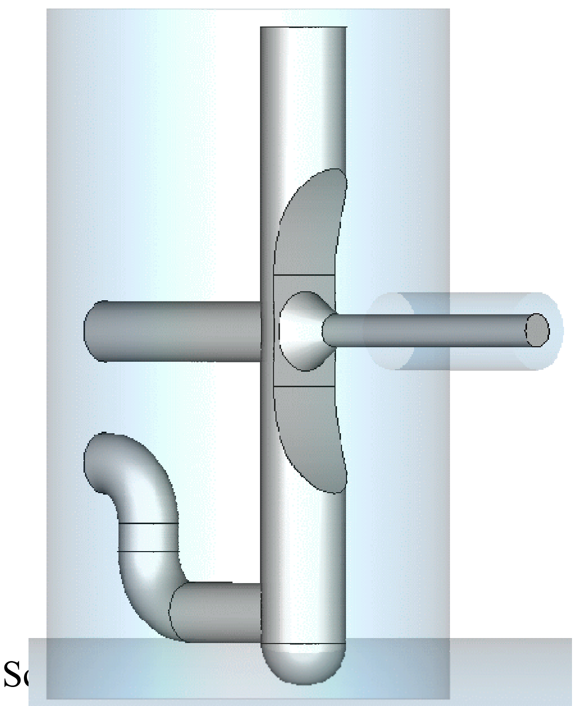

Comparison in Damping Performance of HOMs

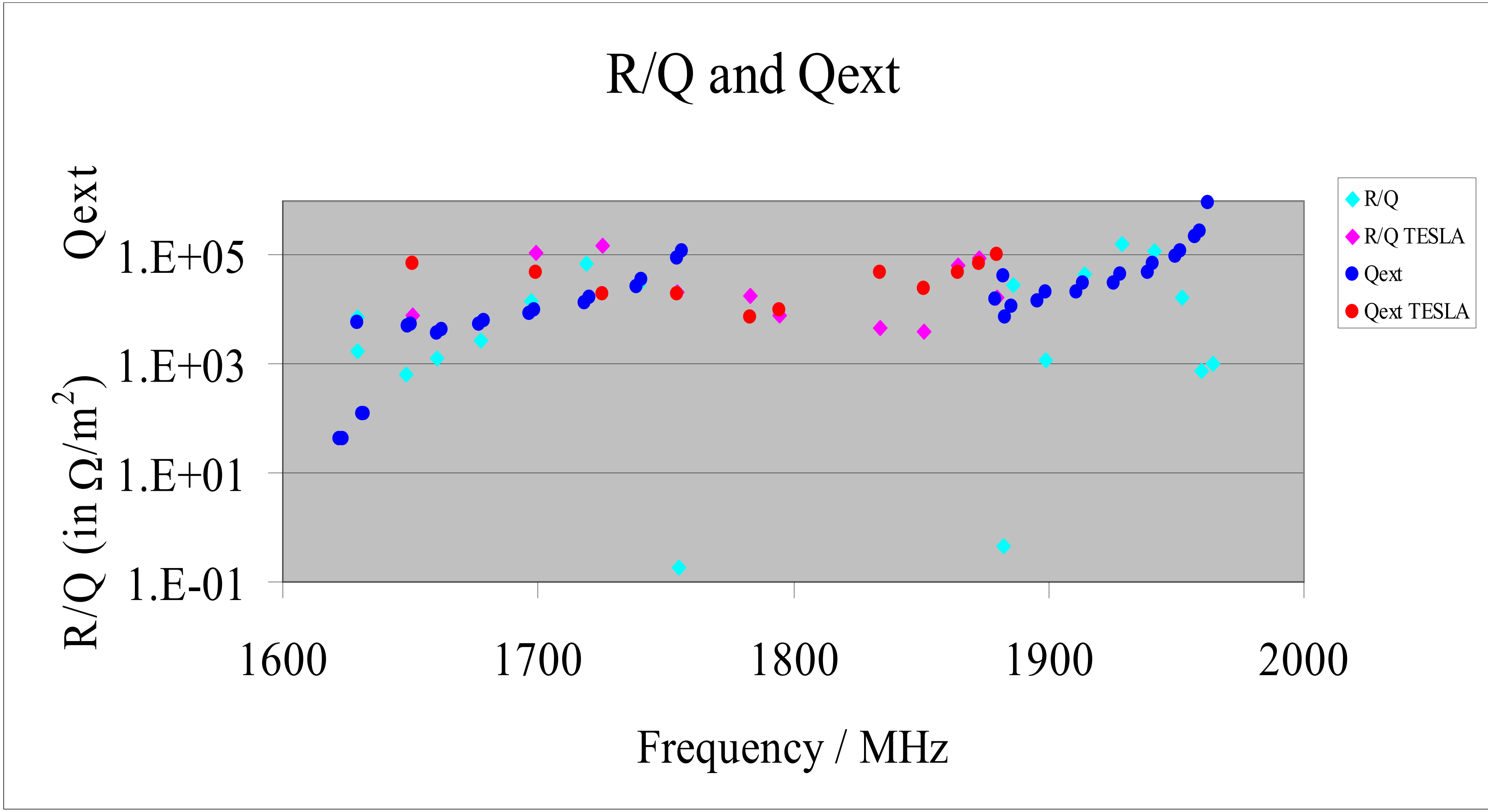

Suppression of Multipacting in HOM Cylinder by better HOM coupler design

By Y.Morozumi @ KEK

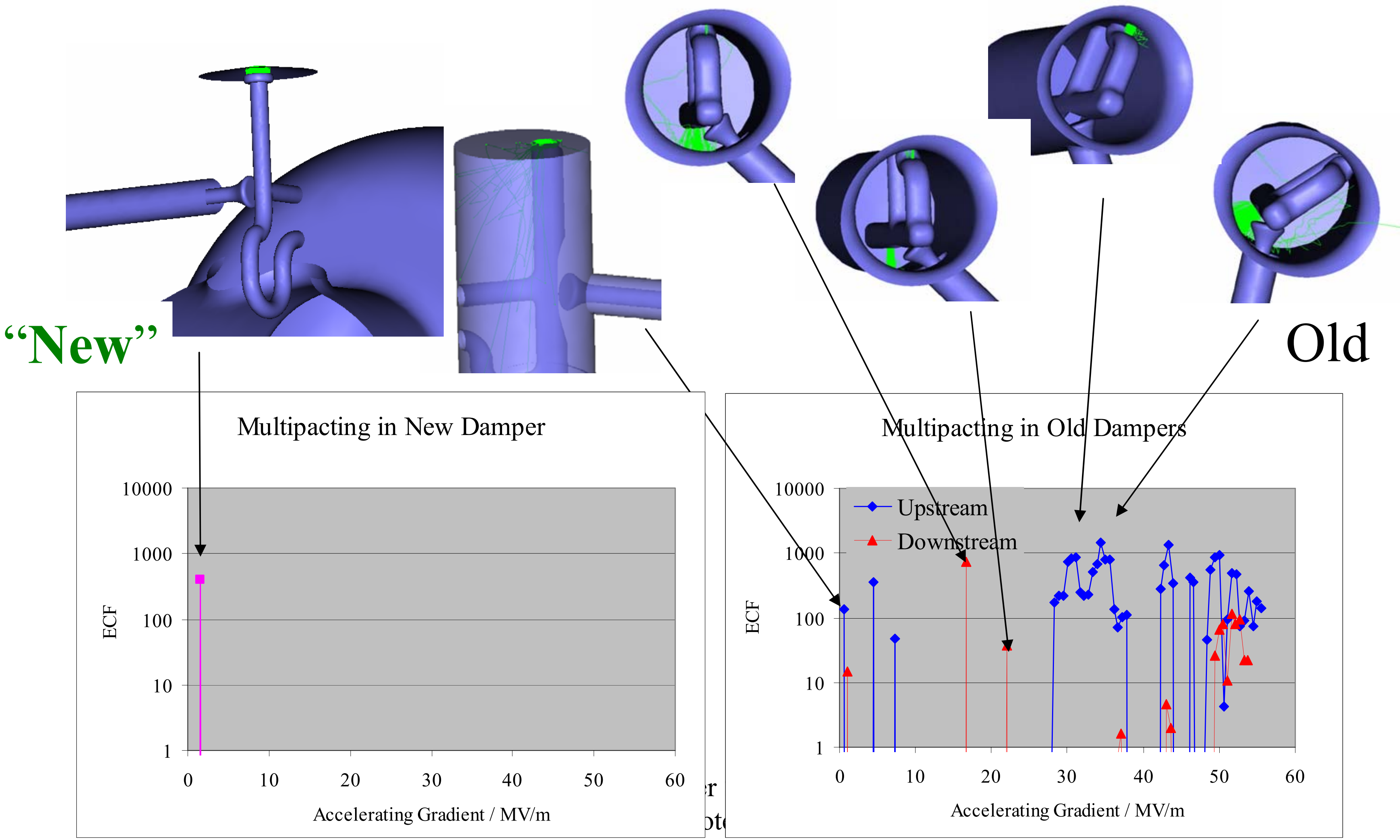

Cavity Design comparison with TESLA

	TTF	STF 45MV/m	Advantage/Disadvantage
Operation gradient	23.4MV/m 35MV/m XFEL TESLA800	45MV/m	1-1.1 TeV in 40km tunnel. If superstructure, 33km for 1TeV
Cavity shape	Iris ϕ70 Beam pipe ϕ78 cell taper 14^{O}	Iris ϕ60 Beam pipe ϕ80/ϕ108 cell taper 0^{O}	Tighter tolerance due to severe wake field
R/Q[Ω]	1036	1144	10% higher electric efficiency
Ep/Eacc	2.00	2.31	
Hp/Eacc[Oe/(MV/m)]	42.6	37.8	Eacc max 46-49MV/m
Cell-to-cell coupling	1.86	1.55	F-flatness more sensitive on fabrication error
Tolerance[μm]	250	170	
Sensitivity for Lorenz detuning[Hz/(MV/m)^2]	1	1.18	Wide detuning range
Lorenz detuning[Hz]	200 600	~1500	Need wide range tuner
He jacket material	5t Ti	3t SUS316L	No matter with Japanese high pressure code
RF transmission power[kW]	240 350	500	Need higher input coupler

5. Lorentz Detuning

Frequency detuning by Lorentz force

Frequency Detuning during RF Pulse

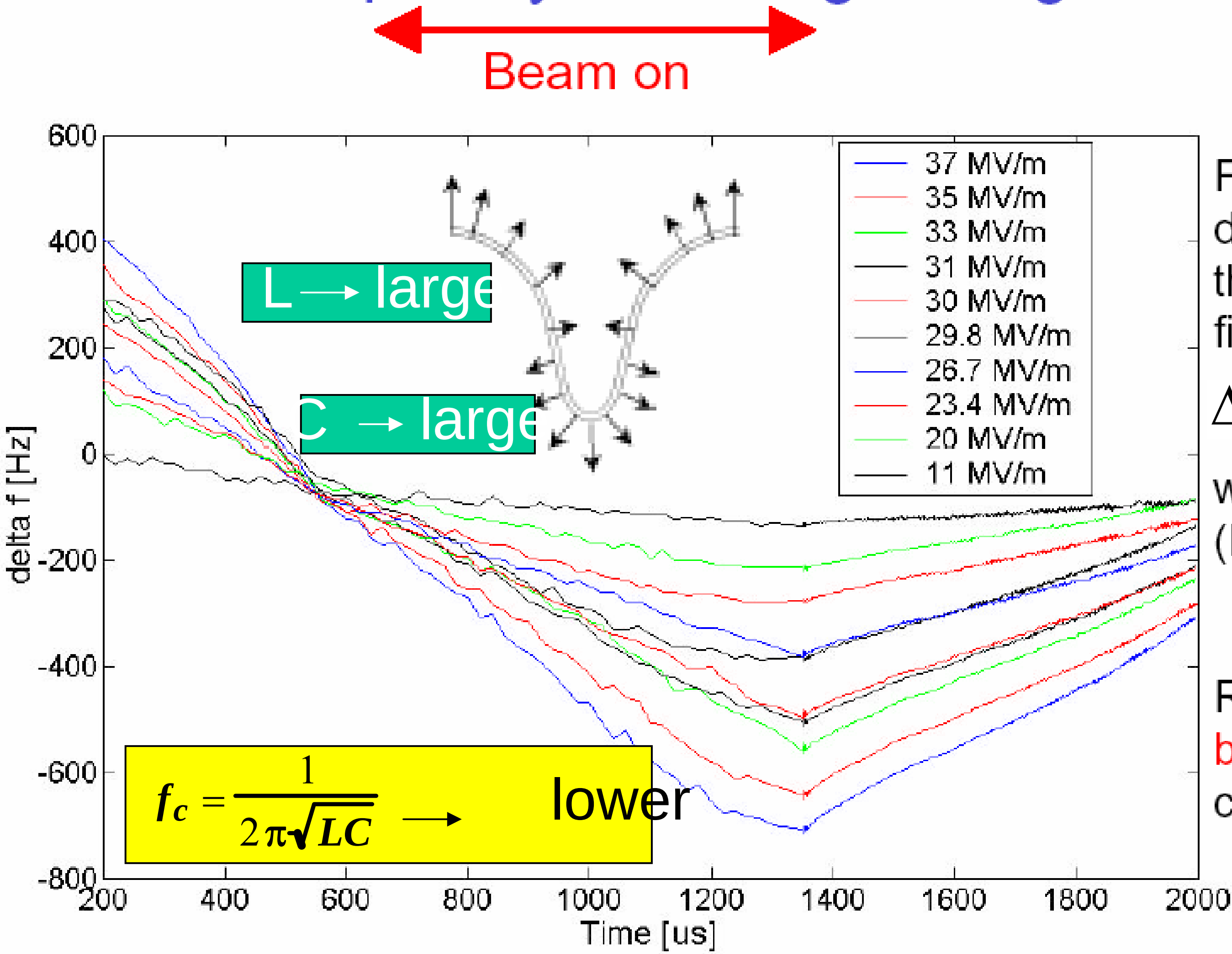

Frequency detuning due Lorentz forces of the electromagnetic field in the cavities:

$\Delta f = -K \cdot E_{acc}^2$

where K " 1 Hz / (MV/m)^2

Remember: Cavity bandwidth with main coupler is " 300 Hz

Frequency and Phase Control by Piezo tuner

Lorentz detuning can be compensated with Piezo tuner control

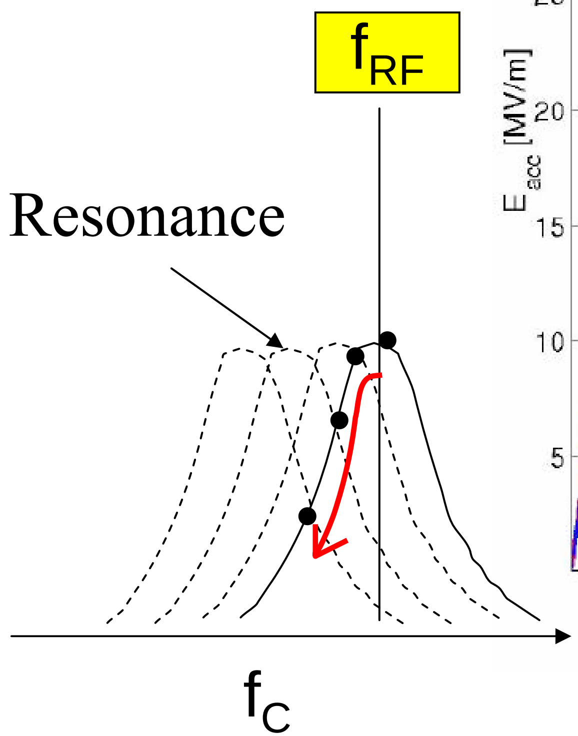

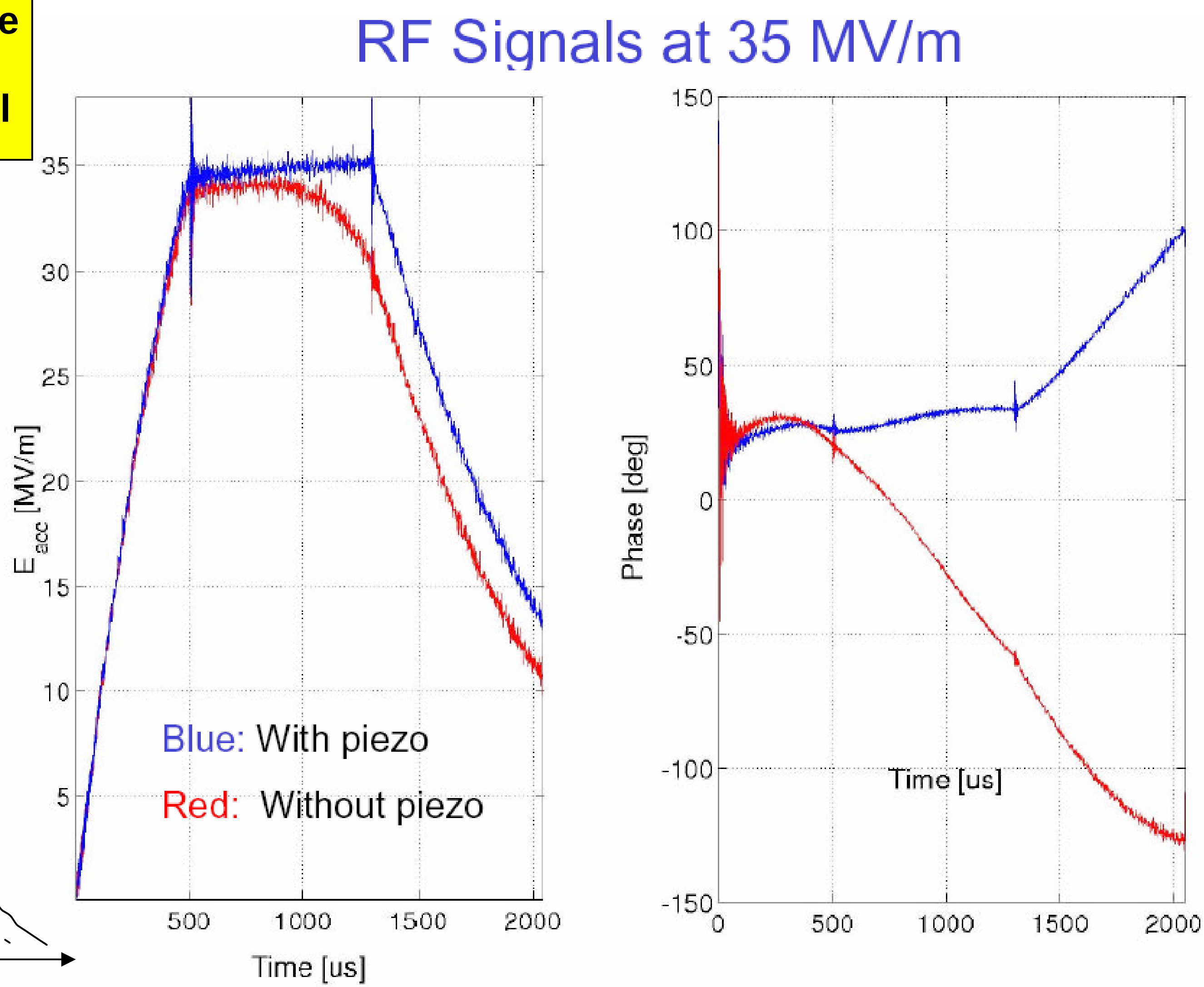

Tow components of Lorentz Deformation

Noguchi's slide in the 1st ILC school

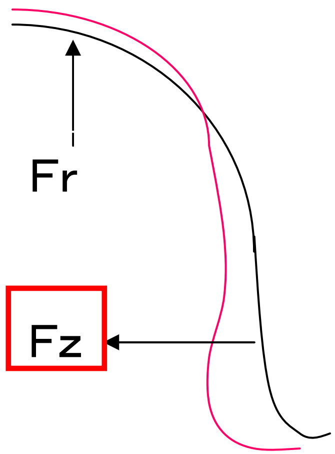

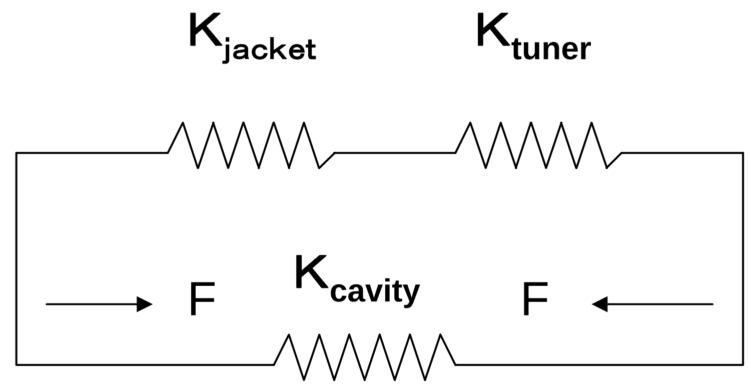

$$\Delta f = \sum_{\text{mode}} a_k \, \delta f_k \approx \sum_{\Delta l = 0} a_k \, \delta f_k + \frac{d\,f}{d\,l}\frac{d\,l}{d\,F} F$$

$$= A E_{acc}^2 + \frac{d\,f}{d\,l}\frac{B E_{acc}^2}{K_S}$$

Rigid Stiffness at Jacket and Tuner are also Very important against the Lorentz Detuning.

		TESLA Blade	STF Slide Jack	STF Ball Screw
A	Hz/(MeV/m)^2	0.5	0.5	(1.2)
B	N/(MeV/m)^2	0.047	0.047	0.051
df/dl	Hz/μm	320	320	370
dF/dl	N/μm	3	3	1.8
KS	N/μm	13	80	60
Kjacket	N/μm	26	96	58
Ktuner	N/μm	26	500	1700
Δf (30MV/m)	Hz	1490	620	1360
Fine Tuning Stroke	μm	3.7	1	2.9

Design Philosophy for Lorentz Detuning Tuner System

1) Use well established technology
2) Rigidity during handling
3) Wide Range Tuning Design
4) Easy Replacement
5) Less heat loss
6) Less X-ray Damage
7) Keep the possibility to move out of vacuum chamber

1), 2) ⇒ Screw Ball Tuner

3) ⇒ Mechanical resonance

4), 5), 6) ⇒ Locate both tuners around 100K shield

Coaxial screw ball tuner

Principle of the Lorentz Detuning used mechanical resonance

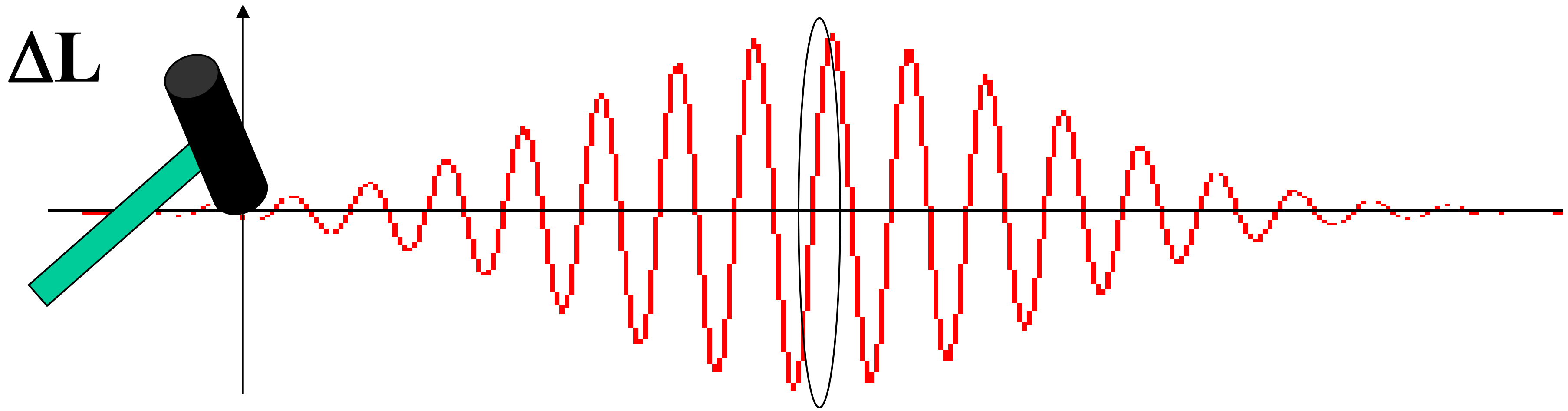

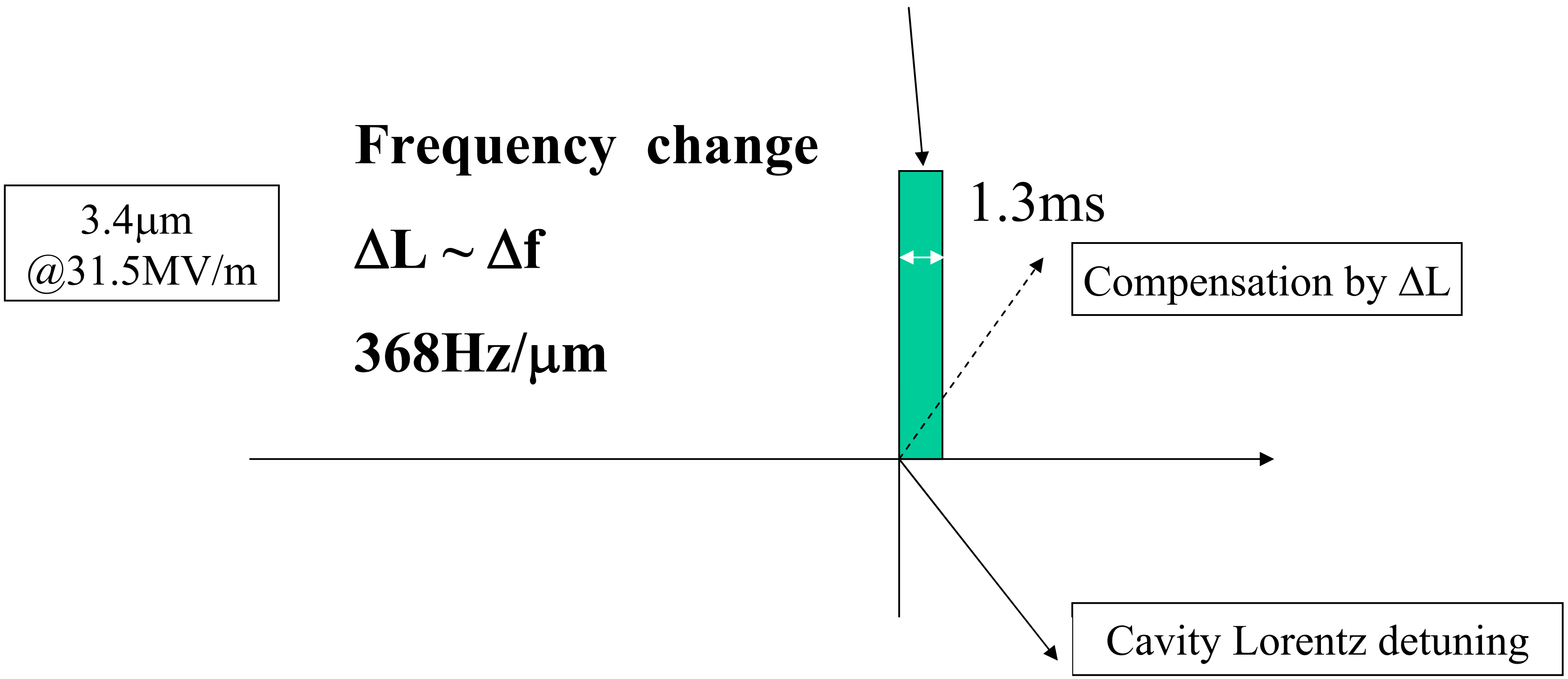

Comparison of Lorentz Force Deformation between different cell shapes

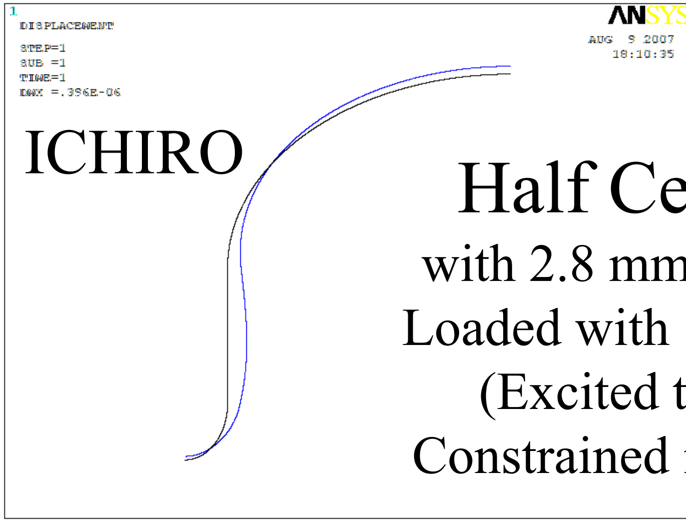

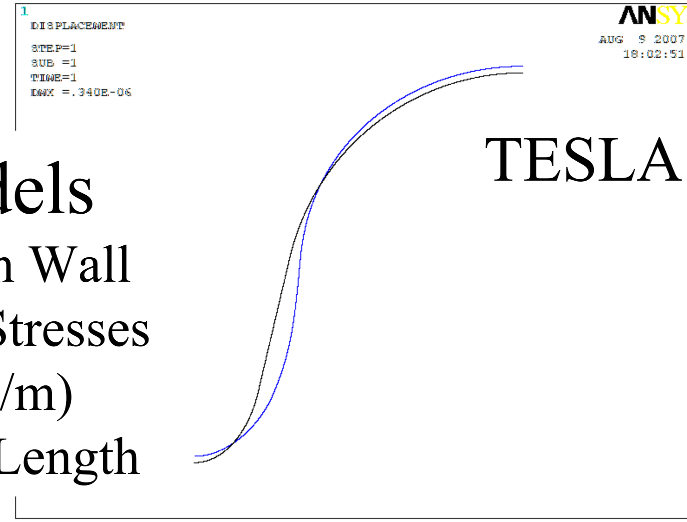

Half Cell Models

with 2.8 mm Niobium Wall

Loaded with Surface Stresses

(Excited to 40 MV/m)

Constrained in Axial Length

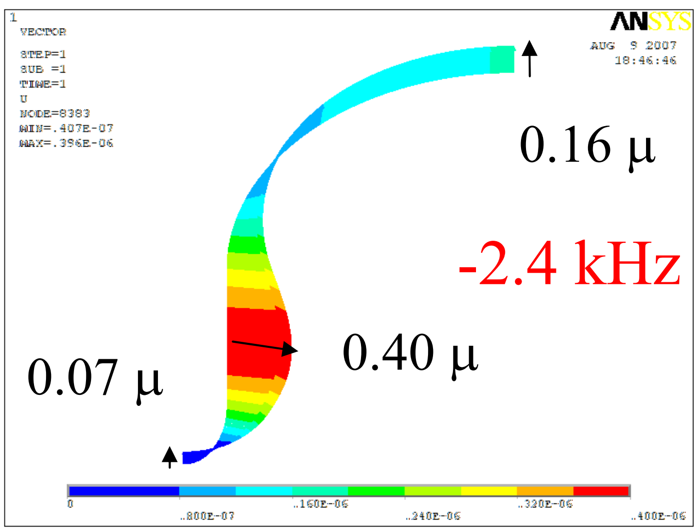

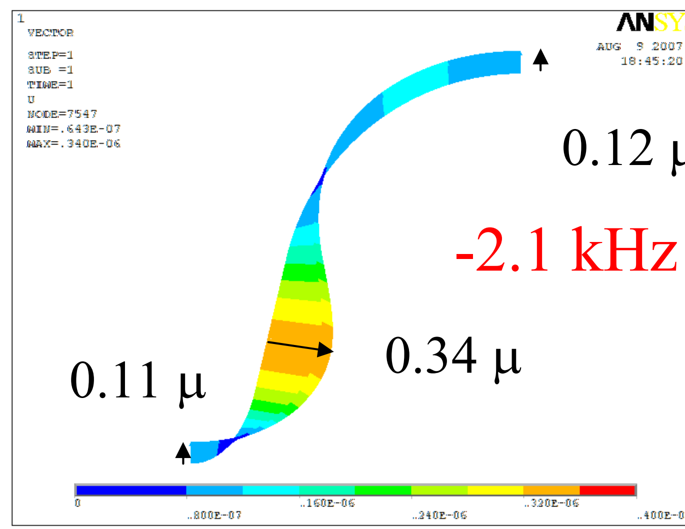

Optimization of Stiffener Location against Lorentz Detuning

Eacc=38MV/m

by H.Yamaoka

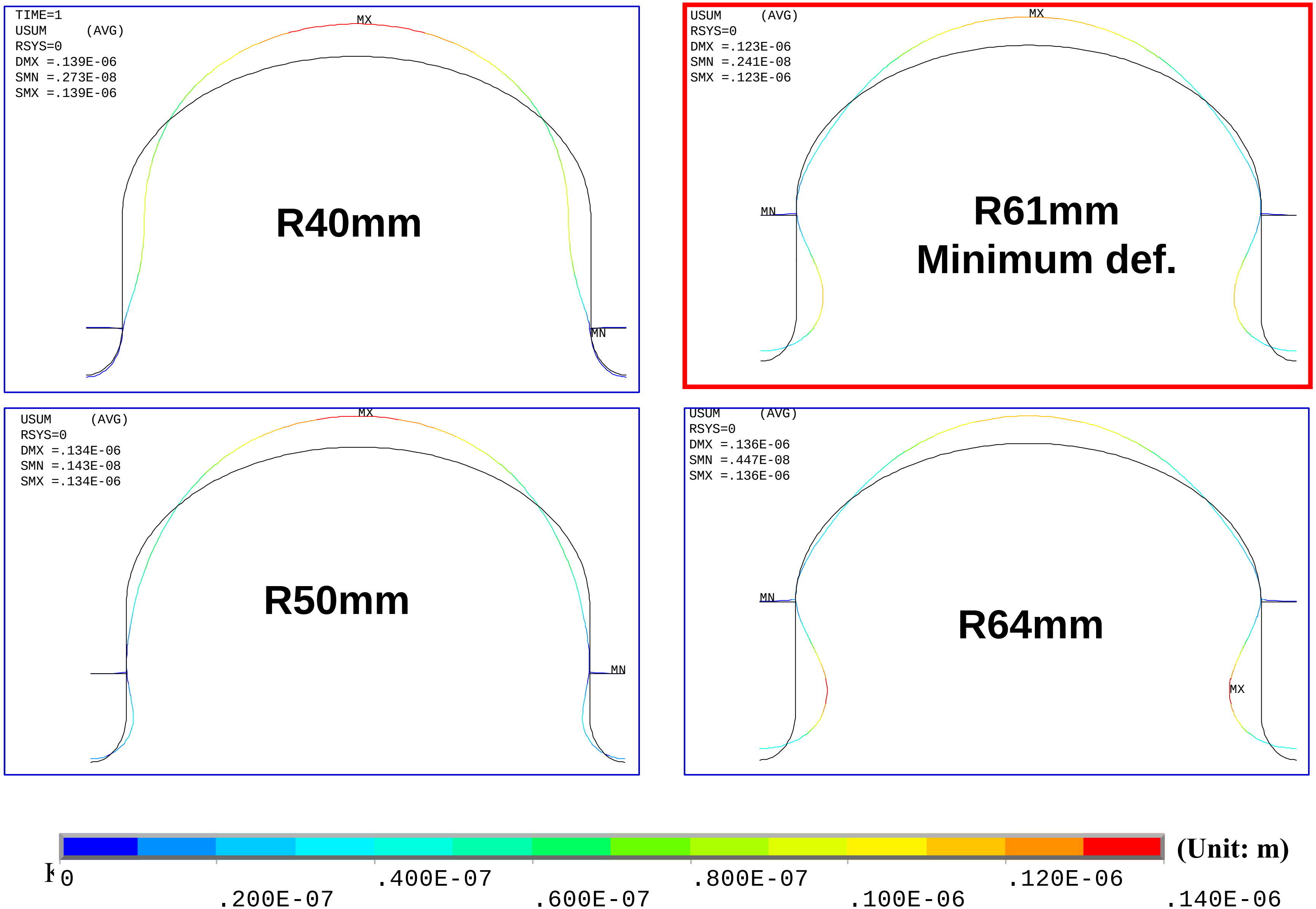

Comparison of Tuners

Screw Ball tuner

Saclay-II

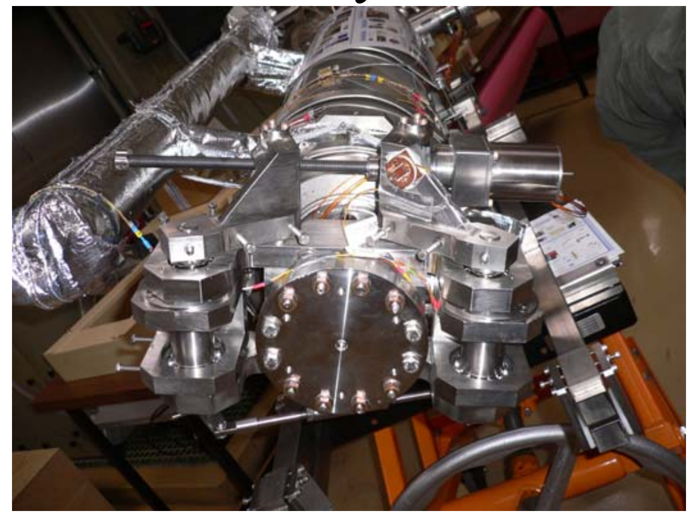

Blade Tuner

Jack tuner

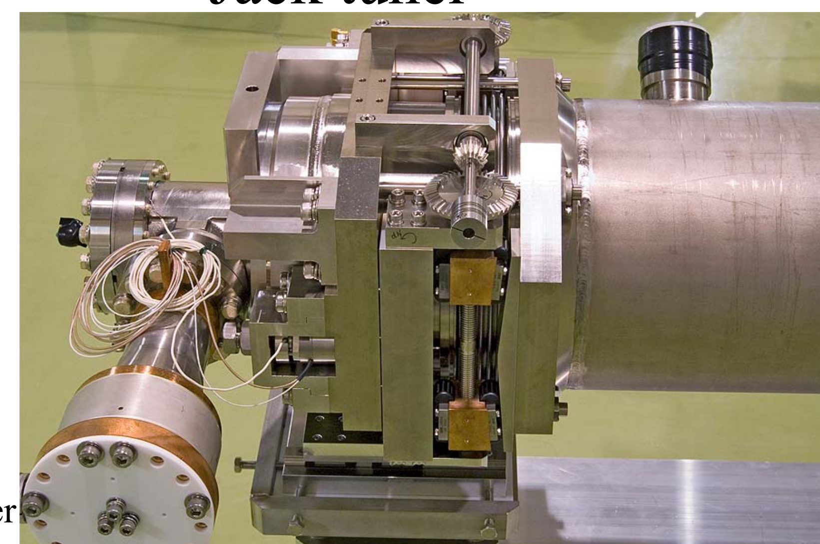

Mechanical Resonance of a multi-cell cavity

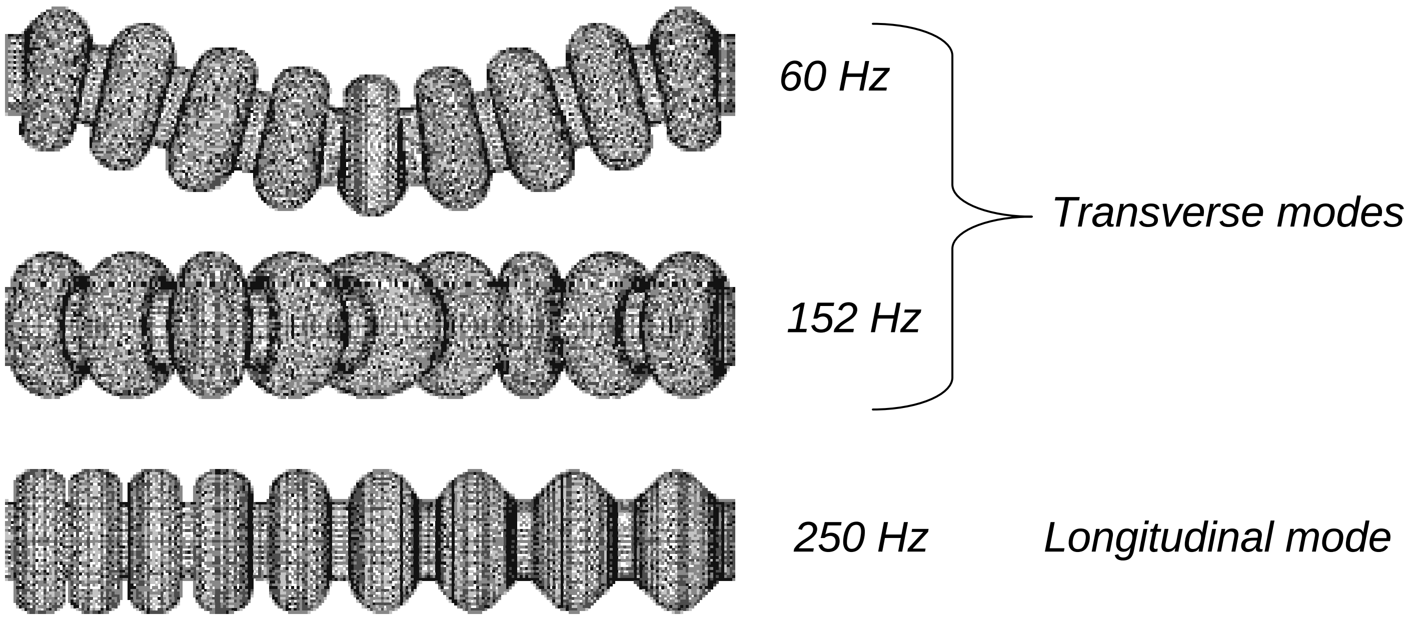

TESLA structure

The mechanical resonances modulate frequency of the accelerating mode.
Sources of their excitation: vacuum pumps, ground vibrations…

Calculation of longitudinal mechanical resonance w/wo He vessel by H.Yamaoka

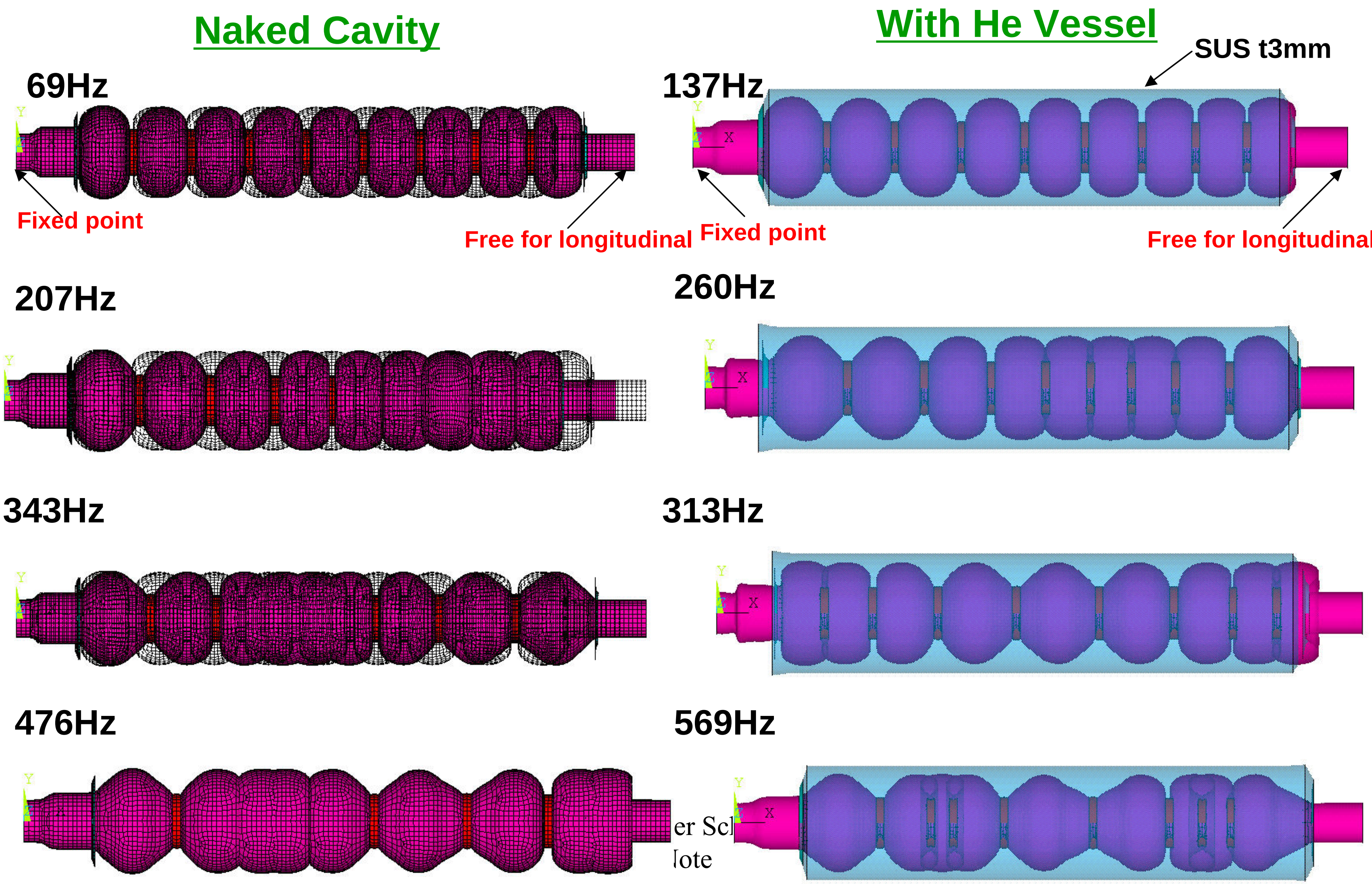

Comparison of Tuner Designs

		Screw Ball	Jack	Blade	Saclay-II
Location	Motor	80K or out of vac. vessel	Out of Vac. vessel	He vessel	Beam tube
	Piezo	80K or out of Vac. vessel	End plate	He vessel	END plate
Tuner mechanism		Coaxial ball screw	Slide Jacky	Twist	Lever type
Motor driving power		0.06gf/μm, 0.1W			
Piezo tuning range		~3000			
Resolution [Hz]	Motor	0.1			
	Piezo	0.1			
$\frac{df}{dl}$ $[\mathrm{Hz}/\mu\mathrm{m}]$		368	320		320
$\frac{dF}{dl}$ $[\mathrm{N}/\mu\mathrm{m}]$		36.4	80	13	

6. RF Input Coupler

Three types developed for ILC

CC-coupler

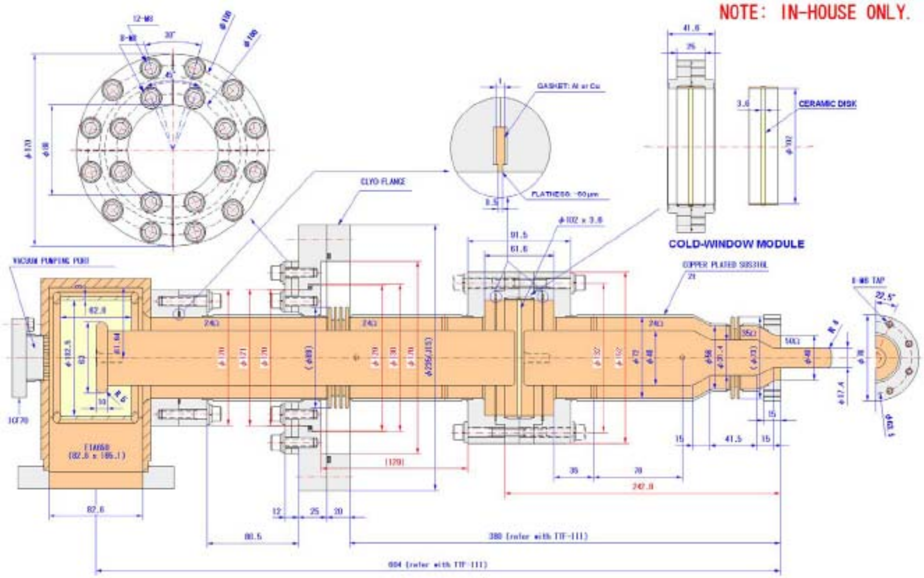

Double disk windows

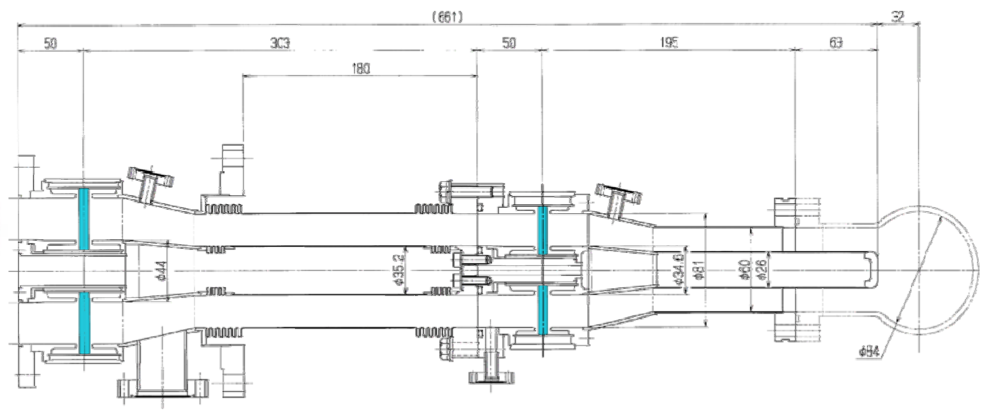

TTF-III (**BCD for ILC**)

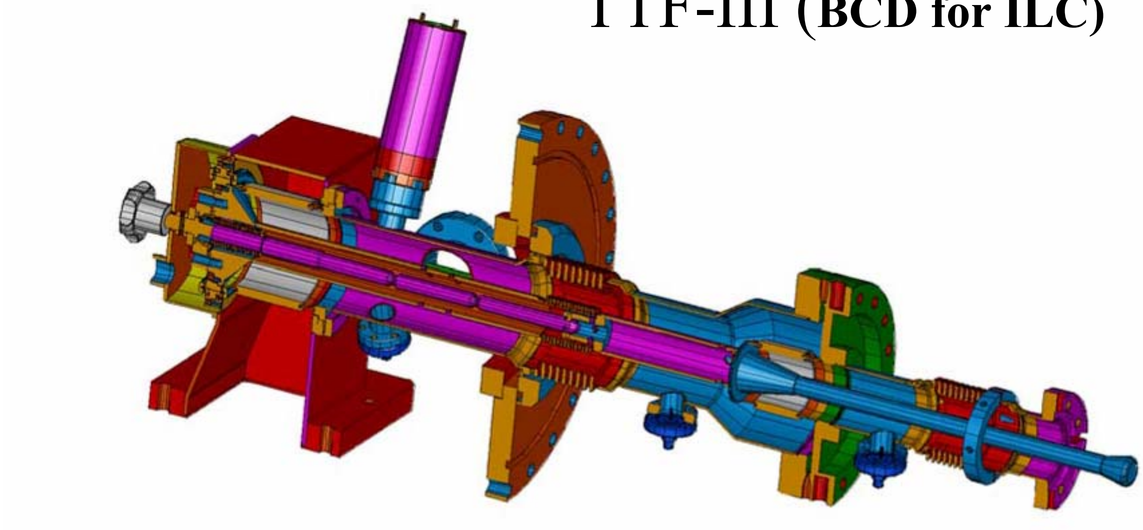

Input Coupler Designs

			CC-coupler	STF-BL	TTF-III
Designed RF Power [kW]			500 (2000)	350(1300)	250(1000)
Pulse width [ms]			1.3 (1.5)	1.3(1.5)	1.3
Repetition [Hz]			5	5	10
Average rf power [kW]			3.25	2.3	3.2
RF processing time [hr]			16	50	20
Thermal Loss [W]	80K	Static	1.24	5	6
		Dynamic	1.5	3	3
	5K	Static	0.54	1.1	0.5
		Dynamic	2.0	0.2	0.1
	2K	Static	1.8e-4	0.05	0.06
		Dynamic	0.18	0.03	negligible

Can be reduced the dynamic loss at 5K and 2K in CC-coupler by using higher RRR cooper material, for example RRR=40.

Input Coupler Design @ KEK

By Matsumoto and Kazakov @ KEK

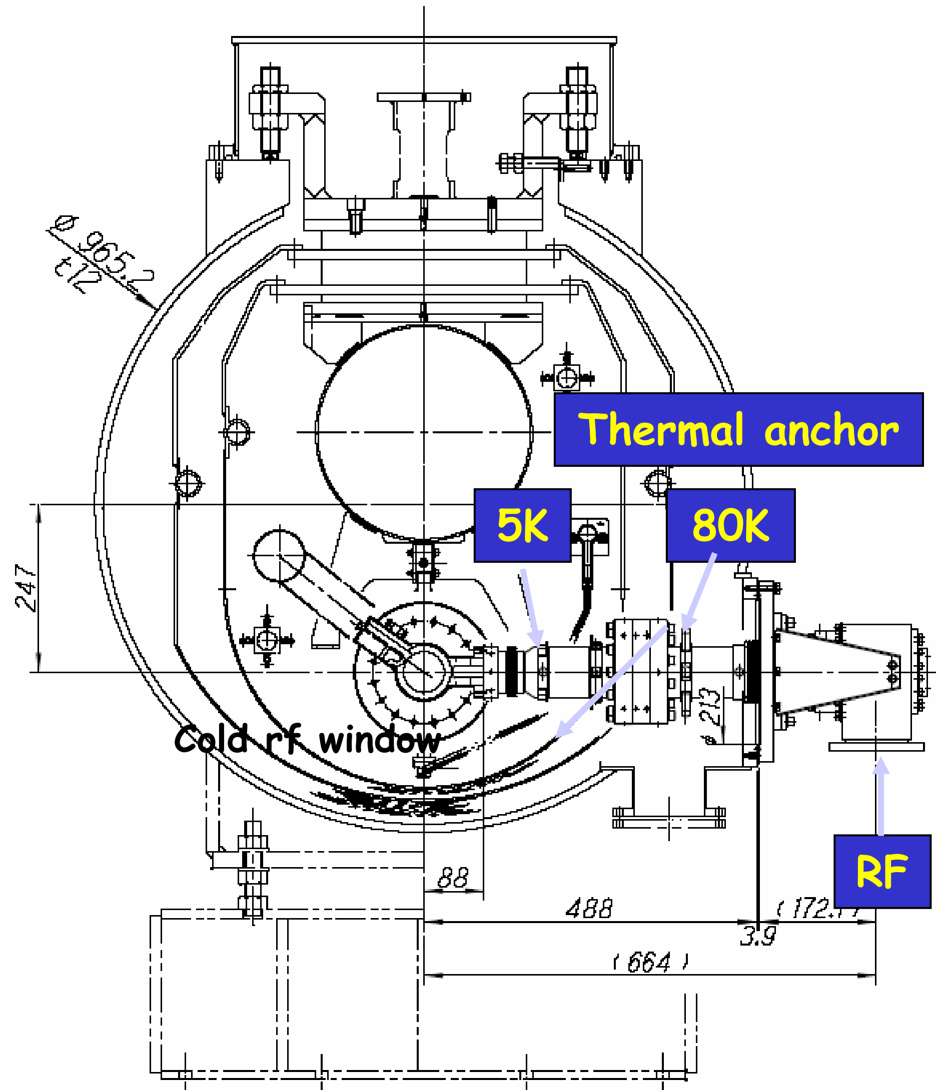

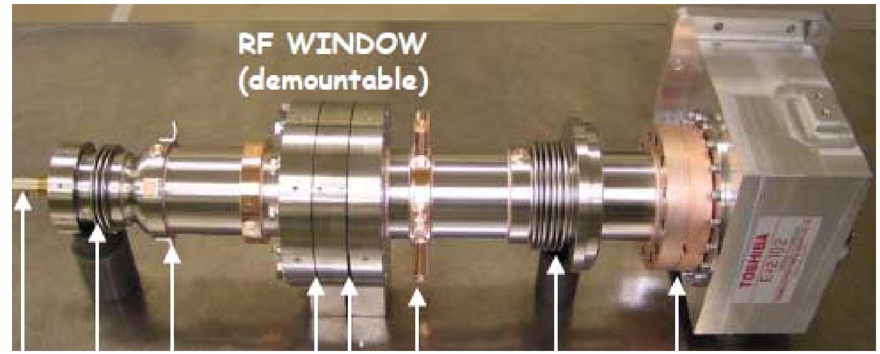

Major Parameters

Input rf power: 500 kW

Pulse width: 1.3 msec

Repetition rate: 5 Hz

Average rf power: 3.25 kW

Thermal loss [W]

	80K	5K	2K
Static:	1.24	0.54	2.6x1e-4
Dynamic:	2.14	2.88	0.25
Total:	3.38	3.42	~0.25

RRR: 3.5 (measured data)

ELECTRIC FIELD GRADIENT AT INPUT POWER OF 500-KW

Maximum electric field gradient in the air side for warm window.

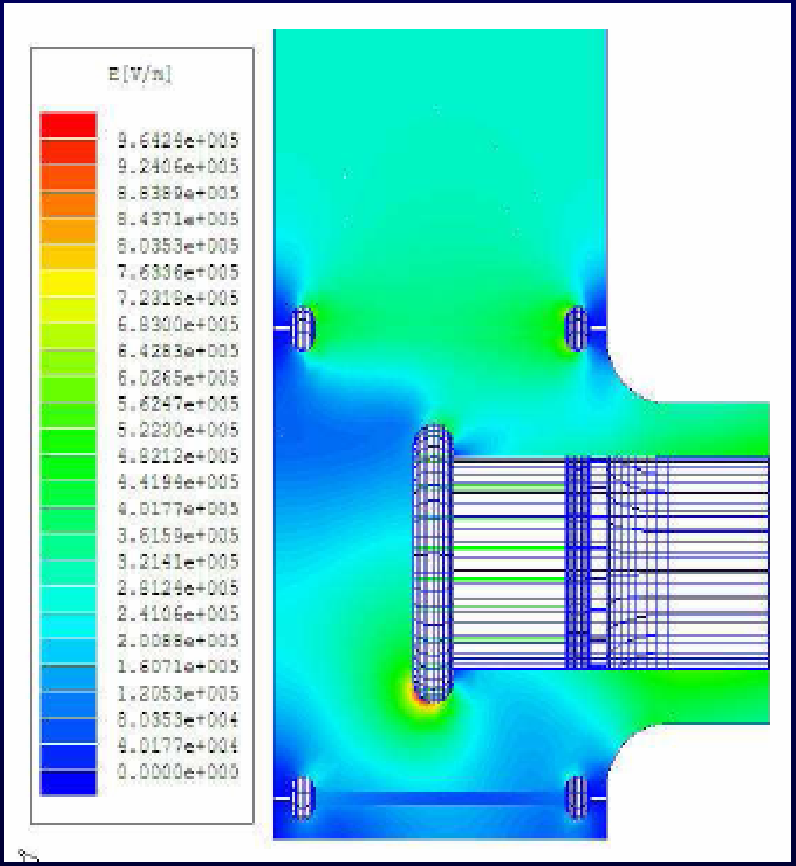

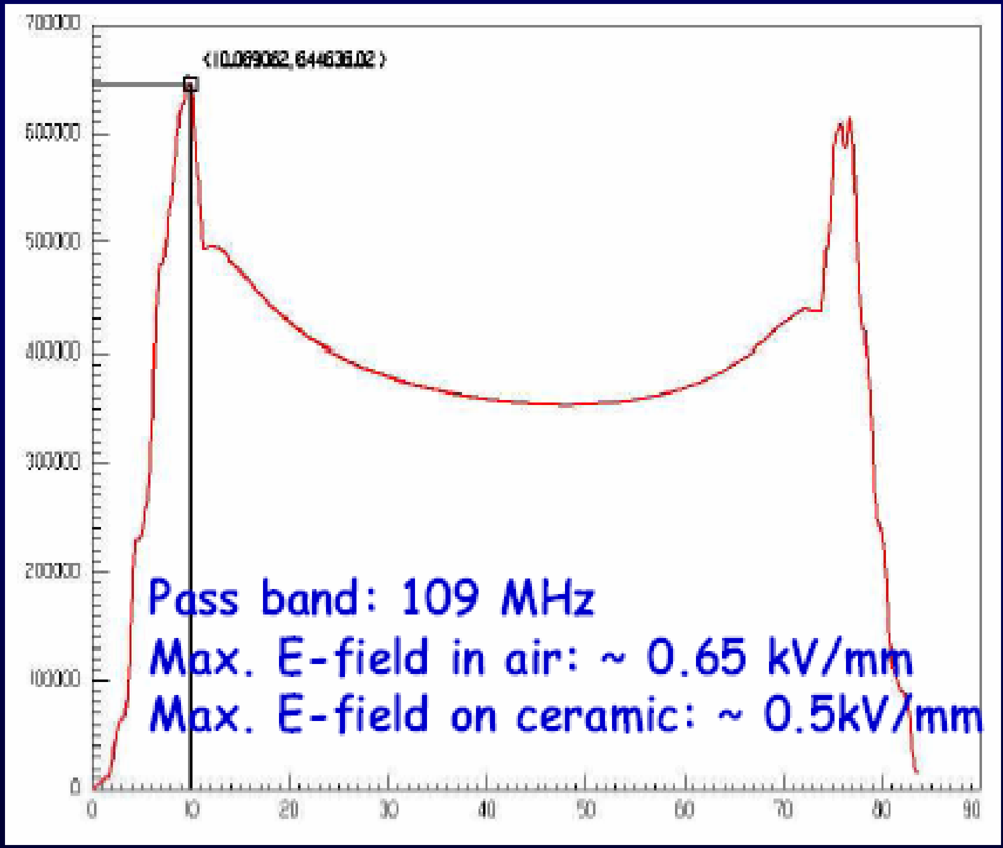

MO flange

Leak tight in LHe-II, No gap at sealing

Mo-flange(ϕ130), Cu ring

Capacitive Coupling Coaxial Line for Input Coupler

Capacitive coupling coaxial line should have advantages; By H.Matsumoto and S.Kazakov

1) Good thermal insulation ability between the warm and the cold sides.
2) Reduce the brazing difficulty for the ceramic window.

Concept of capacitive coupling coaxial line

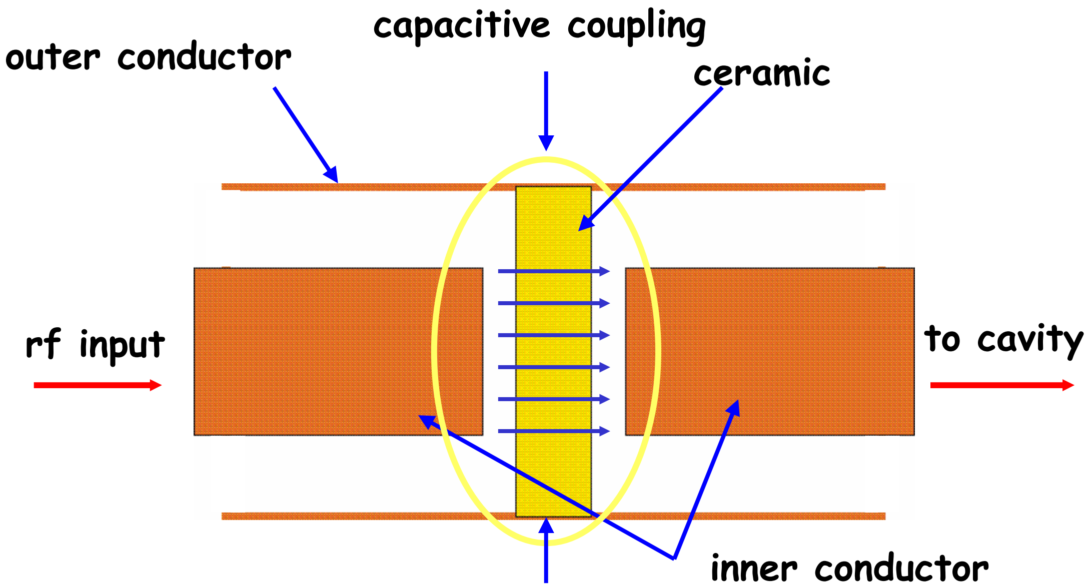

Easy to braze between cooper and ceramic disk.

Well established in warm technology

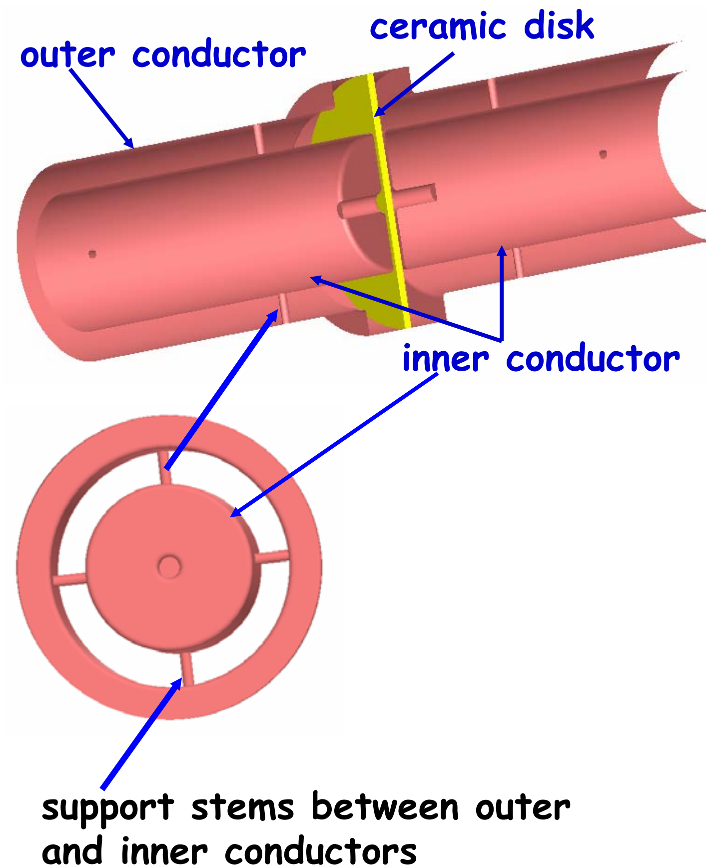

INDUSTRIALIZATION with MODULAR STRUCTURE

Input coupler comprises of four modules:

1) coaxial transformer
2) coaxial line
3) rf window
4) antenna at cold side

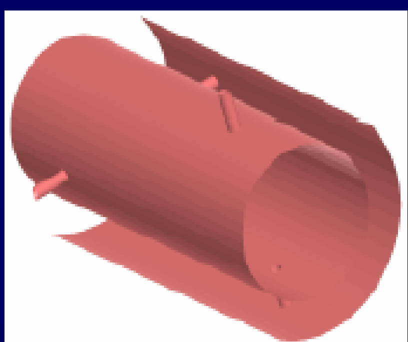

Each pair of rods is mounted in the gap between the inner- and outer-conductors, and are rotated 90 degrees from each other.

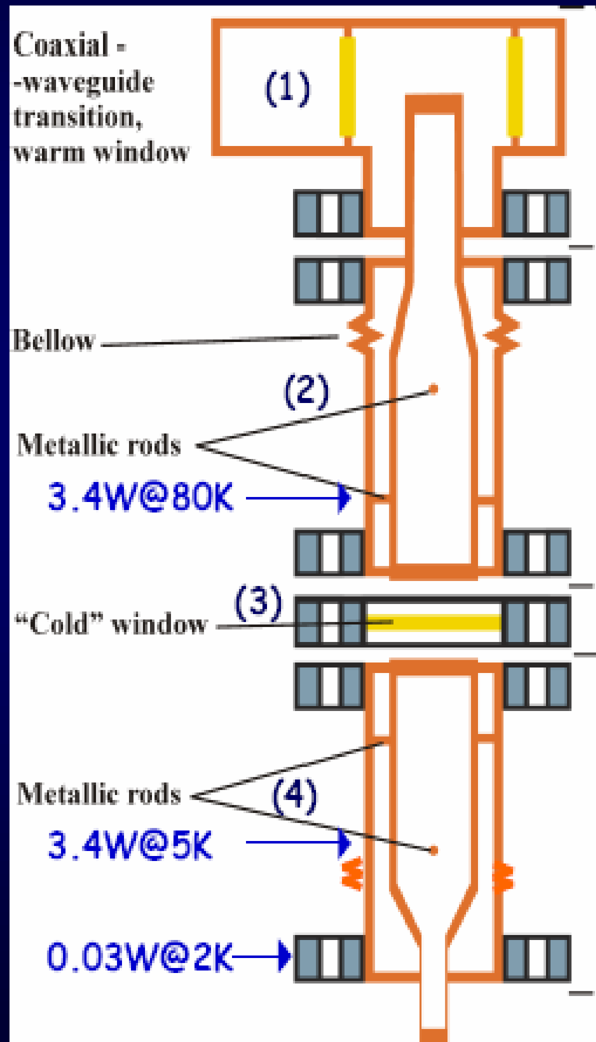

The complete input coupler can
[1] be divided into four relatively simple parts to **ease fabrication and assembly**. If we assume that the inner conductors are not attached rigidly to the waveguide, we **need only two**
[2] **bellows to absorb the movement of the coaxial line** due to thermal contaction and
[3] expansion between cool down and warm up.

The fabrication of each module
[4] **technical requirements dose not overlap for each parts.**

Average power: 3.25-kW (500-kW, 1.5-msec, 5-pps) RRR: 3.5 (measured data for copper plated layer)

500kW Input coupler high power test stand @ STF

Coaxial capacitive input coupler

By H.Matsumoto and S.Kazakov

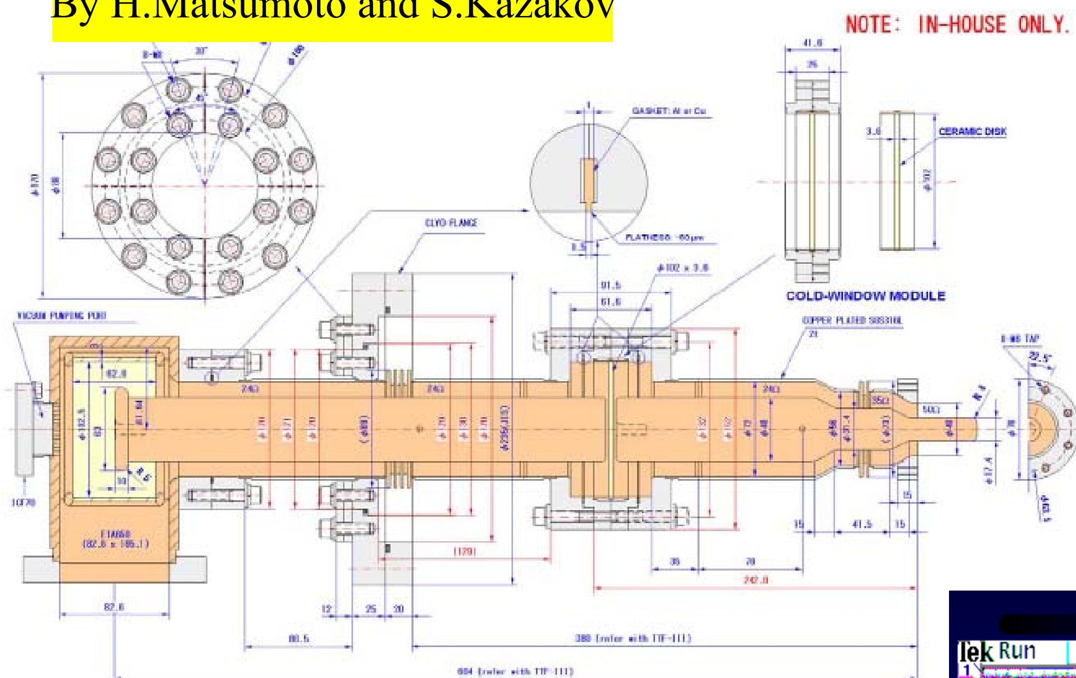

Successfully demonstrated the high power performance up to 2MW!

The specification: 500kW, 1.5msec, 5Hz @ 45MV/m operation

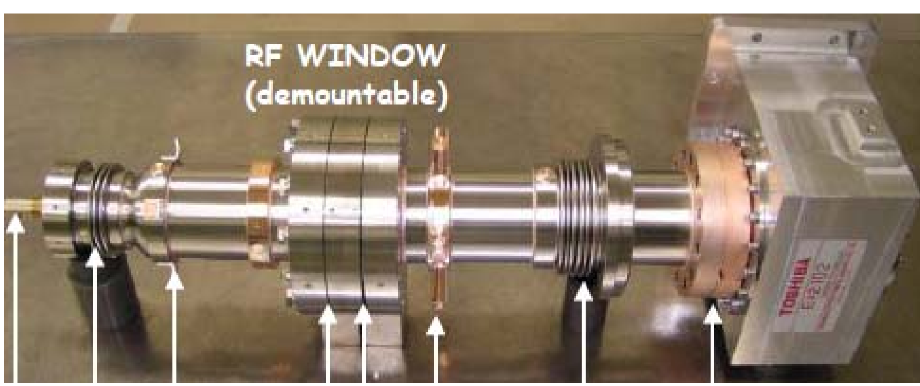

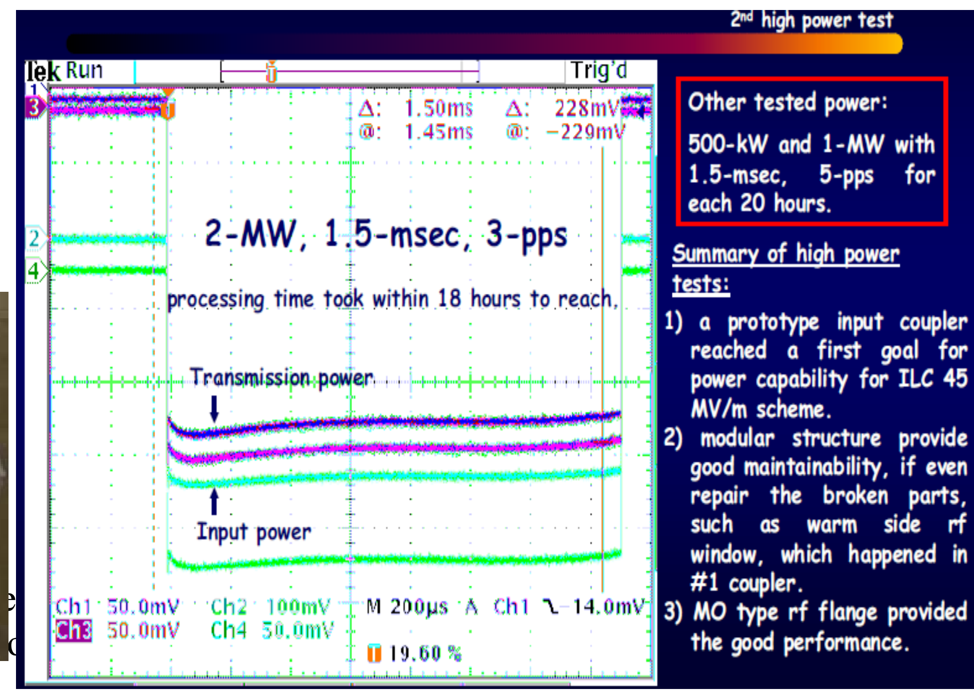

Successful High Power Test @ STF 0.5 Cryomodule

By T.Saeki on 17 August 2007

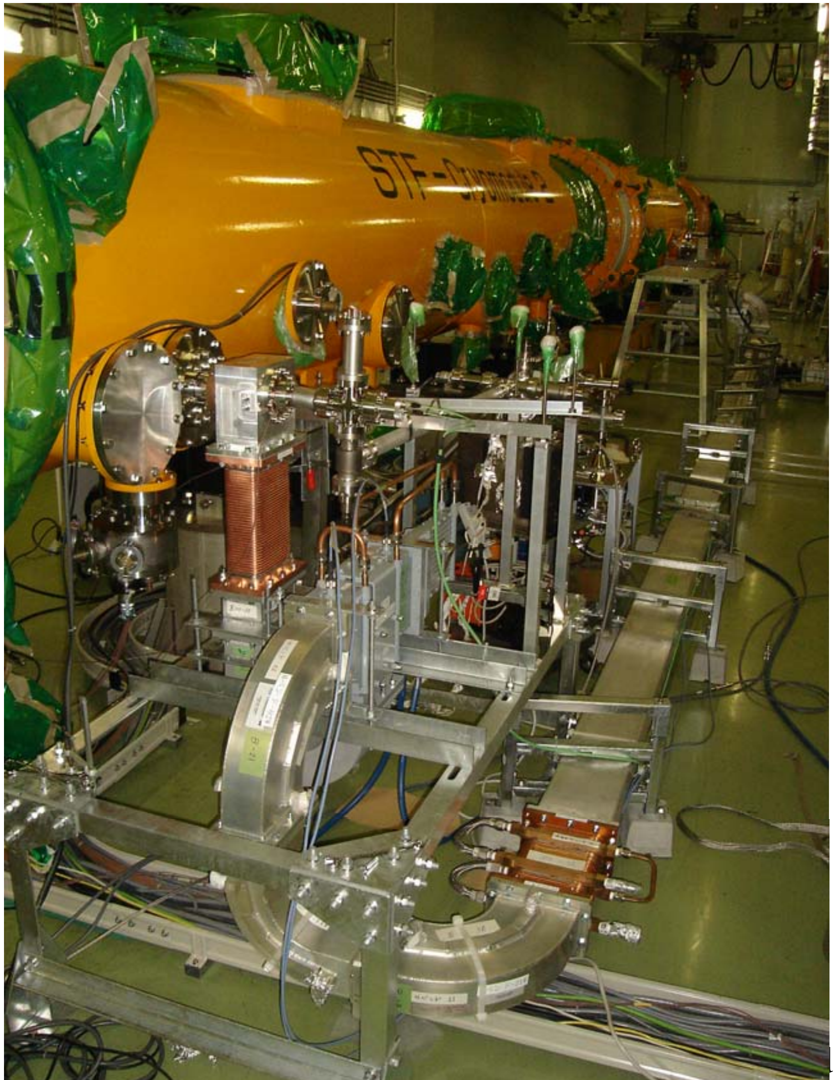

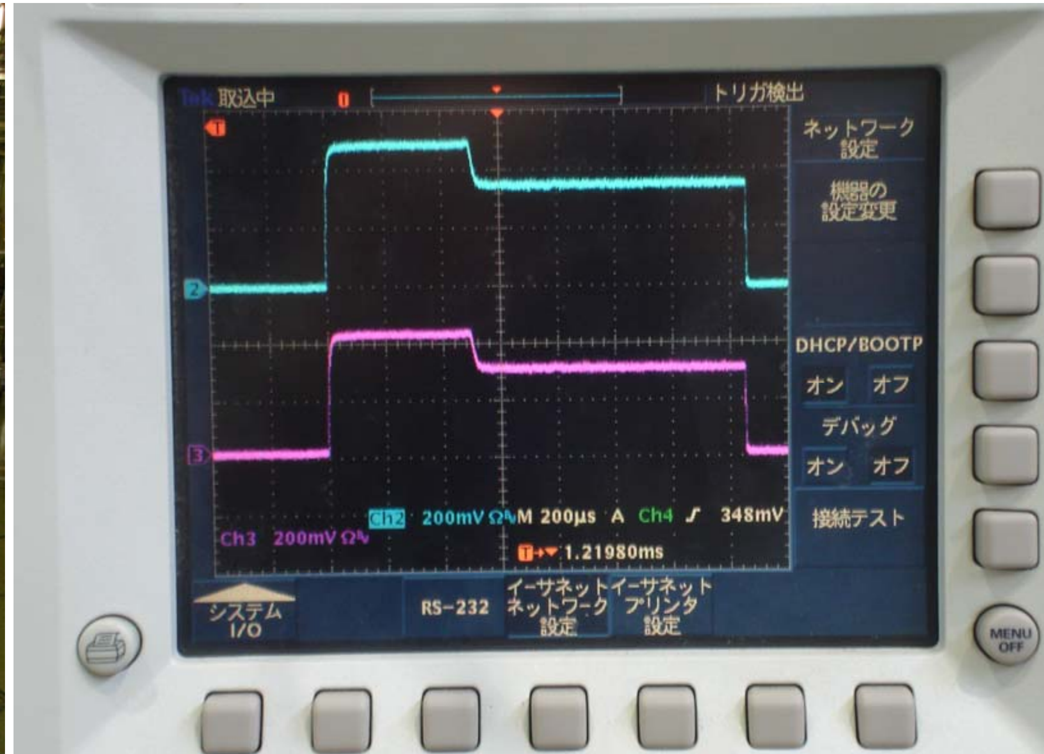

250kW, 1.5ms, 5Hz
(Reflection mode)

7. Niobium Cavity Fabrication

7.1 Deep Drawing

7.2 Trimming of half cell

7.3 END group fabrication

7.4 Final EBW assembly

7.5 Nb film coated cavity

Note

Overview on cavity fabrication

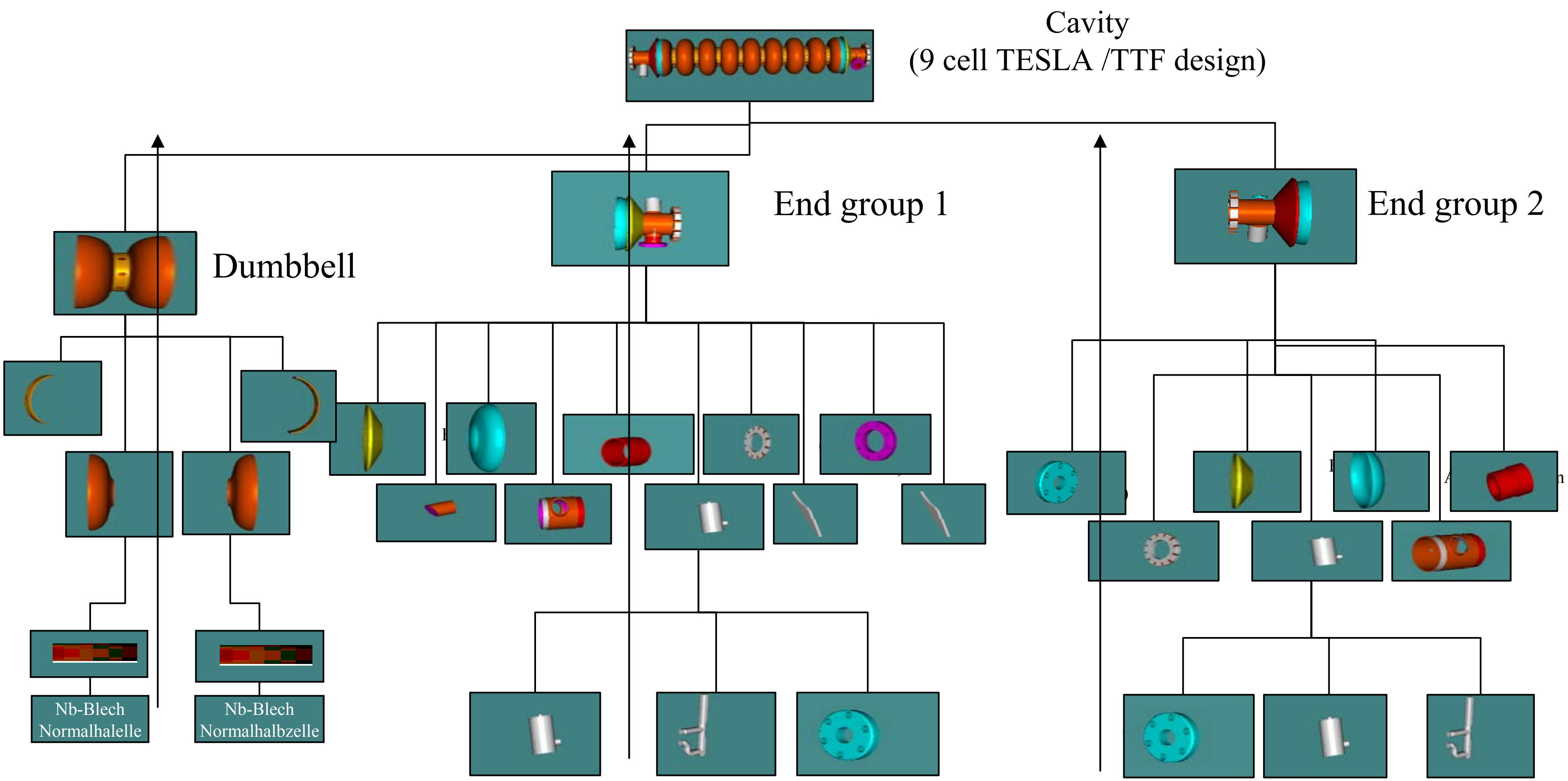

Cavity fabrication and preparation sequences
for the TESLA / TTF cavities at DESY

1st ILC workshop at KEK Tsukuba Japan
A.Matheisen
for DESY and the TESLA Collaboration

7.1 Deep Drawing

Kikuchi Workshop

80t press for 2.8t Nb half cell (1300MHz)

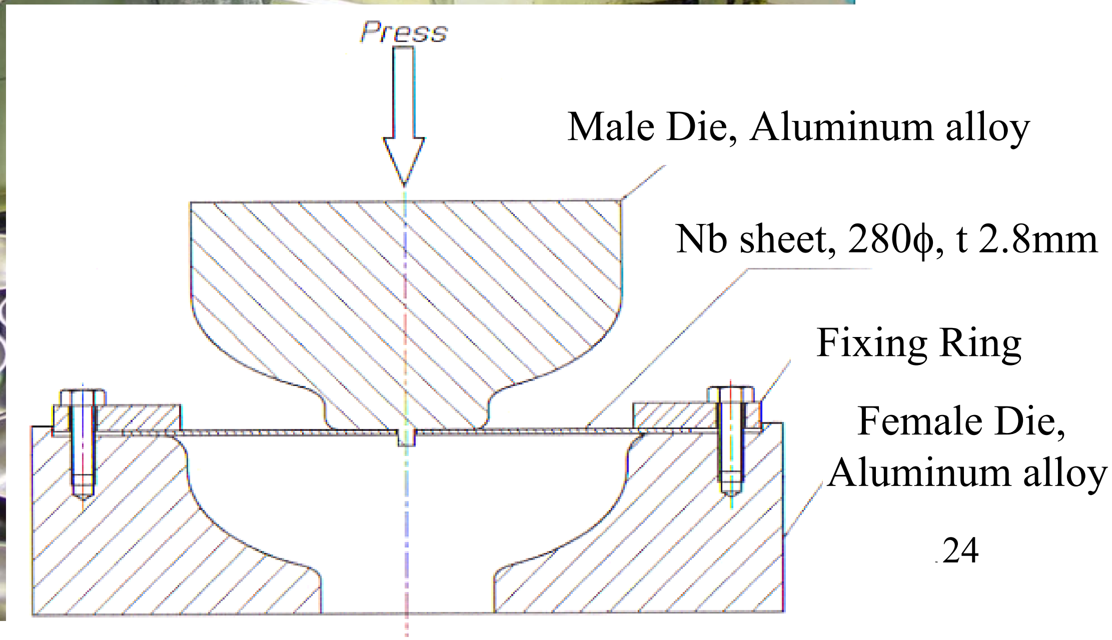

Local Elongation

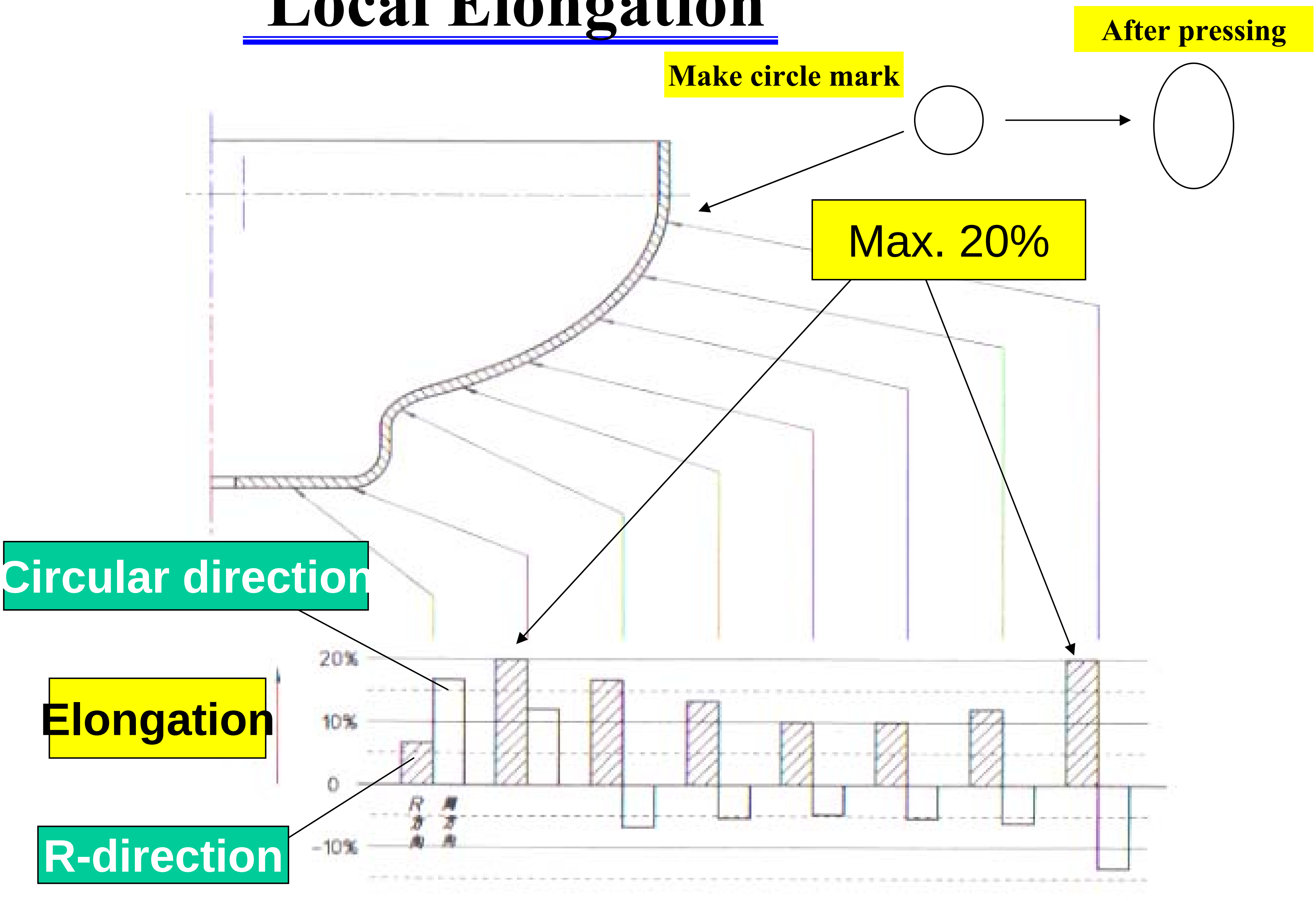

7.2 Trimming

Ishizuka Workshop

Iris Trimming

Equator Trimming

Trimming Configuration at Equator section

So far, KEK has used CBP 100-200μm to make smooth the equator EBW seam. The left trimming shape needs CBP 10 times, and the right trimming configuration needs only CBP twice.

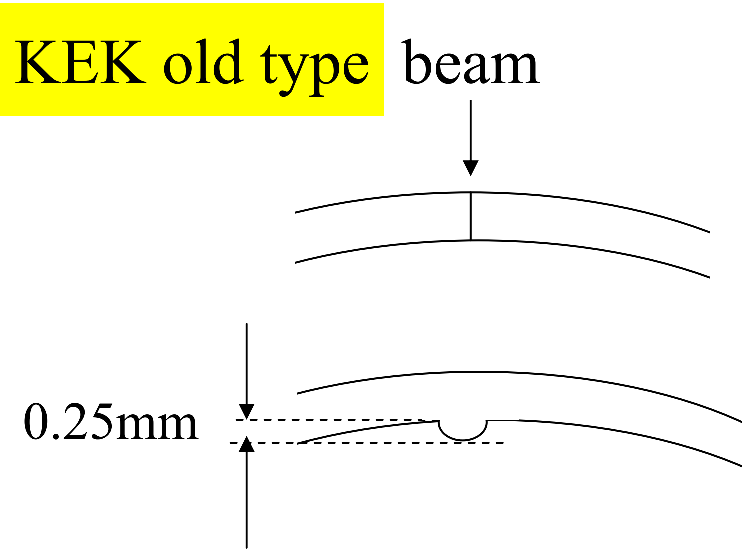

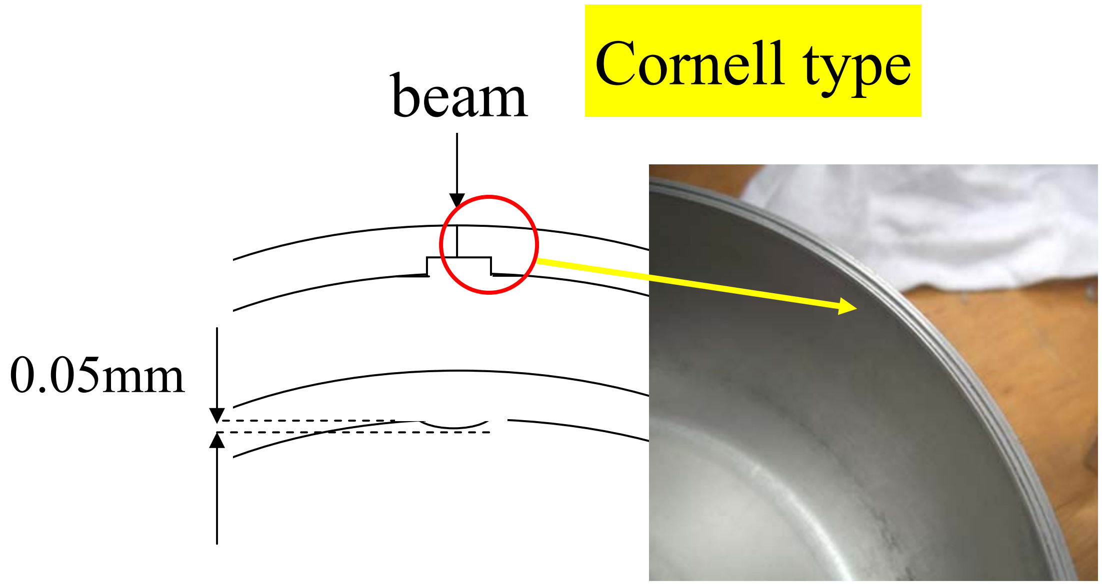

Needed CBP ~10 times

CBP only twice!

Cornell trimming configuration is very useful to smooth the EBW seam by less CBP.

Note

Fabrication Error on half-cell cup

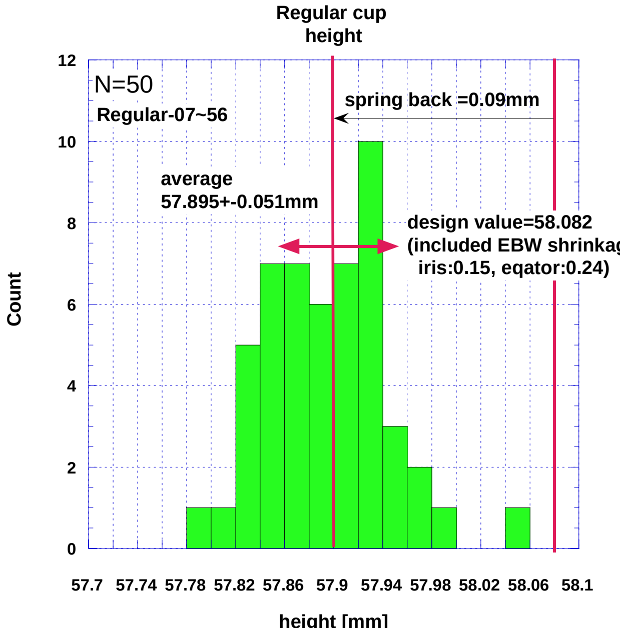

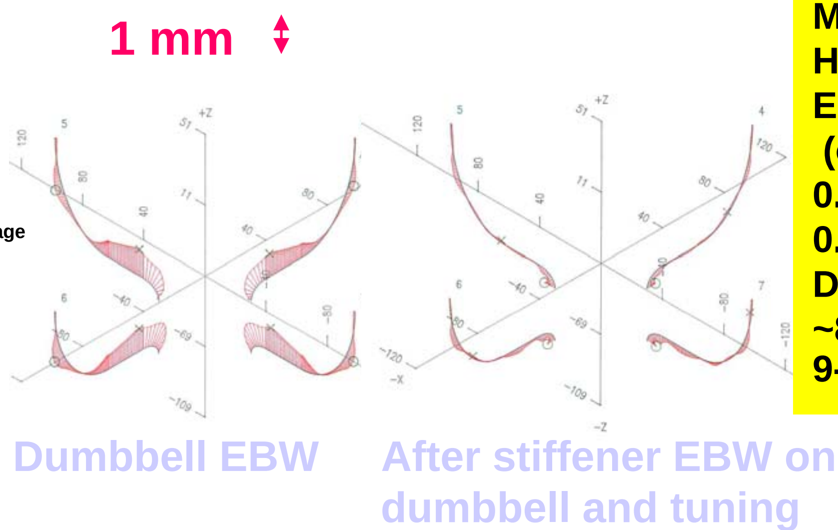

Machining error: 50μm
Half cell spring back:90μm
EBW shrinkage
(old trimming configuration
0.42 ± 0.13mm @ equator
0.15 ± 0.04mm @ iris
Dumbbell fabrication error
~80μm after tuning
9-cell length error:0.7~0.1mm

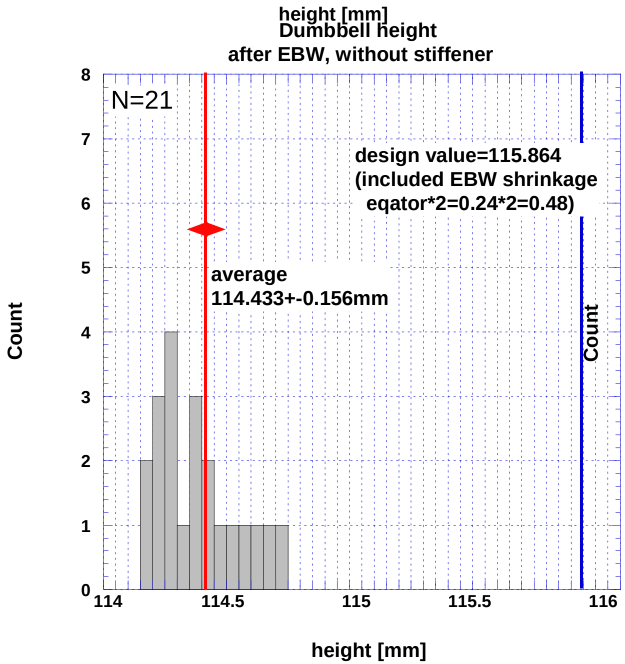

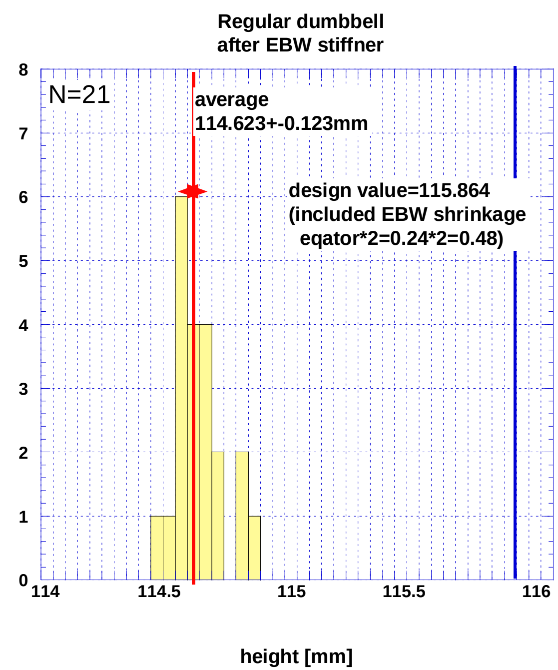

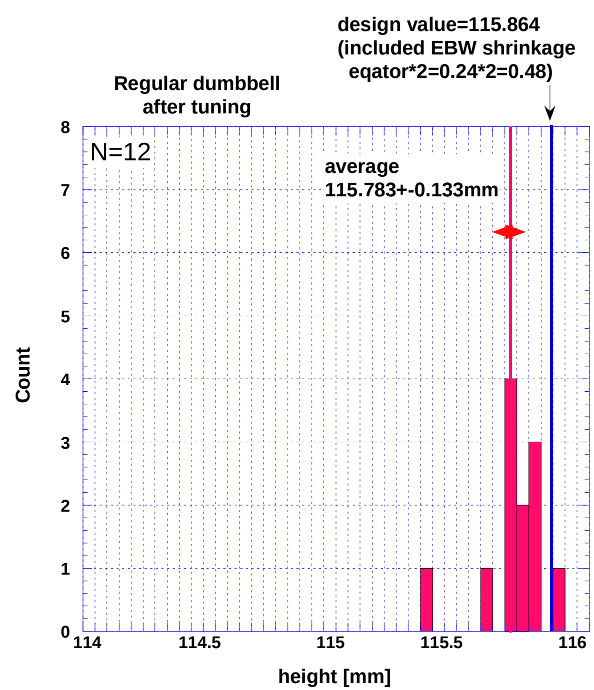

EBW of Dumbbell with stiffener

Electron Beam Welding (EBW)
In KUROKI corporation

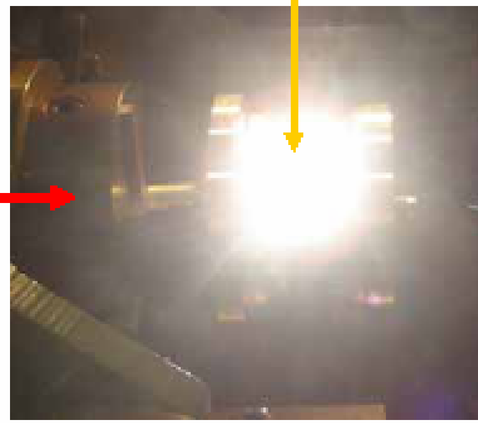

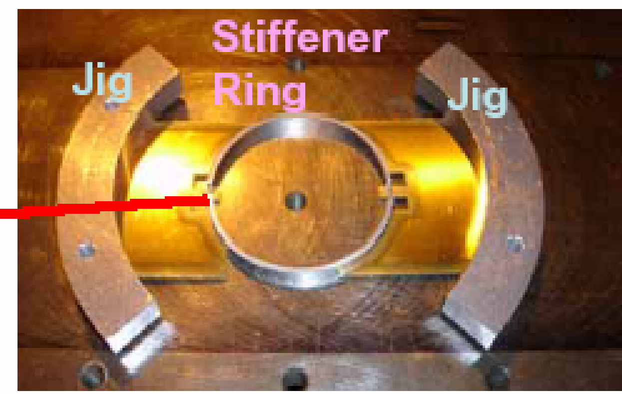

Insert stiffener-ring into the iris part of dumbbell.

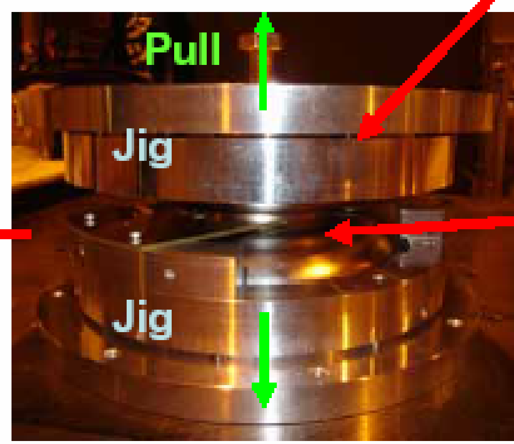

Pull and extend dumbbells to insert stiffener-ring.
=> EBW (dumbbell + ring)

Dumbbell with stiffener-ring after EBW.

EBW Conditions at KEK

KEK Data

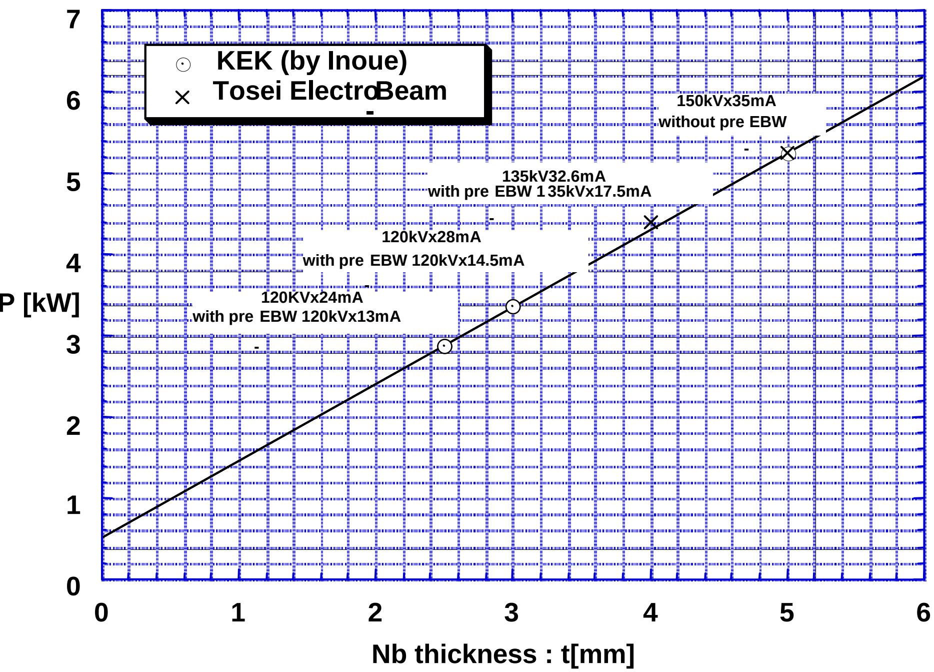

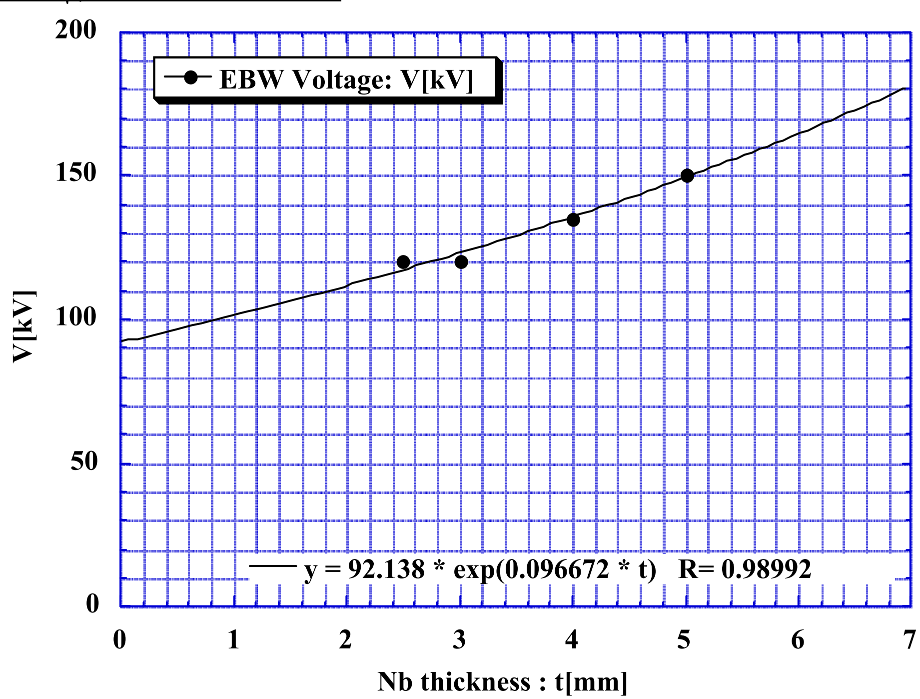

Dumbbells and END Cups

PAL

Note

7.3 END Grope fabrication
-Beam Pipe fabrication (thicker Nb tube case)-

Rounding ends

Bending

Closing

Thickness: 4t ~ 6t

After EBW

Press

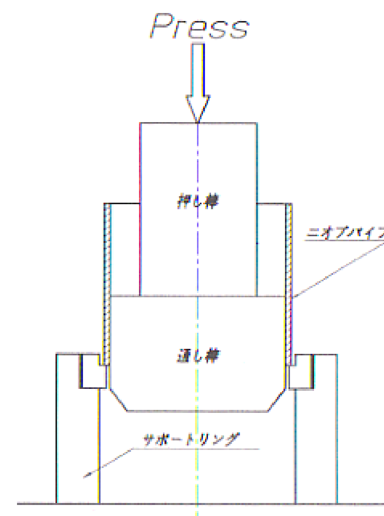

Drawing

Circular die

Oil pump

Circular tube

HOM Coupler Parts

END base plate for Helium Vessel

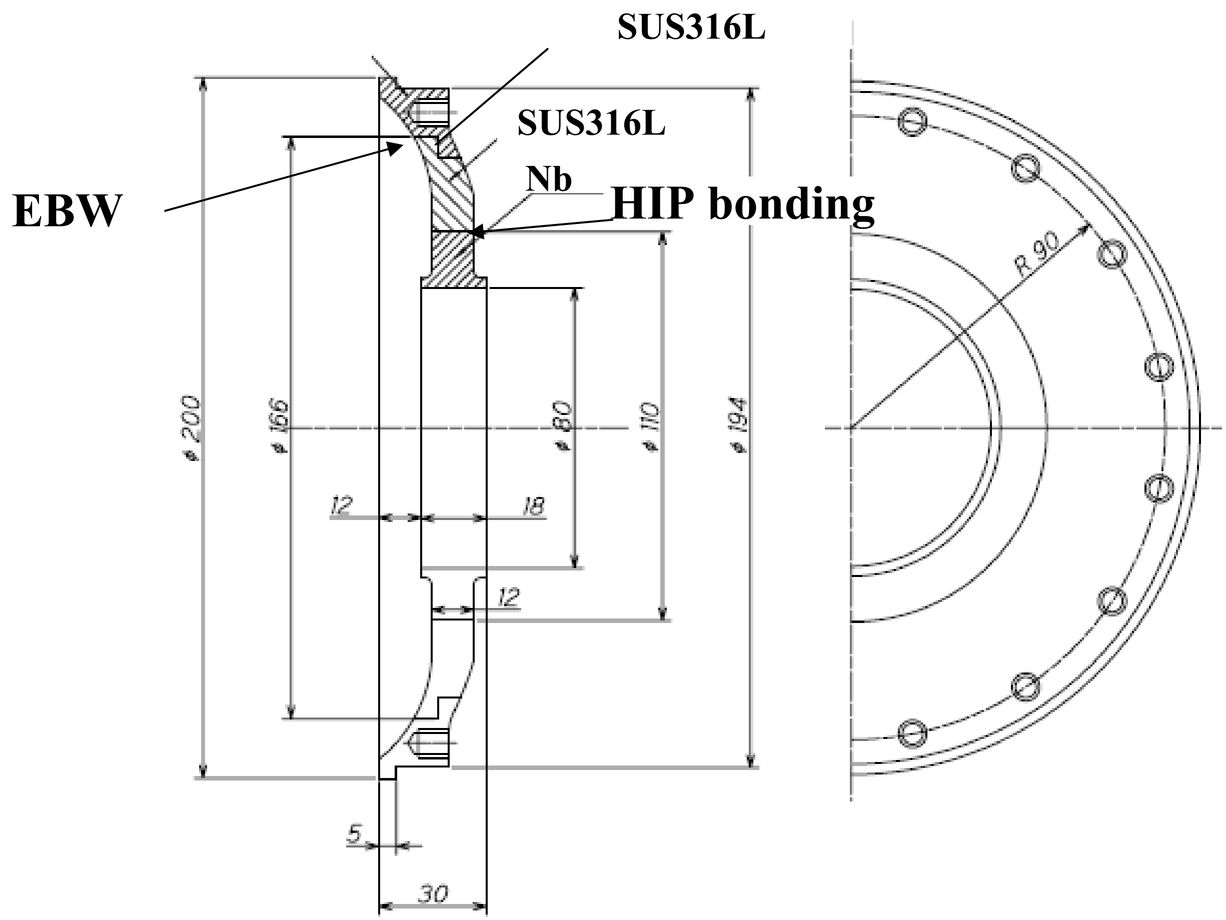

Nb/SUS bonding by HIP

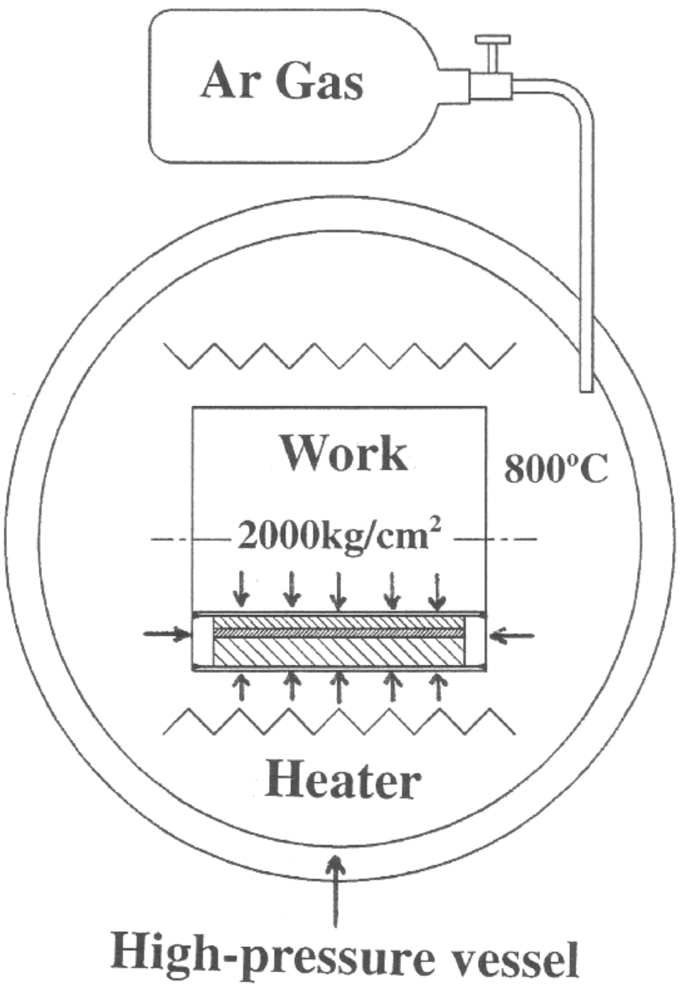

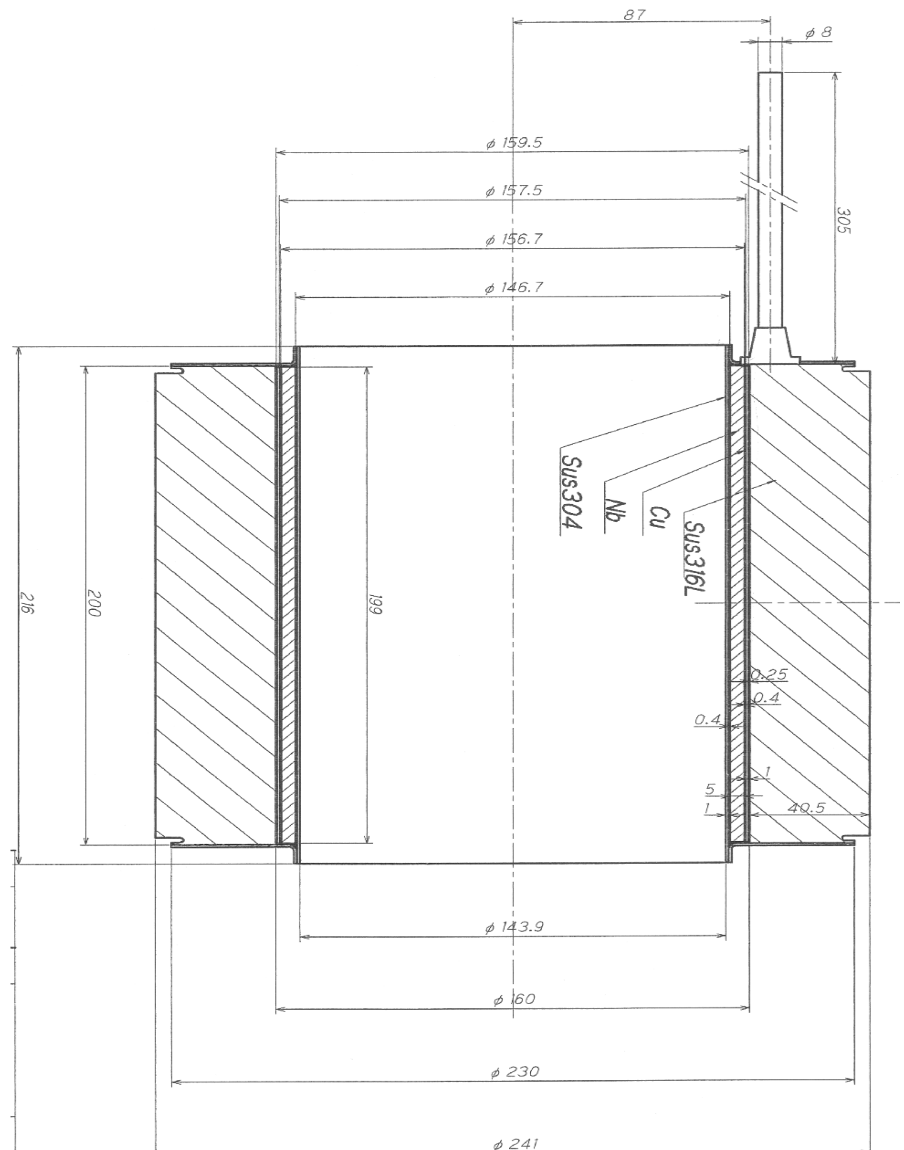

Care for the thermal stress at the base plate

By H.Yamaoka

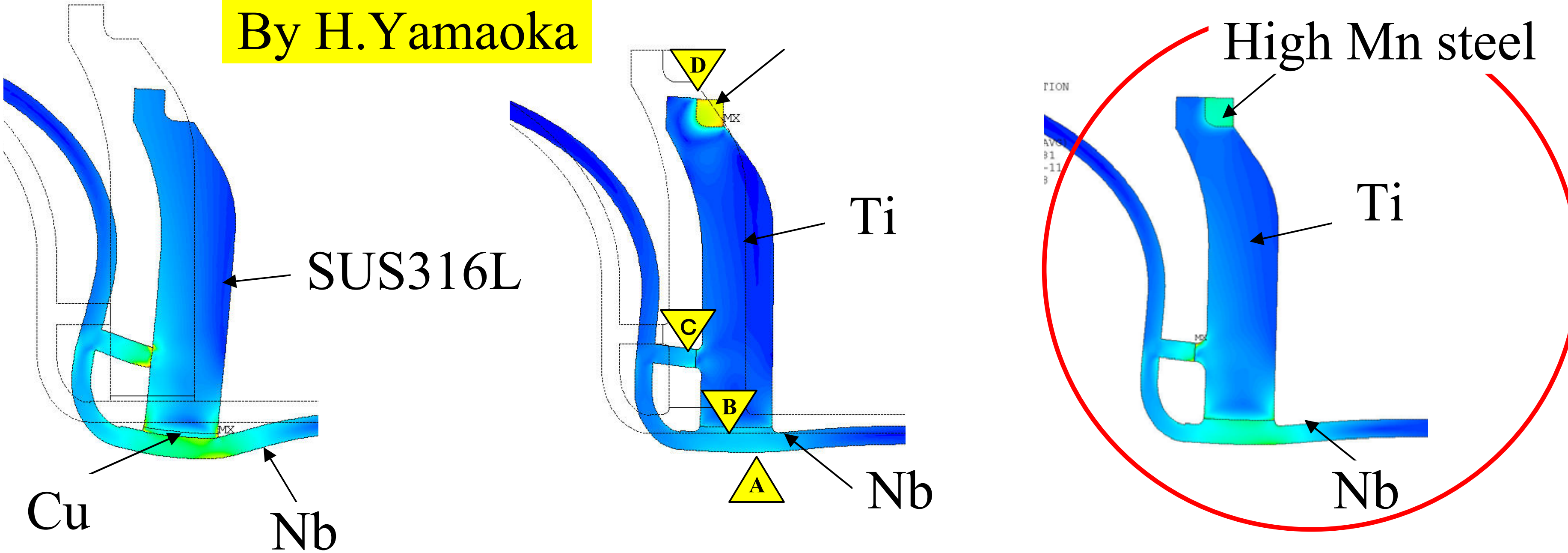

Nb/Cu/SUS316L **Nb/Ti+SUS316L** **Nb/Ti+High Mn steel**

Stress concentration

	A [MPa]	B [MPa	C [MPa]	D [MPa
Nb/Cu/SUS316L	250	500	500	
Nb/Ti/SUS316L	100	100	200	470
Nb/Ti/High Mn Steel	100	100	200	80

Thermal expansion coefficient

	$\alpha = \frac{\int_{77K}^{300K} \alpha(T)dT}{300-77}$ [E-6/K]
SUS316L	16.0
Cu	17.0
High Mn steel	9.8
Ti	8.4
Nb	5.0

EBW of END Group

SFC

7.4 Final EBW Assembly

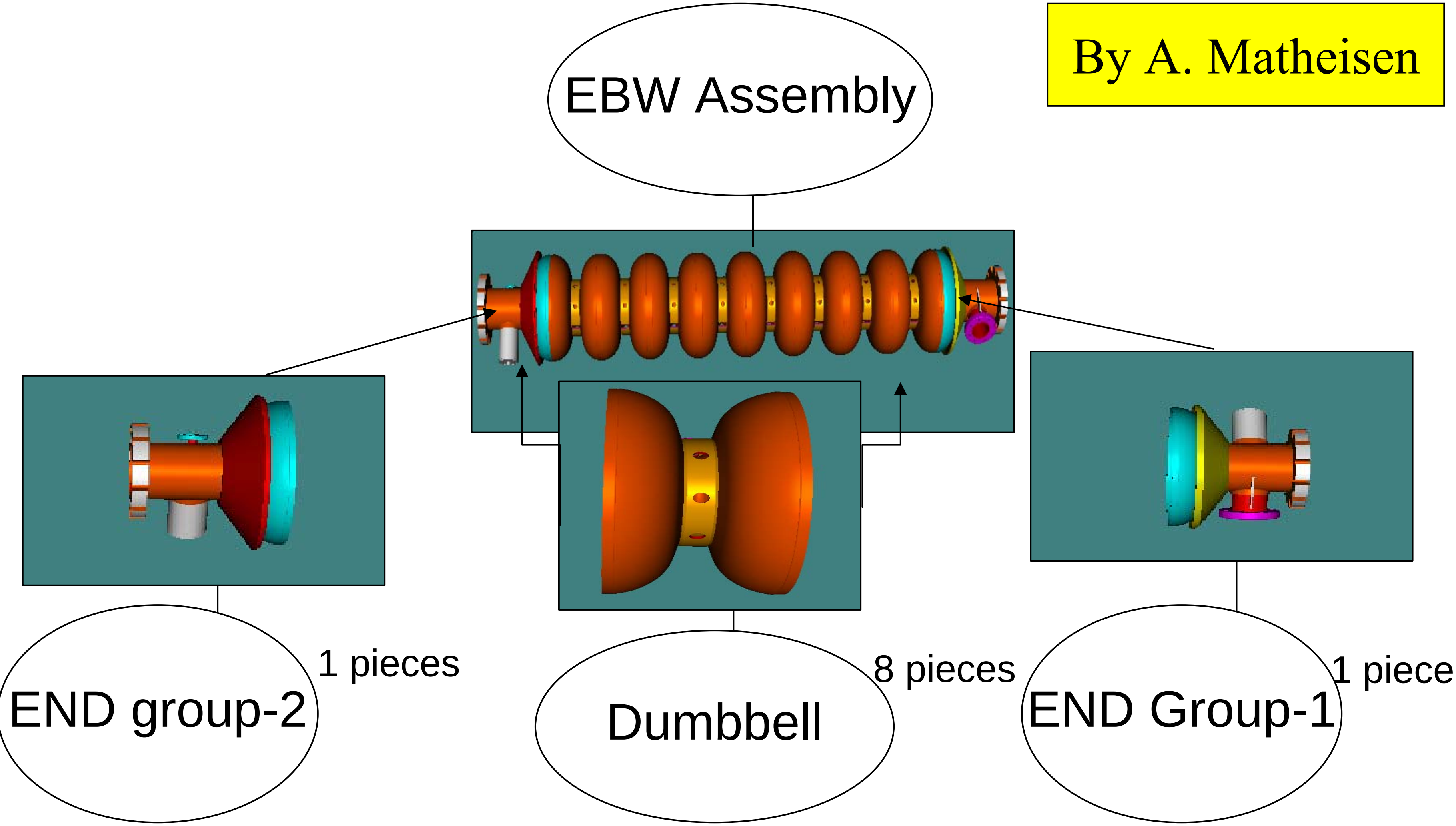

EBW Assembly of Cavity

EBW of dumbbells

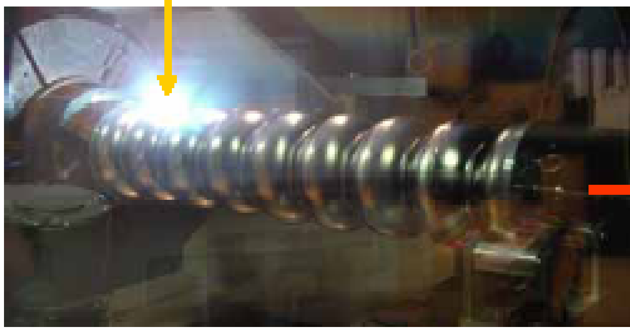

EBW of end-beam-pipe

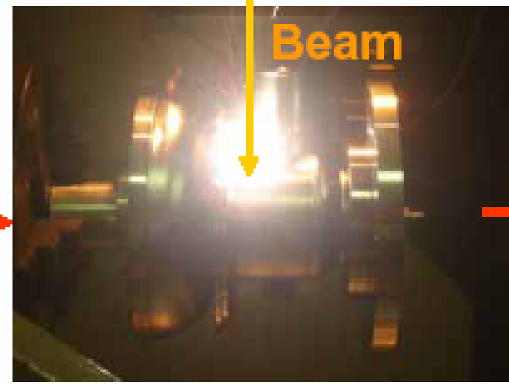

End-beam-pipes with HOM and flanges

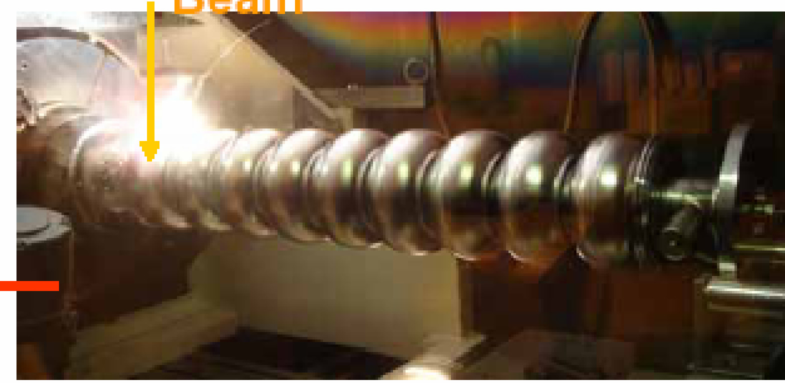

EBW of end-beam-pipes and cell-part

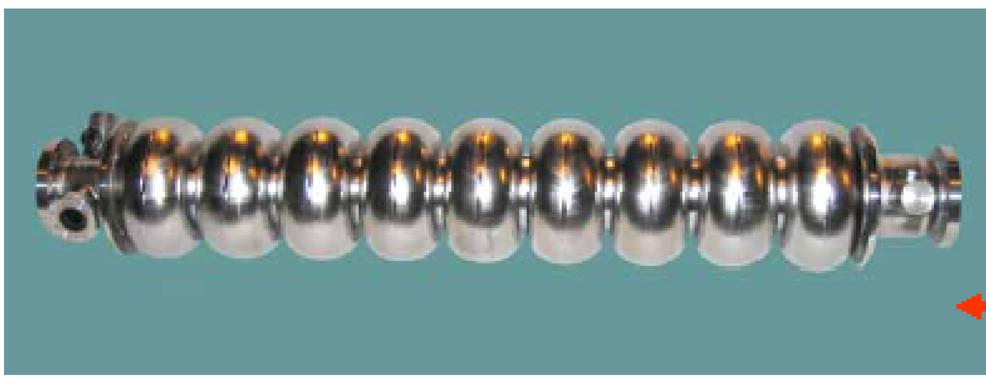

Four 9-cell ICHIRO high-gradient LL Cavities were successfully delivered to KEK ! (4 July 2005)

Completed Ichiro 9-cell Cavity

Kuroki Welding Company

7.5 Nb film coated cavity

CERN

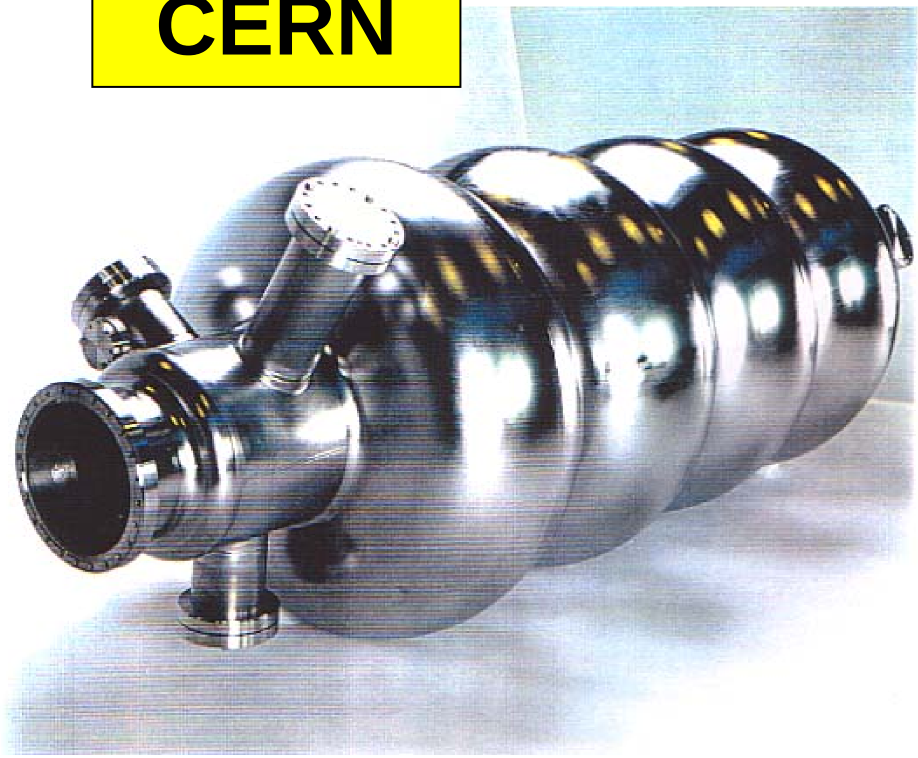

LEP-II 352MHz

niobium bulk cavity

Copper half cell before Nb coating

(electropolished)

Nb Coating Method at CERN

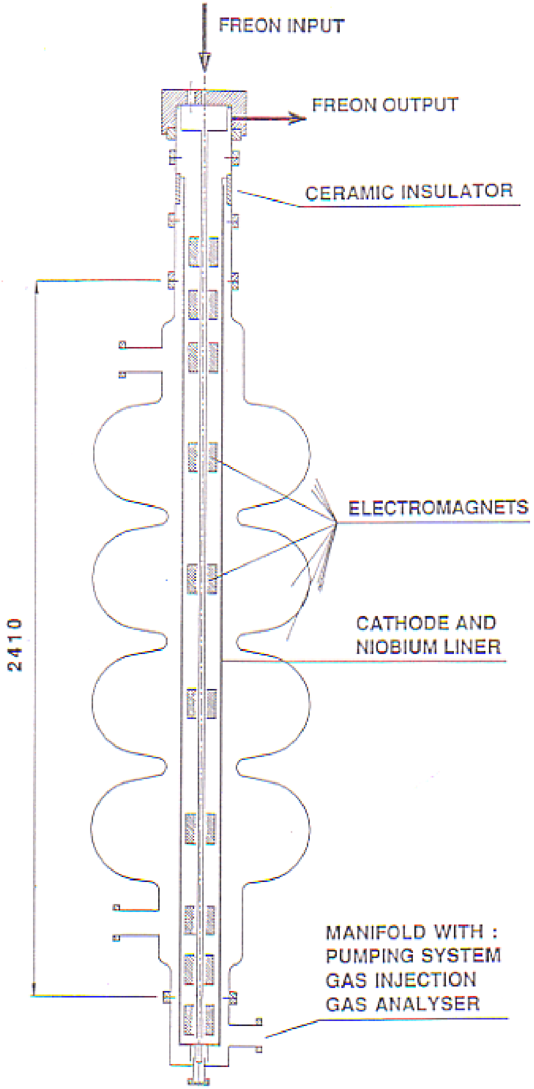

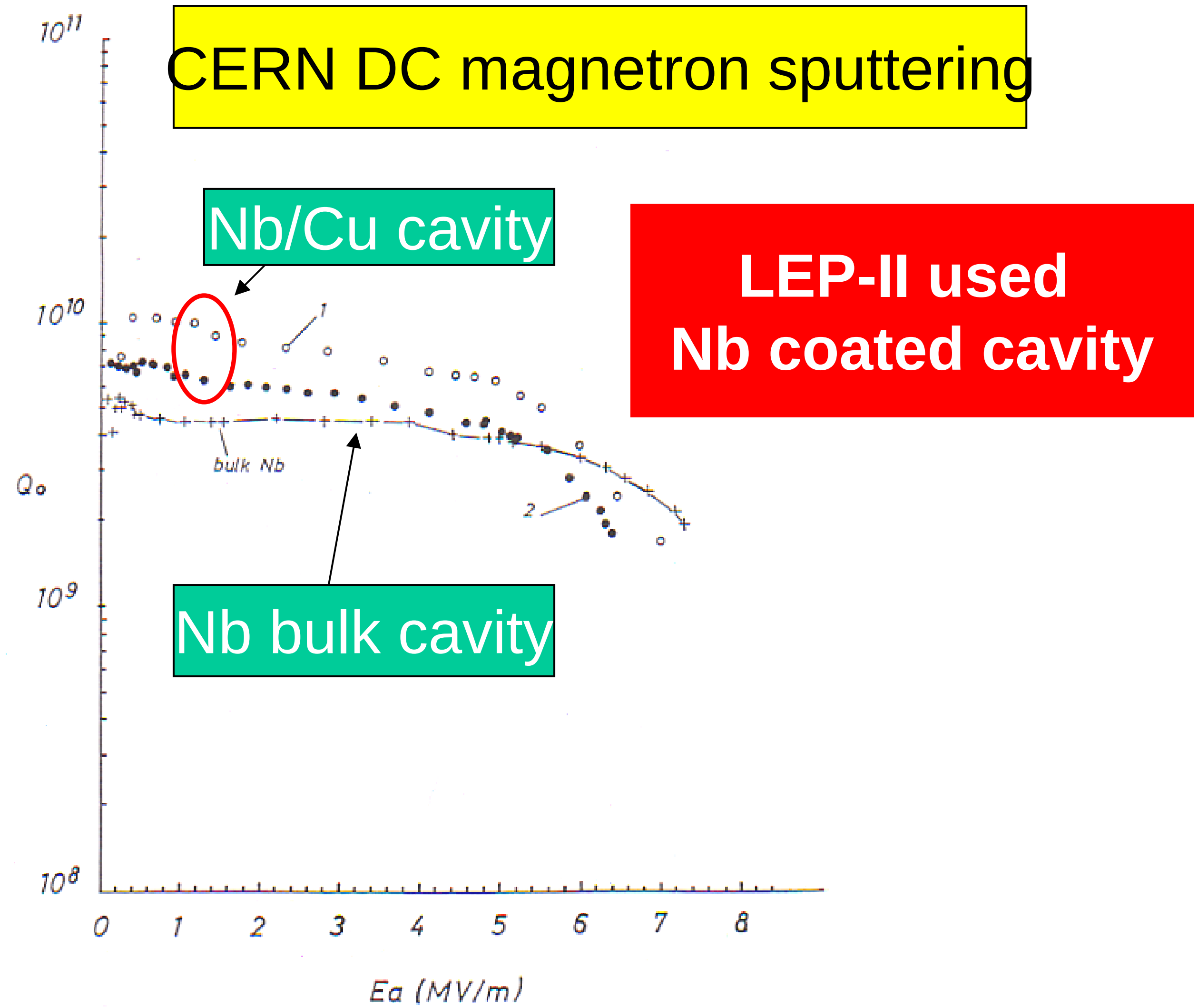

Steeper Q-slope in Nb coated cavities

Saclay 1500MHz

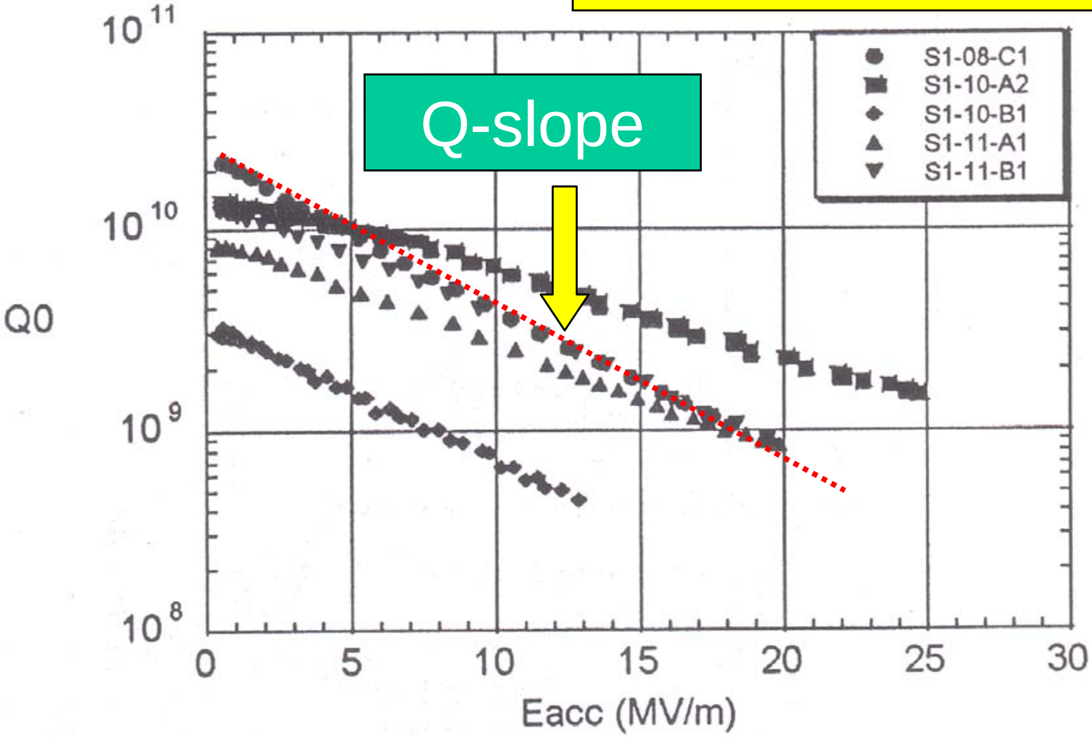

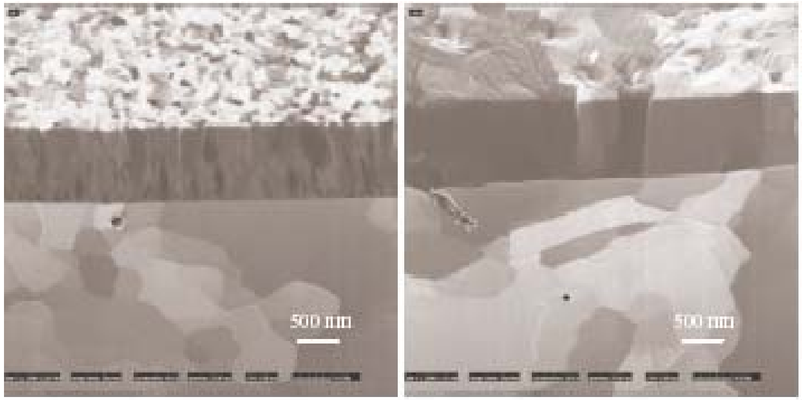

Figure 4: Cross sectional FIB images of niobium films on oxidised (left) and oxide-free (right) copper substrates

Problem: Q-slope
It is no problem at low gradient 5-10MV/m. It brings a serious Q dropp at high gradient. Many studies are under way but so far application o technology has no hope for ILC.

Note